UNIVERSITY OF SOUTHAMPTON

FACULTY OF ENGINEERING AND THE ENVIRONMENT

Industry Doctoral Training Centre

Volume [1] of [1]

Investigation into methods to identify and accurately locate misfired explosive charges following drill and blast operations

by

Kenneth Liddell

Thesis for the degree of Master of Philosophy

February 2021

UNIVERSITY OF SOUTHAMPTON

ABSTRACT

FACULTY OF ENGINEERING AND THE ENVIRONMENT

ISVR

Thesis for the degree of Doctor of Engineering

INVESTIGATION INTO METHODS TO IDENTIFY AND ACCURATELY LOCATE MISFIRED EXPLOSIVE CHARGES FOLLOWING DRILL AND BLAST OPERATIONS

Kenneth Liddell

Drill and blast tunnelling typically requires firing scores of explosive charges in a predefined sequence and from time to time, an explosive charge will fail to detonate, or will fire out of sequence; this event is known as a misfire. This research investigated a variety of techniques to reliably detect and accurately locate explosive misfires following drill and blast operations.

Previous related investigations into blast monitoring aimed to optimise the blasting process and fragmentation, or to minimise the environmental impact of tunnelling operations. In contrast, this research focused on spatially locating an individual shot by utilising its unique blast induced impulse signature.

Acoustic signal detection and analysis have been employed to uniquely identify the impulse point of origin. Signal classification was carried out on low energy and high-energy impulses from tunnelling/mining operations. Initial results have shown that even using an individual sensor, it is possible to discriminate between impulse origin locations as acoustic paths increase from millimetre-scale to meter-scale. We have shown that, in steel reinforced concrete beams and slabs and in natural rock mass, multiple impulse signals, made at same position, correlate strongly, but impulses originating from different positions showed significantly reduced levels of correlation. We found that higher energy impulse signals generated by small explosive charges, in contrast to mechanically induced impulses, also exhibited strong correlation.

Significantly, early experimental results have shown a strong correlation between low energy impulses and high-energy impulses originating at the same location during blasting in natural rock. This opens up the possibility to establish a methodology to classify impulse origins and thereby to potentially identify the locations of misfires.

Table of Contents

Table of Tables

Table of Figures

Academic Thesis: Declaration of Authorship

I, Kenneth Liddell

declare that this thesis and the work presented in it are my own and has been generated by me as the result of my own original research.

[**INVESTIGATION INTO METHODS TO IDENTIFY AND ACCURATELY LOCATE MISFIRED EXPLOSIVE CHARGES FOLLOWING DRILL AND BLAST OPERATIONS**]

.....

I confirm that:

1. This work was done wholly or mainly while in candidature for a research degree at this University;
2. Where any part of this thesis has previously been submitted for a degree or any other qualification at this University or any other institution, this has been clearly stated;
3. Where I have consulted the published work of others, this is always clearly attributed;
4. Where I have quoted from the work of others, the source is always given. With the exception of such quotations, this thesis is entirely my own work;
5. I have acknowledged all main sources of help;
6. Where the thesis is based on work done by myself jointly with others, I have made clear exactly what was done by others and what I have contributed myself;
7. None of this work has been published before submission

Signed: .....

.....

Date: 4 February 2021 .....

Acknowledgements

I would like to acknowledge my supervisors Dr Matthew Wright and Dr Jen Muggleton for sharing their extensive expertise in relation to acoustics and vibration analysis and their guidance regarding the research itself.

I would also take this opportunity to state my appreciation to Dr Patrick Foster and Dr Andrew Wetherelt of the University of Exeter for their invitation to conduct the explosives research at the Camborne School of Mines (CSM). Thanks to Mr David (Gus) Williams, the CSM Mine Manager who freely shared his extensive knowledge of mining and blasting techniques and who ensured my safety underground. In particular he enabled the many blast trials that were carried out at the Holman test mine at Camborne. Together we have spent many hours drilling rock, preparing charges and holding our breath hoping our data collection systems would do their thing. I appreciate his encouragement and the shear physical effort he contributed. I'd like to take this opportunity to thank Mark Kaczmarek and Mike Osman for colourfully sharing some of their combined experience of mining and blasting techniques.

I acknowledge the contribution and support of Cobham Tactical Communications and Surveillance (Domo) Ltd: and the provision of EngD funding from EPSRC grant EP/G036896/1, the Industry Doctoral Training Centre in Transport and the Environment

Finally, I would like to acknowledge and thank my wife Linda for her love, support, encouragement and patience, especially during the preparation of this thesis.

EPSRC

EPSRC
Engineering and Physical Sciences Research Council

Cobham TCS (Domo) Ltd

COBHAM

Definitions and Abbreviations

ANFO	Ammonium Nitrate Fuel Oil (Explosive)
CC	Correlation Coefficient
DAQ/DAU	Data Acquisition Unit
Detcord	Detonation cord. High explosive packaged as a 10 -15 mm diameter cord
EMP	Electromagnetic Pulse
Fall of ground	Unplanned release of debris, or rock from the tunnel roof or walls
Flyrock	Any fragmented material expelled from the blast face
Fragmentation	The size distribution of rock fragments following blasting operations
GHz	Giga Herz
ISEE	International Society of Explosive Engineers
kHz	Kilo Hertz
LF	Low frequency
MSHA	Mining Safety and Health Administration (USA)
MCFO	Multi-mode Fibre Optic
MIC	Maximum Instantaneous Charge (kg) / Maximum Instantaneous Charge Weight (kg)
ML	Main Level
ms	Millisecond
Muck pile	The mass of fragmented rock ejected by blasting operations
Nonel or NED	Non-electric detonators (shock tube initiation systems)
Overbreak	Unplanned/excess removal of rock during a production blast
PED	Programmable Electronic Detonators
PETN	Pentaerythrito Tetranitrate (Explosive)
PPV	Peak Particle Velocity
Q	Rock Tunnelling Index
RF	Radio Frequency
RFID	Radio Frequency Identification
RMR	Rock Mass Rating
SD	Scale Distance (m)
SMFO	Single Mode Fibre-optic
Spalling	The ejection of fragmented rock during a blast

TBM	Tunnel boring machine
Throw	The horizontal movement of rock ejected by blasting operations
UCS	Unconfined Compressive Strength (rock or concrete) (MPa)
USBM	United States Bureau of Mines
VCC	Variant Castle Cut
VHF	Very High Frequency (radio frequency electromagnetic radio waves 30 MHz to 300 MHz)
VoD	Velocity of Detonation (m/s)

Chapter 1 Introduction

This chapter presents the background to the problem description underlying the research carried out on misfire detection and blast induced impulse localisation during underground blasting operations.

This chapter outlines the research aims together with a description of the technical approaches considered. The chapter concludes with an overview of the thesis structure and chapter summaries.

1.1 Problem Description

Rock tunnelling involves rock excavation to make a void; and rock support to maintain the opening that could otherwise begin to close. Drill and blast techniques are employed around the world throughout the underground mining industry; in tunnelling and for the excavation of underground spaces. Excavations using explosives in preference to mechanical means enable the controlled and economic removal of large volumes of ore and rock relatively safely and quickly. The blasting process also provides a degree of control over the rock fragmentation, which is essential to permit handling and removal and to enable downstream processes to be carried out. The efficiency of the method is dependent on combinations of the local geology; explosive compounds employed; the drilling techniques used and the design of the drill pattern.

Explosives were quickly established as being of vital importance in civil engineering and in mining. However, their widespread adoption has inevitably resulted in accidents and injuries arising from their manufacture; storage; transportation and usage. Incidents derived from poor practice, misuse and system malfunctions continue to occur Verakis, (2001, Bajpayee, Rehak et al., (2002, Verakis, (2003, Bajpayee, Rehak et al., (2004). In particular where drill and blast is used in tunnel construction scores of explosive charges are fired in accordance with a predefined geometric pattern and firing sequence as determined by the blasting engineer. The aim of the blast design is to optimise the rate at which tunnelling progresses, known as the Advance Rate.

From time to time, an individually charge will completely, or partially fail to fire, or fire out of sequence; this event is known as a misfire. The USA's National Institute for Occupational Safety and Health (NIOSH) describe a misfire as the complete or partial failure of a blasting charge to explode as planned. The explosive, or pyrotechnical products that remain in the ground, or in the muck pile might be triggered by any mechanical effect during digging, milling or crushing stages of the mining (or tunnelling) process, causing injuries or fatalities to blasters or operators.' Certain types of explosive materials e.g. Ammonium Nitrate Fuel Oil (ANFO) mixtures, or slurries that are highly visible pose no danger if they fail to fire. They often become exposed and when unconfined and separated from their initiation systems cannot be initiated. Other blasting components such as detonators, boosters, primers and detcord remain sensitive to heat, shock and vibration and present a very real danger in downstream processes if they remain undetected.

The International Society of Explosives Engineers (ISEE) gives a wider definition of a misfire: ‘a blast or specific borehole that failed to detonate as planned…’ this encompasses a complete failure to detonate, partial detonations and detonating at the wrong time. A blasthole firing before the intended time delay, or out of sequence, can be just as problematic as not firing at all.

The significance of this research is not only to detect whether a misfire has occurred, but to allow the fragments of the initiation system to be found more easily. Identifying which shot in a sequence failed to fire greatly assists the responsible engineer to locate the hazardous products in a safer and faster manner. As the blast sequence progresses rock ejected from a specific region of the blast face will end up in known areas, therefore the products of a misfire will also likely be in predictable locations. Before further work can continue, all unfired products must be accounted for and safely removed.

Earlier research focused on optimising the quantity of explosives used and minimising the adverse effects of blasting resulting from excess ground vibration or air over pressure. In contrast this research focused on improvements in safety underground by developing a methodology to detect and locate explosive misfires. Although a misfire is primarily a risk to safety, the legal requirement to safely manage the incidence of a misfire means that when it has occurred, or is suspected of having occurred, the work underground must cease until such times as the misfired explosives have been recovered.

Despite advances in explosives initiation technologies there is presently no reliable method available to determine whether every charge has fired correctly in the firing sequence. The potential consequences of a misfire are economically severe and potentially catastrophic with risk of injury or loss of life and consequently every reasonable measure should be taken to avoid and deal with a misfire Verakis, (2001, Verakis, (2002, Verakis, (2003, Liu, (2011)

Current practice infers the occurrence of a misfire from visible indicators during the post-blast inspection such as unexpected blast outcomes; the presence of unfired explosives; the presence of other initiation components; excess flyrock; poor fragmentation; unusual vibration traces etc. All of these raise the possibility that a misfire may have occurred, but none of them indicate which specific charge(s) may have misfired. Since the interpretation of these indicators is subjective and requires tunnelling engineers to visually assess the blast area they are temporarily exposed to potential hazards while they conduct the post blast inspections. Following a blast there is a minimum time period where it is prohibited to re-enter the blast area (typically 30 minutes) due to the potential for the fall of ground, or the presence of noxious fumes from the blasting process.

It would be preferable to have a reliable, real-time misfire detection method that did not require any human presence near the blast face and that the required blast data could be derived exclusively from the blast process and not open to subjective interpretation of secondary indications. This research aimed to obtain data from directly explosive charges as they fired and to remotely monitor the blast process.

1.2 Research aims

The aim of this research is to develop a methodology that would increase the probability of reliably detecting and spatially locating a misfired explosive charge in the context of underground transport tunnel blasting.

The research had the following objectives:

- Investigate more reliable techniques to identify and locate misfired explosive charges
- Outline the implications of employing this technique in tunnelling.
- Develop a remote monitoring methodology for tunnel blasts

To achieve the aims set out above, two streams of investigation were carried out:

Investigation into a means of reliably generating and transmitting a signal that would confirm a successful initiation of an explosive charge, or create an alert of a potential misfire at a safe monitoring location.

The second objective was to devise a method whereby it would be possible to remotely monitor the blast-induced vibration generated by each charge fired in the sequence and establish, with a high degree of confidence, whether each individual charge had been successfully initiated.Thesis structure

This thesis is broken down into eight chapters.

1.2.1 Chapter 2

Through an introduction to tunnelling techniques and in particular the use of explosives in underground tunnelling, this chapter expands on the problem description.

The likely causes of misfires and their implications are outlined, together with the available statistics on the incidence of misfires. The literature review expands on past interest in blast monitoring and approaches to blast control. The attempts to minimise environmental impact of excess air over pressure and ground vibration using signature hole blasts were highlighted due to the potential to apply the measurement techniques to this problem.

An introduction is made of other, more advanced signal correlation techniques for event positioning and of seismic ray tracing in 3D applications. Finally, the potential to exploit Time Reversal Mirror theory and the research approach are described.

1.2.2 Chapter 3

Introduces the Exeter University test mine in Cornwall. Outlines the initial technical approaches to the identification of misfires with a brief summary of the outcomes for ‘return-line’ misfire detection investigation.

The chapter concludes with the need to develop remote monitoring techniques to monitor blast parameters and reliably detect a misfire and identify its specific location.

1.2.3 Chapter 4

Chapter 4 examines the applications and benefits derived from monitoring blast induced-vibration and outlines the need in relation to explosive misfires for being able to spatially locate the point of origin. Some related use cases where the source of acoustic signals have been spatially isolated using signal cross correlation: are explored.

The chapter introduces the concept of Time Reversal Mirrors (TRM) and looks at the literature around the subject of TRM theory. It expands on the specific combination of blast induced vibration monitoring and the specific application of TRM.

1.2.4 Chapter 5

Chapter 5 outlines the initial investigation into impulse measurement experiments carried out on a fibre board lab bench. These measurements opened the door to investigating the potential to localise signal in solid and pseudo-unbounded media.

1.2.5 Chapter 6

Chapter 6 describes the measurements and analysis of impulse experiments carried out on a steel reinforced concrete beam and on a steel reinforced concrete slab.

1.2.6 Chapter 7

Chapter 7 describes experimental work carried out at the Exeter University Camborne School of Mines test mine using commercial, mass-manufactured detonators to generate impulses in rock. The use of standard detonators as the impulse generating mechanism standardised the mass of explosives used in the main series of experiments. It also localised the source of the impulse to the size of a pin head as only 0.6g of explosive is used in the manufacture of the detonators.

The progression of experiments at the CSM quarry investigated the possibility of correlating small blast induced vibration and quantified the spatial degradation of the correlation coefficient. The mine facilitated monitoring of several small scale production blasts and investigation using far field measurements.

1.2.7 Chapter 8

Chapter 8 reiterates the main learning from this research and draws the main conclusions from the experimental work. It outlines the practical considerations on the applications of the techniques described and concludes with recommendations for future work.

Chapter 2 Explosives in Tunnelling and Misfires

2.1 Explosives in tunnelling

Tunnel blasting is much more complicated operation than surface bench blasting used for creating a transport cutting in road construction in the open countryside, since in tunnelling the only free surface where initial breakage can occur is the tunnel face. The optimal weight of explosive charge required to efficiently blast rock was originally derived by Langefors U., (1978). Due to the higher degree of charge confinement, larger volumes of explosive charges are needed than in bench blasting where a free face exists and the expulsion and fragmentation of rock is relatively easier Persson A. (1994). Tunnel blast design has a direct influence on the efficient removal of rock and therefore on the tunnel construction time and costs Zare, (2006).

2.2 Improvements in tunnelling technologies

Improvements in the efficiency of drill and blast operations have followed technological evolution in drilling techniques and in the types of explosives available.

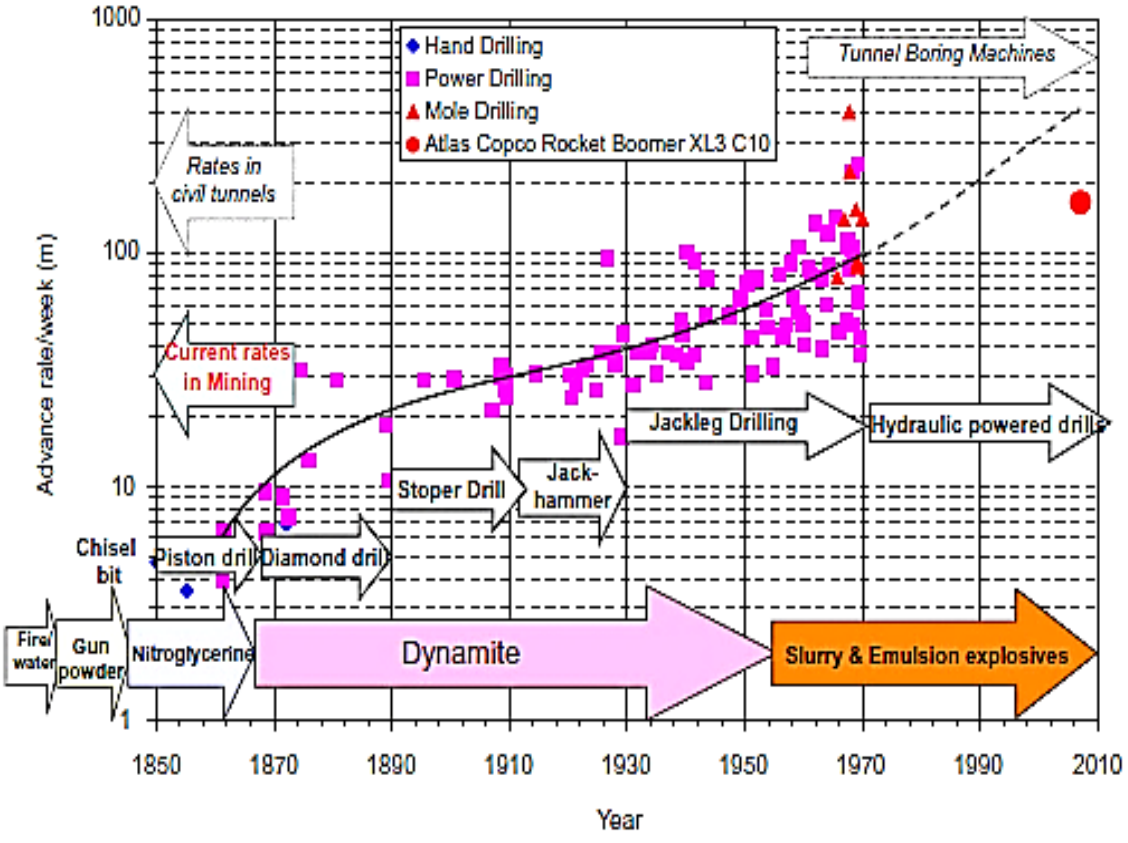

Figure 1 Chart showing improvements in Tunnelling Advance Rate (metres/week) vs technology innovation Sandvik, (1999)

In complex geologies, as in most mining operations, the use of Tunnel Boring Machines (TBM) is generally ruled out due to the increased need for adaptability, therefore drill and blast becomes the only commercially viable option.

A tunnel blast begins with creating a predefined pattern of holes that are first drilled then charged with premixed or site sensitised explosives. Commercial explosives are mostly ammonium nitrate or nitro-glycerine based. The complete charge is a combination of a detonator which controls the initiation sequence, a booster and the bulk charge. The charges are typically fired sequentially with a delay of around 100 ms between each one, but frequently there is a need to fire pairs of or clusters of charges depending on the shape of the tunnel and the local geology.

2.3 The tunnelling process

The construction of surface road and rail cuttings often requires bench blasting in rock. During blasting material is expelled in the direction away from the rock mass into free space. Active prevention of excess rock removal, known as over-break, is often necessary. Figure 2 shows an example how over-break is mitigated using a row of uncharged holes. These holes have been drilled to define the limit of rock breakage.

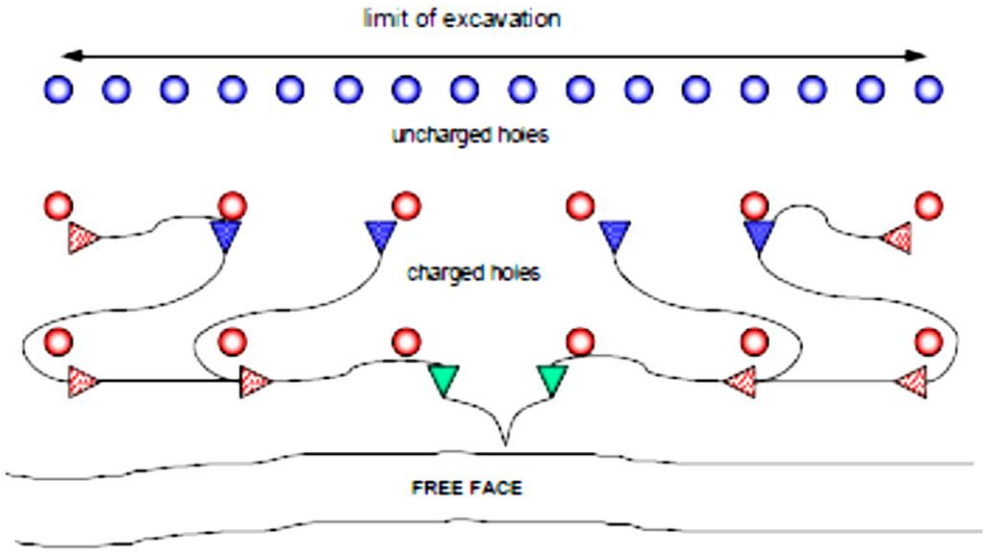

Figure 2 Line drilling layout, showing the free face and the direction of rock movement

In contrast to surface blasting, the starting point for the tunnel blast is the creation of the free face where each successive blast will direct the fragmented rock into it. Since the only free face is initially perpendicular to the direction of the tunnel advance, this technique creates a pattern of long, narrow free faces by drilling extra-large holes into the tunnel face which will remain un-charged. These holes are intermixed with regular charges holes, which when fired, blast the rock into the empty ones. This narrow engineered free face is called the ‘cut hole’.

Various stages of the blasting sequence can be understood Lee, (1994) . The first blasting event that actually removes rock is described as 'the cut'. The purpose of this step is to introduce a larger free face into the rock. The importance of the design of this stage cannot be overstated. Adderly examined the role of cut design in his PhD thesis and detailed how excessive blast induced vibration can be directly linked to ineffective cut designs Adderley, (2009). Common cut designs were investigated in depth shown in Figure 3.

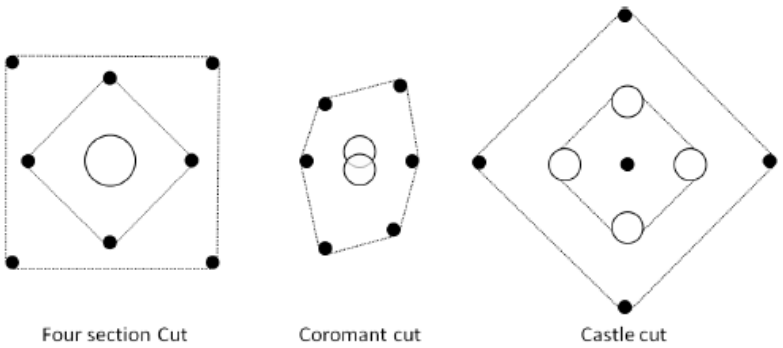

Figure 3 Drilling Patterns for Common Cut Designs. Reproduced with permission Adderley 2009.

A detailed investigation into the impact of the 'cut' design required in the first step of tunnelling using drill and blast methodology was carried out by Adderley (2009). Figure 3. Illustrates a selection of designs that could be chosen for the initial blast pattern. The smaller solid dots show bore holes charged with explosives, the larger circles are larger diameter reemed holes that serve as a free face within the rock. In his PhD thesis Adderley established the link between excessive blast-induced-vibration and ineffective use of explosives during the execution of first crucial cut hole firing sequence. Poor cut design results in excessive consumption of explosives in the first fractions of a second of the blast; resulting in an unproductive blast with uncontrolled generation of undesired vibration remote from the blast site.

After a few hundred milliseconds after the blast is initiated a void will be created into which the subsequent Stoping charge holes develop; sequentially ejecting material out of the rock mass. The perimeter holes are usually fired with detcord as an explosive. Detcord is a narrow (~15mm diameter) cord of high explosive that is loosely fed into the blast holes and since it is decoupled from the surrounding rock, does not crush and weaken it when it fires, but generates fissures that track between the smooth blast profiling holes. These are therefore employed to create the smooth wall finish desired for the tunnel finish. In Figure 4 below shows the work operational sequence in tunnel development Sandvik, (1999). All images reproduced with the kind permission of Sandvik.

- Survey the tunnel face
- Drilling
- Explosive charging
- Blasting the 'round'
- Mucking away

- Scaling
- Roof support

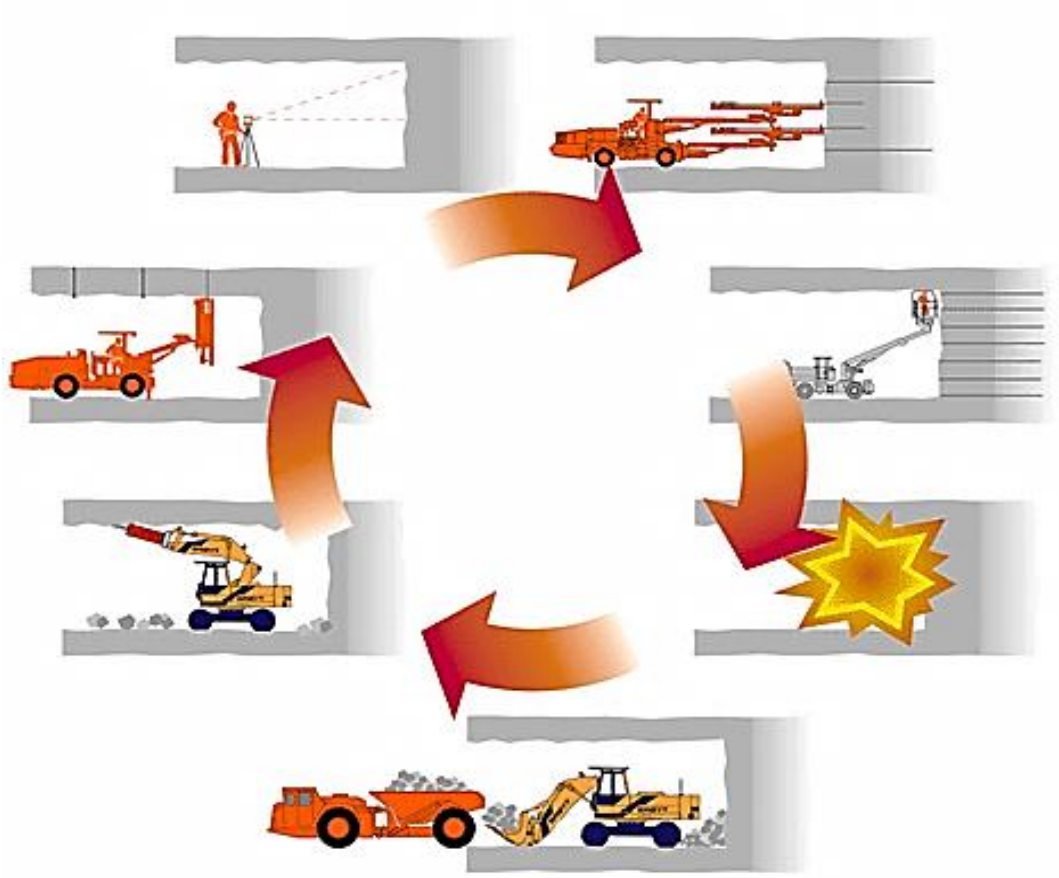

Figure 4 Operational sequence in tunnelling. Sandvik, (1999)

Tunnelling can require combinations of several drill and blast methods; the combination of which are intended to result in smooth wall blasting. The intention is to limit the degree of unplanned removal of rock, called 'overbreak' during blasting.

Overbreak is undesirable in transportation tunnels where a smooth engineered finish is what is desired. Four common methods used in tunnelling are:

- Line drilling
- Trim blasting
- Pre-splitting
- Bench blasting

An example is shown Figure 5. This technique involves creating a line of closely spaced holes, drilled around the intended periphery of the tunnel, operating in a similar fashion to the perforations on a postage stamp.

These are the contour holes and they are not always charged with explosives. The blast holes are then drilled and charged at normal intervals inside these fracture-limiting contour holes.

In line drilling normal charges and firing delays are employed. However in order to produce a smooth surface finish to the newly exposed rock face a row of uncharged holes are made to attract and concentrate blast induced fissures, where they terminate Figure 5 Lee, (1994).

At the outset of the process to create the tunnel gallery no free face exists, therefore, an artificial free face is created by blasting into a group of larger drilled holes. The void created in this stage is known as 'the cut'. The cut is engineered by drilling a few extra-large holes at the centre of the blast pattern. In the example shown in Figure 5 below, the central diamond area is where the primary free face is created by drilling a couple of 80 mm diameter holes. The first blasts numbered 1 -4 are designed to 'burn the rock' creating a free face that develops radially outwards as the blast sequence continues. The numbers shown are the blast sequence for the full round.

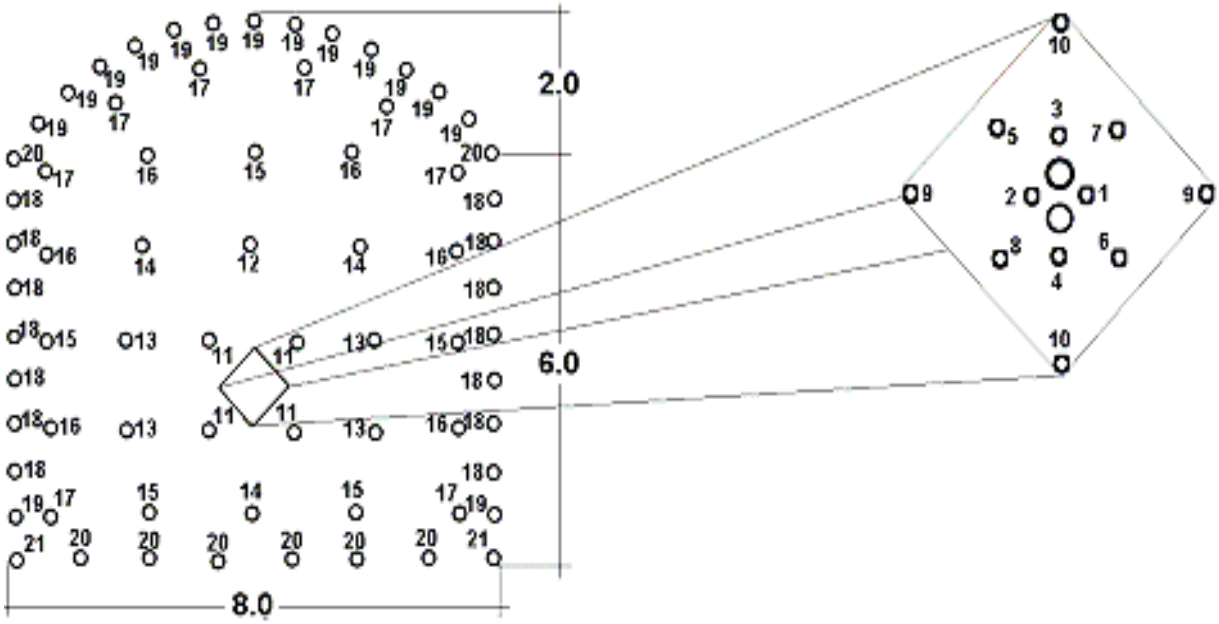

Figure 5 Drilling and firing pattern for a horse shoe shaped tunnel showing a typical pattern of terminating blank holes at the intended boundary of the new tunnel Lee, (1994).

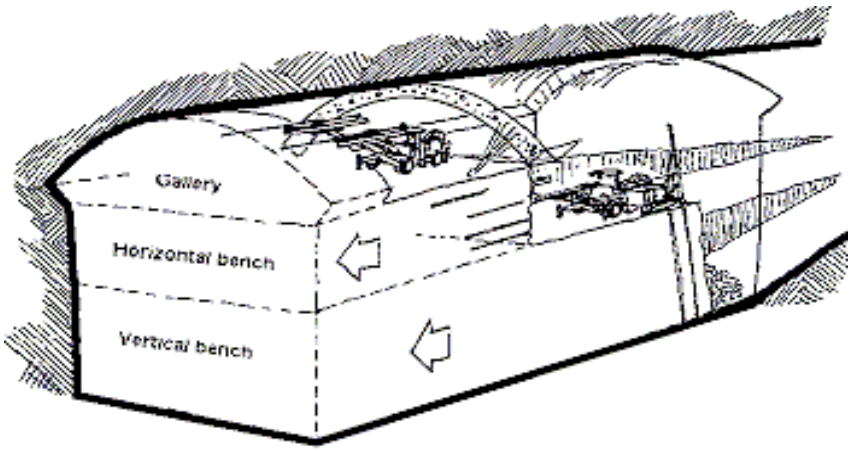

Figure 6 Large tunnel development sequence Lee, (1994)

The technique by which a large tunnel is developed is shown in Figure 6 Lee, (1994). It shows that the first step is the creation of the gallery zone under the new tunnel roof; with the next step blasting the horizontal bench; then finally the vertical bench.

The gallery is created using combination of drill and blast methods, with a firing sequence like the one in the figure below. The second phase of operations is the horizontal bench, where additional horizontal boreholes are created; blasting rock upwards and away from the tunnel wall. Drilling and blasting in this horizontal bench blasts rock upwards into the newly created void in the gallery until the available 'headroom' is sufficient to allow vertical boring operations. Smooth wall blasting techniques are employed at the tunnel walls only. When sufficient headroom has been created, vertical boreholes are made and the rock in the vertical bench is removed. Figure 7 shows the blast sesquence with the red zone being the first material to be expelled from the blast area.

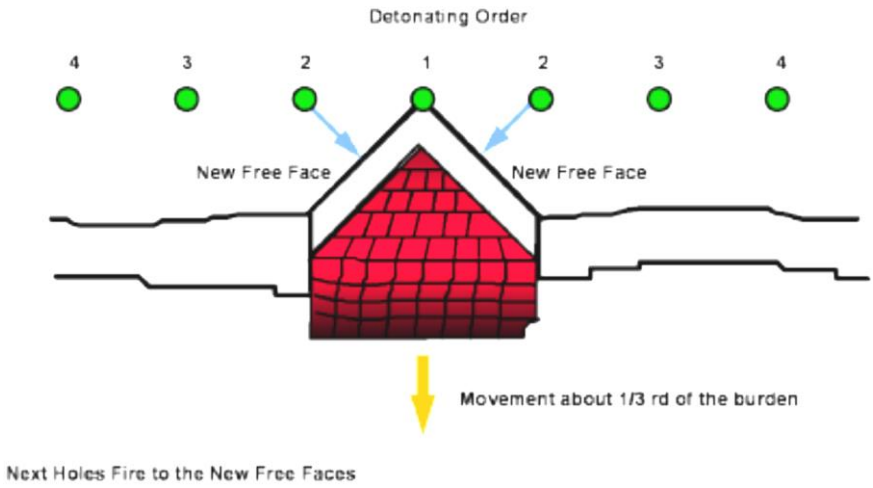

Figure 7 Blast sequence in a vertical bench. Sandvik, (1999)

Drilling holes in blast face has become increasingly efficient due to continual improvements in drilling equipment. Combining drilling techniques with site sensitised explosives (SSE) is making the blast set up faster and safer.

2.4 Blast design and constraints

The blast design requires decisions to be made on the drilling pattern, the firing sequence and timing delays as well as the type and quantity of explosives in each blasthole. Each one will be charged with a combination of detonator/primer and column charges. Examples of readily available bulk explosive materials are ANFO, SEE/slurries. A cast primer such as Pentolite™ (or nitro glycerine explosive such as Perunit™) will be required to initiate the bulk explosives Farnfield, (2012).

Although classed as high explosives and sensitive to shock, heat and friction, successfully initiating bulk column charges, such as ANFO, requires very specific conditions to be created before they will actually detonate Farnfield, (2012). Depending on where the chosen explosive is used in the blast, several types of column charge explosives may be used in combination. SSE are fast and efficient to load and have the safety advantage of not becoming explosive until they are pumped into the blast hole and they reach their design density Sandvik, (1999, Farnfield, (2012). With SSE emulsions the explosive mix/concentration may be changed in the hole so that no special explosive is needed in the contour holes that create the boundary of the planned tunnel. For efficient loading the SSE loading truck and the service platform of the drill rig may be used together. For small diameter short holes it has long been the practice to charge shot holes with a primer Farnfield, (2012) consisting of a detonator inserted into a cartridge of sensitive explosive. Subsequent cartridges of explosive need not be sensitive to a detonator but only to a primer cartridge Sandvik, (1999, Farnfield, (2012).

The impact of unwanted vibration outside of the tunnel blast zone is a factor that frequently limits the amount of rock that can be removed at any one time. The maximum quantity of explosives that is permitted to be fired at any one time is called the Maximum Instantaneous Charge Weight (MIC) and is quantified in kilograms. The amount and choice of explosive compound that is used in any one hole is a key parameter affecting the blast performance therefore, there emerges a trade-off between the volume of fragmented rock achievable and the permitted vibration radiating from an individual charge, or from the superposition of vibration from multiple charges. The chosen timing delays between charges control how the vibration from each individual charge combines constructively, or destructively with those from other charges in the sequence at some specific remote location. The vibration experienced at a remote monitoring point is directly related to the local geology; the distance from the blast face; the firing delay times and to MIC of explosives fired.

In addition to the MIC of explosives, the rate of energy released varies between explosive types employed which are commonly characterised by a parameter called the Velocity of Detonation (VoD). This is the velocity that the explosive reaction propagates along a length of the charge. Effectively, the higher the VoD, the more

energy is released per unit time, therefore the greater the breaking force. More rock can be removed by higher VoD explosive compounds.

The expected vibration created by a blasting can be modelled by the blasting engineer. So called signature-holes where a non-production holes is drilled and used to accommodate a test fire can be set up close to the blast face. The resulting vibration trace is then recorded at a remote point of interest (such as a specific building near the blast site), to give an indication of the expected vibration amplitude and frequency characteristics that could be expected from each of the shots in the production blast. The vibration measured from the signature hole is then incorporated into commercially available software together with the planned shot timing sequence to model expected outcome. However, the MIC and firing sequence timing are just two of the parameters that influence vibration. Variability arises with how consistent charge loading; rock burden and hole-hole spacing Yuill, (2001).

2.5 Detonator types and initiation systems

Three types of detonators are in general use. Each one of them has an initiation line, a detonator with a selectable delay element, a priming charge and a base charge component.

The purpose of the detonator is to produce a sufficiently energetic shock wave to initiate the primer, which in turn initiates the main volume of explosive material known as the column charge. Each of the three types illustrated here are commonly available, but the 'Non-el' (non-electric) types are the most widely used.

2.5.1 Electrical Detonators

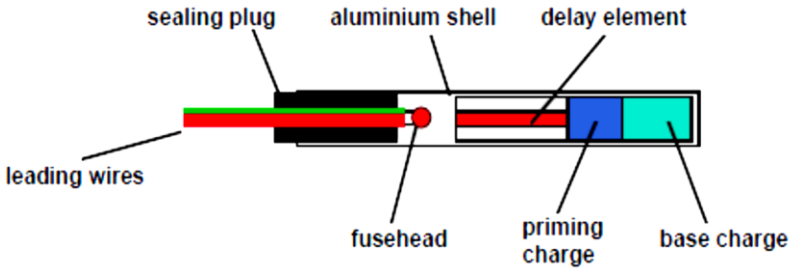

Figure 8 Delayed action detonator. Farnfield, (2012)

The electrical detonators operate when a sufficient current is delivered through the control wire to melt the fuse head and begin a pyrotechnic reaction I the delay element. A specified number of milliseconds later the priming/base charge fire.

2.5.2 Shock Tube Detonators (Non-electric, or 'nonel' detonators)

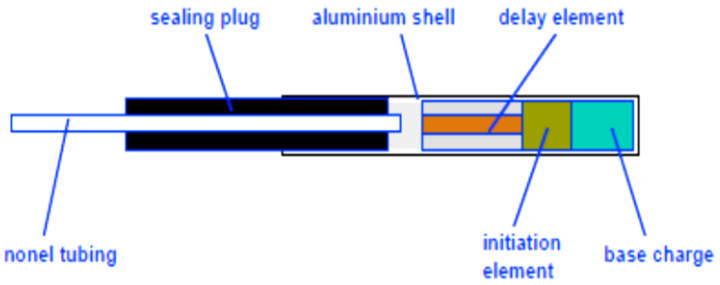

Figure 9 Shock tube detonator construction Farnfield, (2012)

When initiated the explosive powder combusts and propagates down the tube at a rate of 2,100 m/s. Such a small amount of powder is used that the explosive effects are contained within the tube, which does not burst open. Shock tubes are used to convey a signal from the operator to the blast site. When this signal reaches its destination it initiates a delay or an instant blasting cap. Shock tube has replaced electric detonators and blasting caps for many applications because it is far less sensitive to many of the effects of static electricity and radio frequency energy that can cause premature initiation of electric initiators.

Industry figures state that over 6 million km of shock tube are used each year worldwide. Shock tube is used in commercial blasting, military demolition, special effects, automobile airbags, aircraft escape systems and professional fireworks to name a few. New applications are developing almost every day for this amazing product. Nonel (non-electric) detonators are referred to as shock tubes. Shock tubes replace the electrical components in conventionally constructed detonators. The inside surface of the plastic tubing is coated with a thin layer of an explosive/reactive substance that, once activated, propagates a shock wave down the tube at a speed of approximately 2000 m/s. This shock tube has a light coating of explosive on its inner surface that when initiated has sufficient energy to initiate the primary explosive or delay element in a detonator. Since the propagating shock wave is contained within the tube, this has no blasting effect and the tubing acts merely as a signal conductor.

These devices are initiated manually by percussion gun, or by being connect to another detonator.

2.5.3 Programmable Electronic Detonators (PED)

The most advanced design of detonator is the Programmable Electronic Detonator (PED) with their associated control systems. These systems establishes two-way communication with each individually addressable detonator. Theoretically the blast will not be initiated until every detonator has been confirmed operational.

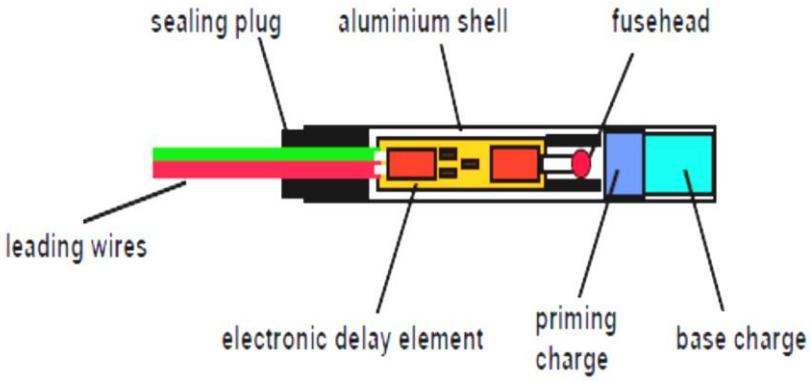

Figure 10 Schematic of an electronic detonator.Farnfield, (2012)

The control system carries out checks including:

- The correct number of detonators in the circuit
- Any missing or poorly connected devices
- The presence of fuse heads in the detonator
- Whether communication to the detonator is possible
- Checks the identity number of each detonator
- Detonator condition (state)

Although these checks are comprehensive and sound fool proof, in practice great care needs to be taken as poorly installed explosives can still misfire or even prevent a blast from ever being ready to fire. Blasts incorporating thousands of charges can still demand hundreds of man-hours to check for continuity and correct installation. The PED system is designed to prevent the initiation of the blast sequence should any of the preliminary checks discover a problem. Even although the system will not fire until the system condition is 'perfect', a misfire could still occur for any number of reasons unrelated to the condition of the blast initiation system.

2.6 Blasting control and monitoring

Controlling the negative effects of blasting is essential during the tunnel construction process to meet safety and regulatory requirements. The most common undesirable impact of blast operations is causing damage to nearby structures on the surface, and more likely, to the newly created areas of the tunnel itself.

The current guidelines for drill and blast practices were reviewed by Nateghi, (2012) in relation to the avoidance of damage to the newly constructed concrete lining of tunnels as a result of on-going drill and blast operations and refined them to their current level.

Routine analysis of the blast vibration time signal itself can be used to verify the numerical count and the timing of each shot. The relative amplitude of each impulse generated by a fired shot indicates how effective any particular charge has been in removing rock.

The speed that ground moves as a result of blasting measured in mm/s and is referred to as the Particle Velocity. Peak particle velocity depends on the effective instantaneous mass of explosives fired i.e where the duration of one charge overlaps with another charge the effective charge mass is greater in any instant (usually within a period of 8 ms). Therefore the effective instantaneous charge is dependent of many factors: number of charges; the distance between each charge and the measurement position: timing delays, length of charge, the blast location as well as the geological conditions of the intervening rock mass. Most other researchers have investigated tunnel blasting methods specifically with a view to reducing the environmental impact of this vibration, to control the rock fragmentation, or to optimise the economic consumption of explosives per linear metre of tunnel gained.

No investigation technique to date, addresses the identification of the physical location of any specific charge in the sequence or even confirmation that any one charge has fired correctly.

2.7 Misfire statistics and causes

Given the complexity of the drill and blast process and the universal adoption of the technique globally, it should not come as a surprise that there is the possibility of technical failure, or the opportunity for the introduction of human error.

2.8 Misfire statistics

Misfire statistics in the tunnelling industry are not readily available, however in the mining industry where there is continuous use of explosives, statistics have been reported, collated and analysed. The industry categories adopted were for coal mines and metalliferous (metal) and non-metal (other minerals). Bajpayee, Rehak et al., (2002) investigated flyrock injuries in the US mining industry over the period from 1978-2000. In that period there were 114 fatalities in total that were related to blasting processes.

Table 1 Blasting related injuries 1978 – 2000.

Industry/Location	**Underground**	**Surface**
Coal	31	19
Metal / non-metal	28	26

In a ten-year period between 1989 and 2000, non-fatal injury rates were significant for the industry.

Table 2 Non-fatal blasting related injuries 1989 - 2000.

Industry/Location	**Underground**	**Surface**
Coal	384	167
Metal / non-metal	200	1,008

In a study to review blasting accident data over a three decade period from 1980-2010, Bajpayee, (2010), categorized all the blasting accident data according to the cause of the accident or activity that was taking place when the accident occurred. The major categories reported, ranked in order of severity are:

(1) Poor blast area security

(2) Undesirable projection of rock fragments beyond planned limits (flyrock)

(3) Premature blast detonation

(4) Misfires and unplanned sequence of firing

(5) Fumes from explosions engulfing people nearby

(6) Accidents during the transportation of explosives

(7) Disposing of unfired explosive components

(8) Miscellaneous/other

Siskind and Kopp, (1995) analysed the modes of causes of fatal and non-fatal injuries and found that flyrock accounted for 58.7% of injuries and explosive misfires contributed to 7.8% of injuries.

Analysing the period from 1978 to 2008 Verakis and Lobb (2012) estimated the 2010 misfire related injuries to be 9.3% of the blast injury total (111 injuries from a total of 1192), ranking in severity behind blast area security and flyrock (60.52%), premature blast (11.65%) and fumes (8.8%).

These figures are taken from the MSHA accident data base and likely record the minimum level since they only reflect the total number of incidents where a notifiable injury occurred.

2.9 Misfire detection

Although infrequent, the incidence of a misfire can cause huge disruption and if undetected, present a risk to life and processing equipment. Therefore a means of determining whether every charge has fired successfully would increase worker safety and also productivity. Hence, the development of a tool to enable the accurate location of each shot that is successfully fired is of interest because of the need to detect and improve the response to handling potential, or actual misfires.

At the outset, blast design aims to remove as much rock as possible in a safe and efficient manner and also to minimise the quantity of explosives used. Engineers design each blast to remove as much rock as possible and to ensure it is in a suitable condition for handling and processing. The rock ejected by blasting is referred to as the muck pile. Producing suitably fragmented rock that is localised in its post-blast distribution is the main outcome of the blasting process and is the over-riding consideration in blast design. Other factors that are taken into account are: minimising the cost of drilling; optimising the cost of explosives spent per tonne of rock removed; minimising blast-induced vibration and air overpressure; avoidance of flyrock and vibration damage to nearby structures.

Until recently the predominant aims of research into aspects blasting and were primarily undertaken to control blast-induced vibration and in particular to limit the ground movement by measuring peak particle velocity at some remote location.

The analysis of the vibration time series is commonly used as a predictive tool to adjust the blast-timing sequence and the MIC.

2.10 Identifying and managing misfires

Procedures to identify whether a blast has fired successfully vary from country to country: Generally the shot-firer or mine captain is the legally designated person responsible for conducting the post-blast inspection in order to determine the state of the tunnel or mine and establish whether work may proceed. Multiple hazards could be present not only from unfired explosive material, but also from toxic products of detonation in the air; unstable rock structures in the tunnel roof, walls and the blast face. Each of these possibilities will be assessed by a visually inspection.

Evidence of a misfire in particular is derived from the rock fragmentation, traces of the explosive rounds; initiation products such as detonators, detonating cord; inadequate rock movement; poor fragmentation, unusual sounds, or vibration traces.

With the exception of finding actual detonators, none of the other indicators in themselves conclusively confirm that a misfire has occurred which consequently introduces a degree of uncertainty into correctly assessing whether the blast area is safe, or otherwise. In addition, if a significant amount of noxious fumes have been created, as can happen when blasting with poorly mixed ANFO, it may be some time before the area can be safely inspected.

Blast holes can fail completely, or partially fire. Partially initiated charges occur for a number of reasons. There is the potential that detonation of the main column charge could have been incomplete due to sympathetic detonation from a neighbouring charge. Other circumstances could leave its detonator unfired which would becoming an operational hazard. Detonators are especially susceptible to initiation from any source of heat, shock, or vibration arising from handling, transporting, or processing of the fragmented rock.

A variety of methods to establish whether or not each individual detonator in a round has successfully fired has been investigated in this research. Previous literature relating in particular to blast induced vibration analysis has focused on the reduction of unwanted vibration released into the area surrounding the blast site through improved blast design. The need to design 'blast initiation sequences that minimise the energy being dumped into sensitive structures' in their resonant frequency bands was highlighted by Armstrong L.W (2000). Methods that predict and model blast-induced vibration have typically concentrated on avoiding damage to the built and natural environment; and the consequential avoidance of litigation. Both Siskind, (1980) and Dowding, (1985) have shown with reference to the built environment, that buildings can withstand certain levels of vibration loading, but it is a combination of the peak vibration levels; the frequency content of the vibration and the duration of the vibration acting on the structures that determine any detrimental impact on nearby structures.

2.11 Misfires causes and modes of failure

Despite the introduction safer more reliable detonators, initiation methods and programmable systems, misfires still occur. They can be manifest as a partial or complete misfire and depending on the cause the implications vary for the construction engineer.

Hopler R., (2006) highlighted that a misfire can result from a failure of the explosives themselves, or of the blast control accessories. The twelve of the most common recognised causes of misfire Energy, (2013) are:

1. Poor wire/tubing connections (corrosion, dirt)
2. Bare splices on the ground, lying in water or wet areas
3. Improper detonator circuit
4. Improperly balanced detonator circuit
5. Current leakage in electrical systems or damaged tubing in non-electric systems
6. Mixing detonators from different manufacturers in the same blast
7. Detonators not wired or connected into the circuit
8. Defective or inadequate firing line
9. Inadequate power supply to fire electrical systems
10. Improperly made primers
11. Using non-water resistant explosives in wet holes
12. Improper loading practices

The causes described above all directly affect the detonator itself. Other effects impact the column charge such as when a primer detonates, but doesn't not initiate a portion of the column. These misfires are often attributed to ground movement cut-offs, inadequate priming, deteriorated explosives, or bridged charges in the borehole where one cartridge fails to initiate. Inadequate training is a significant factor that leads to misfires if the initiation system is poorly installed. Unexpected ground movement during the blast also leads to misfires. The causes and outcomes are so numerous such that unconnected detonators are sometimes mistaken for misfires. Some of these influencing factors listed in Table 3 are outlined here in more detail.

Table 3 Misfire Contributing Factors

Product Failure	Detonator Failure	Human factors
Explosive malfunction	cut-off / column charge damage	Poorly designed Blast
Desensitised explosives	poor rock movement	wrong combination of initiation techniques
Sympathetic detonation	poor delay set-up	inadequate priming
Detonator malfunction	Geological features	collaring errors
Nonel bunch connectors	Dead pressing	drilling errors
Blast-pressure damage to detonators	Water ingress	stemming errors
physical composition of charges		

2.11.1 Detonator Damage

The greatest cause for concern is the where a detonator has failed and a detonator and primer combination remain buried, undetected in the muck pile. This is the most dangerous situation as detonators and primers are sensitive to initiation by shock, heat and friction.

Detonators themselves can be damaged by pressure waves from adjacent holes firing. In this case even when the initiation has worked perfectly, the detonator and consequently the primer and column charge can fail.

2.11.2 Open circuits and damaged control lines

These types of failure afflict electrical and electronic detonator systems and should be discovered prior to blast initiation. Electrical continuity checks will detect and isolate the cause of an electrical short very quickly.

Shock tube systems are very reliable. Second-man checks should identify poorly assembled shock tube bundles and potential spots where shrapnel from one detonator could cut the control lines leading to a second. By loosely burying any surface detonators this problem is generally eliminated.

2.11.3 Explosive desensitising

Commonly used bulk explosives such as site sensitised emulsions, slurries and ANFO owe their ability to support a rapid explosive reaction to the physical density of the explosive compounds. When the material is too dense, the desired chemical reaction is not self-sustaining, but if the density of the material is artificially lowered by the introduction of air bubbles for example, the chemical reaction can propagate through the material. Most explosives are mixed on site and made sensitive in situ often by generating gas bubbles in the mixture and, like dough rising in the oven, the column charge rises in the charge hole until it reaches the critical dense state where it is sensitive to shock and an explosive reaction can propagate through the column charge. Anything that results in an increase in the density of the explosive mixture, even a transient event, will supress or in some case eliminate the explosive properties of that substance.

2.11.4 Dead pressing

ANFO is the classic example of a bulk explosive that can permanently lose its ability to detonate when it has been subjected to a significant shock wave typically from an adjacent firing hole EPC (2010) which results in a permanently change the material density. When this happens even though its own initiating detonator/primer may well have fired the subsequent shock wave cannot trigger the column charge as the composition of the bulk explosive has be permanently affected.

2.11.5 Shock desensitisation

When the explosive in a blast hole detonates a severe shock wave passes into the surrounding rock causing an inelastic response and resulting in fragmentation close to the blast hole. This shock wave then spreads out into the surrounding rock interacting with free-faces and other blast holes. As the wave passes through unfired explosive it causes gas bubble compression causing a transient increase in density which reduces the explosive sensitivity. However, after a few tens of milliseconds, the bubbles expand again and the full sensitivity of the product is returned. However, if its primer is initiated whilst the gas compression is still happening, then the column charge can fail.

Since the magnitude of the shock wave attenuates with distance, the shorter the spacing between charges, the higher the risk of desensitisation misfires becomes and will be more likely to occur in closely spaced charge patterns, such as those found in tunnelling operations.

2.11.6 Cut-off misfires

During a detonation a large volume of high-pressure gas is produced. This gas migrates into the surrounding rock through natural rock faults and blast-induced fissures causing them to open and extend. It is possible for such gas to migrate for a considerable distance through the rock. If the gas penetrates into a hole that has yet to fire it can compress the explosive reducing its sensitivity.

In such cases, it is also likely that the gas will disrupt the explosive column, which can also lead to an in-hole and cut-off misfires. There is a greatly enhanced risk when firing in broken, fissured or soft ground where a ready path for the expanding gas from an explosion to penetrate into neighbouring holes.

Long detonation delays between blasts also give more time for cracks and fissures to develop. Long delays are also common in tunnelling situations e.g. 200-500 ms or more. In surface applications typically inter-charge delays of 18-42 ms are typical.

2.11.7 Risk factors contributing to misfire

If any one of the factors below is present, then the risk of desensitisation increases. If two or more are present, then a detailed assessment of the situation should be undertaken.

Shock Desensitisation is likely where there are combinations of:

- Long detonator delays
- Small burden/spacing buffer
- Lack of free-faces
- Overburdened holes
- Water-logged ground
- Gas desensitisation / hole disruption

2.11.8 Recognising and handling misfires

The current practice to determine whether a misfire has occurred relies on visual inspection of the blast face. Most national regulatory bodies require the blast area to be inspected by a competent person, after firing a round. They are required to carry out a thorough examination of the tunnel face to ensure that all the charges have fired and that there is no indication of a misfire.

Environmental indications of a misfire can include noxious fumes, inadequate ground movement, poor fragmentation, unusual blast sound or vibration trace, excessive flyrock or physical evidence of undetonated explosives.

Unexploded emulsions and slurries can be readily dealt with by flushing out with water. However, residue from detonators, cast primers and detcord all present an immediate hazard. Explosive material could still be present in the newly exposed face, in the muck pile or at the processing plant.

Dealing with a misfire is arguably the most dangerous activity that site managers and shot firers will be involved in during blasting operations. Charge remnants could be detonated if subjected to shock, heat or

friction; such as being drilled into, struck by an excavator bucket, load wheels, or if inadvertently fed through a crushing plant. Unexploded charges may also be accidentally taken off site in road vehicles or to site tips. In any of these circumstances there may be a risk of danger to the operator or to the public, particularly from flyrock in the event of a detonation.

Unexploded charges may need to re-fired or be recovered by hand. All those likely to be involved must realise that this is a potentially dangerous operation due to the numbers of unknown factors present. Great care and attention to detail is required to ensure that this is carried out safely.

Having a clear indication that a misfire has occurred, and the most likely location of the misfired hole, would enhance levels of safety and improve production efficiency.

In general buried explosive material following a tunnel blast could be inadvertently initiated by down-stream operations. Since most explosives are generally susceptible to mechanical handling that results in shock, vibration and heat being delivered to the explosive material; such as digging out, transporting, milling, crushing during transportation.

2.12 Implications of misfires on tunnelling operations

The effects of misfires fall into two main categories: safety hazards and operational impacts. Publicly listed mining companies are being increasingly held accountable by their shareholders and most are now aiming for a ‘zero harm’ philosophy when approaching Health and Safety. The majority of injuries in heavy industry occur when there is a deviation from agreed procedures, and when dealing with irregular occurrences. Misfires, when recognised, certainly fall into both categories.

2.13 Consequential losses resulting from misfires

Misfires resulting in accidents with injuries, fatalities and/or equipment damage involve obvious costs and these vary from one site to another. Depending on where in the round a misfire occurs, will also have an impact on the subsequent blasts.

Uncontrolled blasts can result in tunnel damage, destabilised zones around the blast area, excessive blast induced vibration and flyrock damage to the tunnel or to personnel.

In addition to the potential for injury to personnel, misfire events can result in a variety of consequential losses:

- Cost of time investigating/inspecting the blast zone following a misfire event
- Direct cost in additional drilling, explosives, primers, detonators and labour
- Operational cost as failure of cut hole(s) could result in the loss of the entire round

- Dealing with over-sized boulders requiring secondary breaking
- Increased digging time and greater wear and damage to equipment results in lower productivity and higher maintenance costs
- Haulage vehicles travelling over rough terrain as result of excessive rock throw
- Misfiring of one hole will increase the burden on another hole causing cratering, excessive over-break
- Flyrock causing injury and damage to property outside the designated blast area
- Uncontrolled, excessive vibration levels which could lead to litigation from external claims.
- Overbreak at tunnel profile could result in ground control problems and the need for additional ground support

It is evident that the potential consequences of a misfire could affect most aspects of subsequent tunnelling processes, therefore every reasonable and practicable measure available to blast engineers should be taken to avoid its occurrence Verakis, (2002)

2.14 Blast design, vibration prediction and modelling

The magnitude of the seismic signal generated by a blast is dependent on a broad number of parameters, some of which are controlled by the blast engineer and some are dependent on the performance of the blast. Table 4 outlines the set-up variables determined by the engineer. The interaction of the blast arrangement and the rock will result in variable vibration levels, rock fragmentation size, ejected rock volume and the throw of the ejected rock.

Table 4 Blast set-up variables affecting blast characteristics

Set-up Parameters
Hole diameter
Hole length
Hole location
Deviation of hole position / drilling direction
Charge weight per hole
Stemming
Explosive type and properties
Selection of detonator type and timing delays

Detonator timing accuracy
Rock type and local geology

From work carried out by Adderley, (2009) in the Holman test mine and Olson (1972) other granite mines a dominant characteristic frequency content of that geology was expected around 200 - 300 Hz. Olson's tests were conducted using an MIC of 1.7 kg at a range of 60 m from the blast zone.

As this thesis is concerned with blast misfire detection and location and not modelling potential building damage, the work did not focus on earlier vibration reduction investigations Anderson, (2008), rather on blast vibration characterisation.

2.15 Seismic wave generation mechanism

As a confined explosive is detonated in a hole the resulting rapid chemical reaction generates increased volume of gas and heat creating a quasi-instantaneous pressure build-up. As the explosive material oxidises the gas produced expands to fill the bore-hole volume and exerts a pressure shock into the rock that crushes and fractures the surrounding rock.

Inside the blast hole column charge detonation is initiated at the blind end of the hole by the detonation placed around 2 m away from the free face of the rock. The detonation locally initiates the column charge which then travels from the detonator along the full length of the charge. The pressure induced by the rapidly expanding gases, that are the product of detonation, is referred to as the 'Detonation Pressure Front'. The nature of this pressure front depends on the chemical composition of the explosive; its density; velocity of detonation; quality of the confinement and the nature of the rock mass. Dowding, (1985) described the process continuing as the newly formed explosive gases formed at the detonation front continue to expand into the increasing numbers of voids created by the crushing and fracturing of the rock. This explosive gas pressure acts to propagate the formation of fissures produced by the shock wave front. The explosive gas pressure is maintained until the fractures reach the free face at which time the rock is ejected. The expanding gases also provide the energy to expel the fragmenting rock out of the free face.

The VoD describes how fast the detonation front travels along the column length, this velocity can range from 3000 to 7000 m/s. As distances increase away from the excitation the explosive reaction no longer produces fractures and splitting of the rock, but the rock is subjected to elastic acoustic waves that radiate away from the blast site Liu (1993).

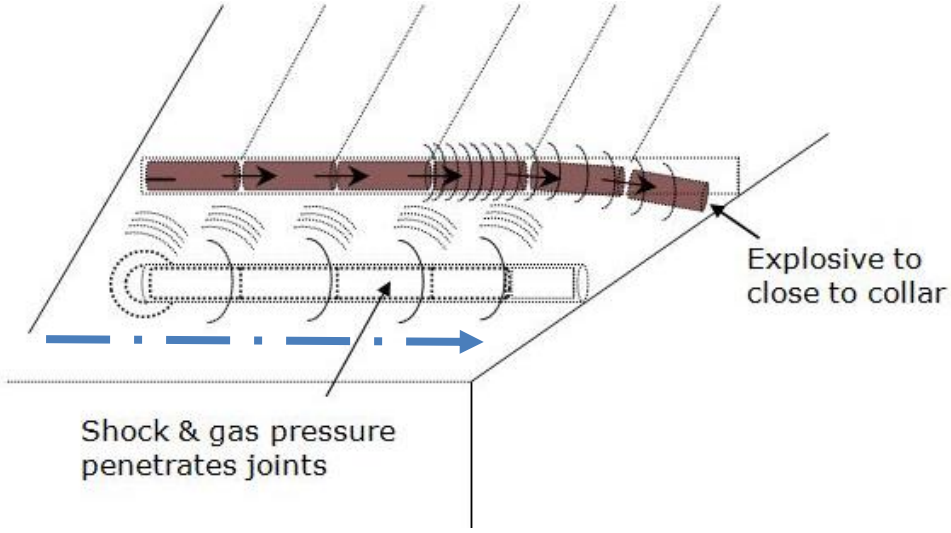

Figure 11 Detonation Pressure Front. Adapted from Revey (1996)

Revey, (1996) described the process of gas expansion in the blast hole penetrating into and expanding fissures and thereby fracturing the rock. Figure 11 indicates the direction of explosive reaction and the potential effect on adjacent blast holes. In the illustration in Figure 11 a partial misfire is depicted at a section where explosive material is ejected from the blast hole before it can fire. The wave train interacts with all of the facets of the rock mass and will experience reflection, refraction and damping by changes in rock density, bedding planes, fractures, presence of water, voids etc. Propagating waves will experience modifications as the wave radiates through the rock. The elastic motion of the media will have a spatial and a time dependency as groups of waves arriving from a multitude of paths will combine constructively or destructively. Anderson, (2008) asserts that the local geology is the primary factor affecting the final wave form amplitude and spectral content.

In the context of tunnelling, rock is inhomogeneous with multiple planar free surfaces (i.e. the blast face, tunnel walls, faults and facets within the rock) which introduce non-isotropic radiation patterns. McLaughlin, Bonner et al., (2004) observed surface quarry blasts from a distance of 2 km and in particular the azimuthal radiation patterns in the frequency band of 0.2–3 Hz. Their primary interest was in the relationship of the Rayleigh and Love waves Nazarchuk, (2017) as being diagnostic for non-isotropic radiation from quarry blasts. Observations show that the Love and Rayleigh wave radiation patterns depend upon the orientation of the quarry benches. They postulate that two possible mechanisms for non-isotropic radiation are (1) the lateral throw of spalled material (i.e. the ejection of fragmented rock) and (2) the presence of the topographic bench in the quarry. The spall of material from surface bench blasting can be modelled by vertical and horizontal forces applied to the free surface with time functions proportional to the derivative of the momentum of the spalled material with an average ballistic velocity of 2–5 m /s to provide sufficient impulse to generate the observed Love waves at the surface. In tunnelling the source will be in the elastic media, but the observation point will typically be at the surface (within the tunnel) on the ceiling or wall mounted transducers. In addition at close range the frequency band will be broader, up to 200 Hz.

Spathis, (2010) outlined a method of estimating the attenuation of blast induced vibration in rock masses. They established that any seismic pulse may be subject to spurious delayed reflectors and wave conversions. However, for all cases the onset of the pulse was observed to be free of any other arrivals and so it was reasonable to assume the rise time measured was due to a compressive, longitudinal P-wave propagating on the most direct path from impulse source to receiver.

2.15.1 Peak particle velocity control

As a guide engineers designing a tunnel blast the concept of the Scaled Distance (SD) was introduced Energy, (2013). The SD is an arbitrary ratio of the distance between the blast site and a point of interest (like a surface building) and the amount of explosives used per shot fired. The SD is defined as:

$$SD = D/\sqrt{m} \qquad (1)$$

Where SD is the scaled distance, **D** is the measured distance between two points and **m** is the mass in kg of explosives per hole.

In the early eighties varying the MIC was the primary technique available to blasting engineers to control the Peak Particle Velocity (PPV) and maintain it below the legal limits at the required point of measurement Anderson, (2008). The measurement location would typically be at the homes of some sensitive resident in the locality of the construction site, or mine.

The SD relates the PPV to the distance between the blast and measurement point and the weight of the explosive charge used.

$$SD = D\ /\sqrt{m} \qquad (2)$$

$$PPV = A \times SD^{-\beta} \qquad (3)$$

Where A and β are site specific constants that typically do not vary a lot from one site to another Anderson, (2008). The great limitation to this method has been the necessary assumption that each of the column charges in a blast sequence are identical, disregarding the variation in explosive strength, or how the shots interact with the rock mass. The technique assumes that distance is the only parameter that will affect the resultant PPV value.

2.15.2 Signature hole method

As discussed in 2.15.1 the duration of the blast vibration and its frequency content are not addressed by the SD and since these parameters had been identified in both damage to buildings and for causing distress to building occupants a second technique called the Signature Hole Method (SHM) addressed these deficiencies. Anderson, (2008) examined the progress of the SHM specifically in the light of improvements in detonator technologies.

The SHM is a more effective tool for estimating the PPV as it utilises a single “signature” blast, with a representative mass of explosive material to be fired near the tunnel face. The underlying principle for the SHM is that each shot in a blast sequence will generate essentially the same vibration at a given remote location. In effect, this assumes that each hole is detonated at the same location, so that the path travelled by the waves is identical. In addition it assumes that all holes have the same explosive charge type, weight and that each shot hole will be identically prepared to produce the same explosive-rock interaction as the signature shot, so that the blast induced impulse will be the same.

When the signature hole shot is fired in isolation the induced vibration signature is recorded at the point of interest which is incorporated into commercial software to extrapolate the to the probable outcome from multiple charges will produce given their allocated timing delays. The PPV estimates are more accurate since a physical representative test shot is fired and the transfer characteristics of the natural rock are measured then modelled in accordance with the blast design.

2.15.3 Limitations of the signature-hole method for misfire identification

The primary intent of the SHM is to control the PPV at a remote point of interest by varying MIC and the timing delays. As such, it necessitates measuring blast vibration in the far field where the vibration amplitude and frequency composition have been considerably changed by the intervening rock mass. This method does not include information that could be post processed to identify the location of an individual shot.

Anderson, (2008) established that detonating a charge in a signature-hole close to the intended blast zone could generate a characteristic blast vibration pattern which could be monitored at key locations of interest. These measurements can then be used to build a predictive model. The measured waveforms are combined with a variety of detonation timing delays with the intent of finding timings that result in destructive interference of the blast vibrations at the target locations.

This method has had limited value because in order to be effective it requires precise control of detonator firing time delays to produce the desired destructive interference at the remote point of interest. Detonator timing delay variability meant that control over the PPV could not be guaranteed. It is worth noting that timing inaccuracy is often not the sole cause of poor blasts EPC (2010) . In-hole explosives performance was shown by Kortnik J (2010) to be dependent on drilling spacing accuracy, loading control and maintaining consistent rock burden all of which affect blast results to a far greater degree than just scatter in delay firing times. These factors have to be controlled first before we can hope to derive the maximum benefit out of advances in PED timing precision.

Continued technological improvement of PED by manufacturers such as the EPC Groupe and Orex has resulted in improving the timing precision and accuracy with timing variations of less than 1 ms widely available. These developments are making the SHM more attractive for controlling blast induced vibration.

2.15.4 Efficient blast design and environmental impact

In the 1980s the US Bureau of Mines commissioned research that resulted in the adoption of the Z-curve Siskind D.E., (1986). This relates the particle velocity as a function of frequency. According to the Z curve, any ground vibration (the peak particle velocity or PPV) produced by a mining operation above the solid line will generate damage to the structures. If the PPV is below the line, the safety of the structure without damage is assured. Another important concept as per the Z curve is that the mining operations can operate at higher PPV values if the generated blast vibration is composed of a high-frequency content. Siskind, (1980)

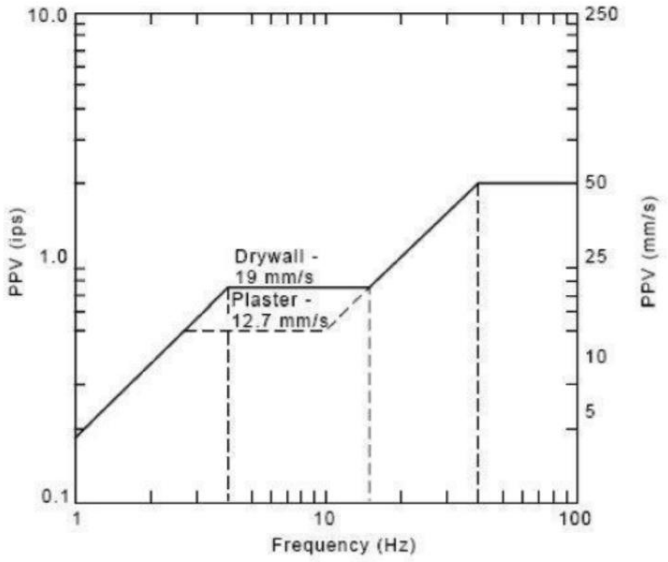

Figure 12 Example of the Z-Curve relating ground vibration frequency and particle velocity

It was at this stage in the research that detonator delay time precision and repeatability described earlier, came into sharp focus. Underpinning the signature-hole method is the assumption that each hole in a blast round will generate very similar vibration patterns at any given remote location as a consequence of local geology and type of explosives employed. It assumes:

- Each hole will fire precisely at the designated timing delay
- All holes are detonated at the same location, therefore the path travelled by the waves is identical.
- All holes have the same explosive charge type and weight
- All holes have the same explosive/rock interaction, therefore the source impulse is the same.

It is self-evident that none of these assumptions can be achieved in practice. However, if the distance from the blast source to the measurement position is large with respect to the area of the blast, then it has been suggested that the assumptions hold with sufficient accuracy to be useful in practice Anderson, (2008).

Once a single signature-hole blast has been recorded, the method uses time-lagged linear superposition to estimate the effect of sequential blasts at the chosen measurement sites.

The contribution from each hole is estimated then the second stage estimates the combined contribution from all the holes planned for that round. The projected timings (within the range of practical, commercially available delays) which are expected to result in the minimum PPV and are then programmed into the blast sequence.

2.15.5 Utilisation of Blast-Induced Vibration

Work to modify the frequency content from blasting is recorded by Thoenen, (1942) followed by a period of consistent studies in the 1980s by Anderson, (2008) Andrews A.B., (1981), Crenwelge O.E., (1988), Hinzen K.G., (1987). Lack of progress was attributed to the inaccuracy of available detonators at that time. There was however a desire to develop an approach that adequately controlled vibration frequency content below 30 Hz since it was these low frequencies that generated most annoyance to building occupants. Furthermore, most buildings tended to resonated at around 12 Hz and were therefore susceptible to damage from vibration containing these frequencies. Anderson, (2008)

Mishra, (2017) showed that there were small differences in vibration wave forms from shot to shot within a blast round and that 'spectra derived from linear superposition matched those predicted, but peak levels are not adequately matched.'

Investigations relating specifically to tunnelling (rather than surface mining) were carried out by Murashita, (1998) where the standard techniques used did not always require a sequence of individual holes being fired, but on occasion there was a necessity for groups of holes to be fired 'together'. At that time engineers were not trying to achieve an instantaneous detonation of multiple holes in practice. Although groups of holes were fired on the same delay (at the same nominal time) in practice, given the limited maturity of technological development of detonators at the time, the inherent inaccuracies of detonator timing was relied upon to give a tight distribution of the effective detonation timing of the group of charges.

PEDs are moving the SHM into a new era since the variability in delay times has become negligible in practice. As a consequence of modern PED timing precision, engineers now have to deliberately create a spread of timing delays to prevent multiple holes firing simultaneously in smooth wall blasting for example where as in the past, the lack of precision could be beneficial to the blasting process, but hampered the control of undesirable blast induced vibration.

The three identifiable stages of a blast are:

- Detonation of the explosive which produced the shock wave and gas pressure inside the bore-hole.
- Interaction of the shockwave with the rock mass, fragmenting some of the rock
- Propagation of the energy not used to fragment the rock as elastic waves.

The characteristic vibration, its amplitude, frequency, content duration etc. all result from the explosive energy released from each hole, their relative timings, reflections and refractions as the waves propagate away from the points of initiation and interacting constructively or destructively at any particular point along the path.

We have stated that the superposition of multiple, time-delayed signature-hole blast wave forms have been used to predict PPV levels at distant positions. Convolution of functional signals and signature-hole waves Anderson D.A., (2008) offers the example in Figure 13 shows a firing timing sequence on delays of 50 ms, combined with a signature-hole blast vibration Figure 14.

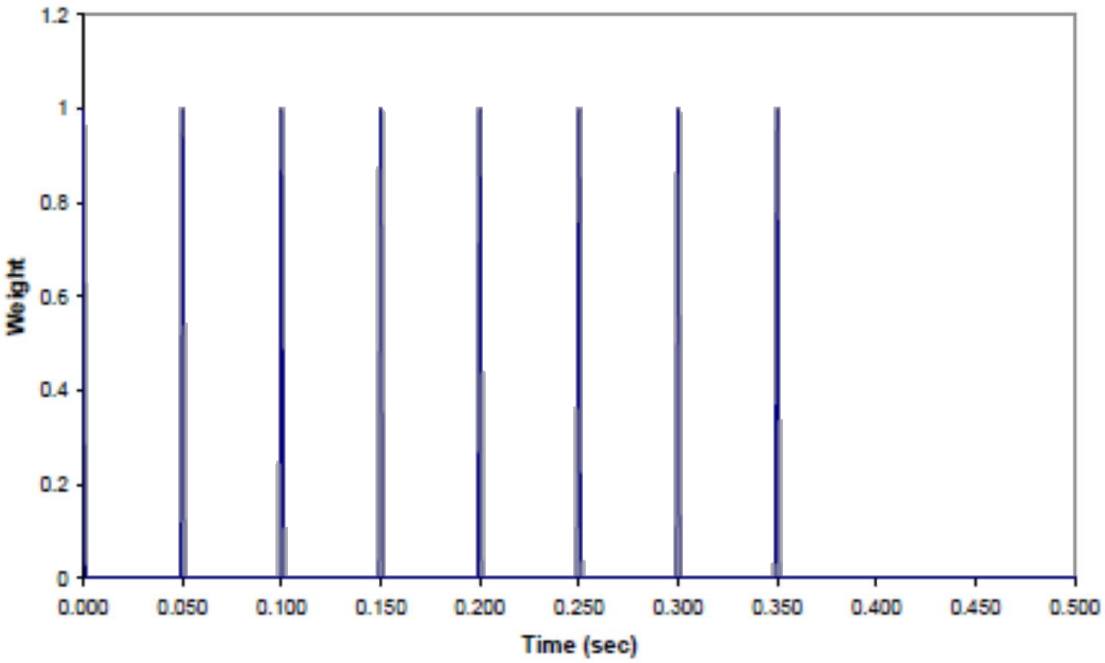

Figure 13 Selected detonator delay times with 50 ms delay

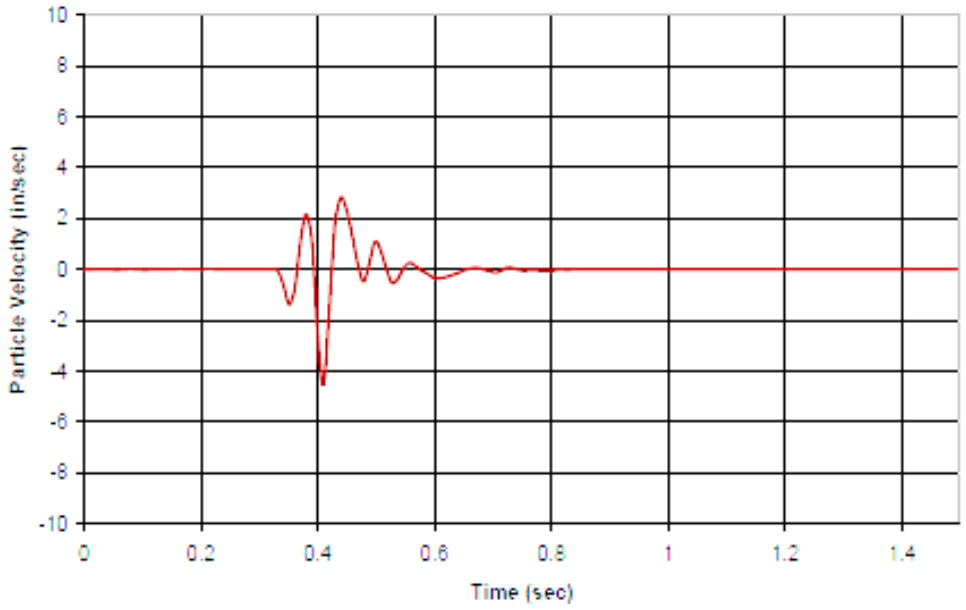

Figure 14 Signature-hole vibration

The resultant waveform is shown in Figure 15 showing the convolution of the two functions with an timing-optimised PPV. In this example, Figure 14 shows a PPV of approximately 3 in/sec. The chosen timing delays of 50 ms between charges results in the trace shown in Figure 15 where the peak is higher than recorded by the individual shot used for the SHM, However, in a blast comprising of multiple individual shots, these shots have to work together and consequently there is a trade off between minimising the PPV and effectively removing rock, hence Figure 15 is displaying the best possible outcome.

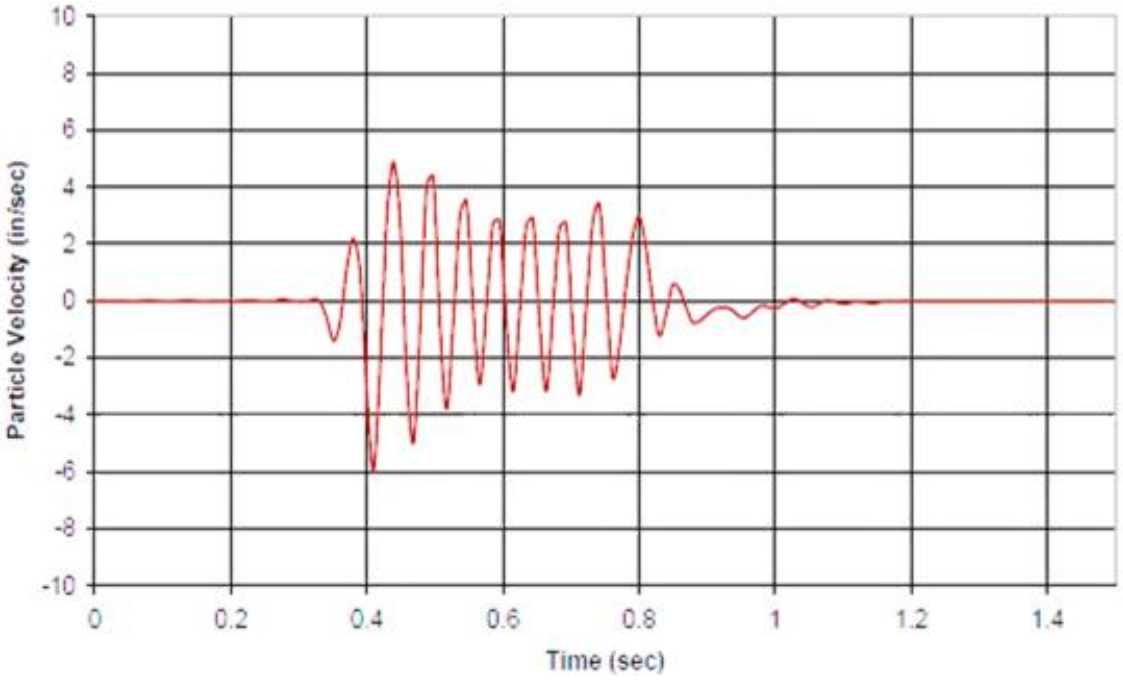

Figure 15 Expected resultant vibration using SHM

The flexibility of this approach is that the comb filter can be used to simulate a variety of possible firing delays which then generates a model of the relative contributions of those timings. The comb filter can be set up to have values at any level between zero and one to weight individual shots with different charge weights. This may be advantageous if it is known that any one borehole will have more or less rock burden relative to the others, or will require more or less explosive charge.

As a predictive method, the SHM still relies on the assumption that the signature-hole will be representative for the contribution from all successive blast holes. It does however have value in that the signature blast vibrations are measured at, or very close to, points of interest i.e. at sensitive locations such as a residential site, or public space. The technique as currently used is applicable in the far field, i.e. where the vibration sources appear to originate from a single point source.

Applying the technique in the near field to differentiate between point sources had not been investigated previously, but the technique would not permit the individual paths to be reconstructed to identify the point of origin of the original impulse. Alone, this technique cannot be used to identify misfires.

Chapter 3 Misfire Detection Investigation

3.1 Initial approaches to misfire detection

The scope of the specification of a misfire alert system, or methodology requires that the probability of detection of a misfire would be as high as practically possible and the false alarm rate low. The essential criteria can be classified as:

- Functional: the solution must work and the results trustworthy.
- Available: for the duration of the blast sequence the system must remain fully operable
- Reliable: the system should have a high mean time to failure and robust enough for handling and set-up in tunnelling/mining conditions.
- Survivable: In the course of a blast it must withstand the extreme physical conditions.
- Practical: In the context of tunnelling and mining the chosen system would need to be acceptable to the users and be cost effective.

Addressing the hazard of misfires can be done at all stages of the blast preparation and loading cycle. Given that the causes of misfires are not solely due to hardware faults caution should be exercised during preparation and careful adherence to procedures during installation; monitoring during a blast and inspection post blast all aim to make the process safe. Preventing, predicting, detecting and locating misfires are possible Farnfield, (2012).

Safe operating procedures have been developed and institutionalised in legislation and regulation as described in Chapter 2. Related competency training to handle and prepare explosives safely are mandatory in most countries. Checking for firing circuit continuity and poorly connected initiation equipment is a small part of safe operating procedures. All of the newer electronic blast initiation systems such as the Hot Shot system manufactured by Dyno Nobel and used at the Camborne School of Mines (CSM) virtually eliminate the potential for misfires due to product failures and connection errors. The detonator control system positively checks that each component is functional against a plan and the control system prevents the round being

initiated if a fault is detected. However, all of the other factors that could contribute to a misfire are still present. Electronic systems prevent blast initiation if a technical failure has been identified, but they do not provide information on detonators malfunctioning arising from blast damage caused once the initiation sequence has begun. None of the blast initiation systems currently available can detect and advise of a fault that develops during the blast itself.

Detection of possible misfires following initiation and commencement of detonation sequence is problematic: primarily due to the rapid and violent release of energy and the inherent danger of flyrock and spalling in the vicinity of the blast.

3.2 Investigation into misfire detection

Several early approaches to assess the outcome of a fired shot were considered when defining the scope of this research and a few were investigated. The monitoring techniques can be divided into intra-borehole sacrificial sensors/indicators and remote sensing. In principle for intra-borehole monitoring multiple sensor options were technically plausible with the aim of utilising the effects of the blast process. Observing parameters such as EM emissions, thermal signatures, light emission and in-hole pressure increases were considered.

In this thesis the principal methods trialled to obtain a detonation confirmation signal from shots in the blast face were fibre optics and nonel (shock tube) systems.

3.3 Transducers and sensors

The requirement for a transducer based system is to deliver a reliable signal from the blast face back to an observation point. The initial scope and detection function were straight forward and a wide choice of sensor candidates was available from simple twisted pairs of wires; low cost optical fibres; photodiodes etc. These approaches were tried during the course of this research and functioned well for individual shots.

For a full face blast with multiple shots, each on different firing times (delays), with the shots fired sequentially and for 100-plus individually charged holes the cumulative delay between the first and last charge being fired

could range between 2 - 5 seconds (if there are hundreds of charges being fired). The challenge for all of these 'return-line' concepts was how to ensure that the signal lines for shots firing later in the sequence could survive long enough to carry their signal to the monitoring station.

3.4 RFID Tags

Radio Frequency Identification Tags (RFID Tags) can be made robust enough to survive extreme handling. Tags are used in the metalliferous mines to designate batches of mineral ore following an inspection of the blast and to identify the provenance of ore batches as they are transported on a conveyor belt for post processing. In these mines RFID tags are programmed with the details of the location and time the ore was blasted and then deliberately introduced onto ore piles. The material is then transported by conveyor belt. The belt conveyor is ringed by RFID tag readers in several locations to optimise the chances of detecting and interrogating the tag as it passes by on the way to the crushing plant or for other treatments. The RFID tags are used in these downstream processes to identify the provenance of the ore as it arrives at preparation plant to optimise the systems settings.

Some blast control techniques include embedding solid steel markers with the explosive stemming. Post-blast, a physical search is conducted to find the uniquely identifiable markers. Knowing where they were initially placed in the blast sequence and knowing where they ended up, informs the preparation of the next blast design.

With both of these approaches, there is an inherent risk that a tag or marker could survive a misfire but become damaged enough, or sufficiently buried, or immersed in water and remain undetected.

Consideration was given to placing RFID tags in the charge hole adjacent to the detonator assembly. If a misfire occurred the assumption would be that the RFID tag would survive intact and locating the tag would enable the detonator to be found. The inspection procedure would include scanning the rock pile for the RFID tag during the post blast inspection.

Long range RFID tags are readily available. The costs are around US$ 20 each. Although this cost does not appear high, it would significantly add to the cost of the explosives and initiation system. These marginal cost increases could quickly scale up to an increase of US$ 2,000 per blast sequence.

Trials conducted at the Holman test mine during routine blasting demonstrated a number of technical drawbacks with this approach.

- The conditions underground were always wet. One of the blast design aims is not to allow the rock to be thrown far from the face, hence it will ideally fall in a heap. A misfire tag could readily be covered by substantial quantities of wet rock.
- There was the potential for the RFID tag itself to be physically damaged by high pressure gases ingress through fissures generated by adjacent shots firing.
- Damage to the RFID tag could also arise from flyrock.

For these reasons, the RFID tag approach was rejected.

3.5 Tracers and markers

Tracers and markers have been used in mining applications for some time Thornton, (2005). Although markers are used in surface blasting to give an indication of rock movement, they are normally constructed from solid steel in order to withstand the blast. We needed something that would be consumed during a successful detonation but survive an adjacent shot firing.

Placing tubes containing a high visibility dye and one with aluminium foil beside the detonator was tried. Neither approach was practical after multiple shots unless a misfired shot was near the top of the face.

The following sensor/communication combinations were considered to confirm the success or failure of a detonation event:

Table 5 Initial approaches to detonator firing detection

Classification	Technology	Concept
Tag / marker	Chemical dye	Chemical dye markers designed to be destroyed by a blast, but survives if charge fails to fire.
Tag / marker	RFID tag (wireless)	RFID tag collocated with the detonator to be destroyed if the explosive charge fires correctly, but made to survive a blast from an adjacent hole.
Physical return signal	Signal wire	Simple resistive monitoring of a twisted pair of wires from a safe observation point. The wires effectively act as a fuse.
Physical return signal	Wired transducer	Pressure transducers /thermocouples / PIN photodiodes etc with a return signal wire to a safe observation point.
Physical return signal	Optical fibre	Optical fibre inside the charge hole, leading back to an observation point. Could conceivably provide insight into a successful blast initiation; blast duration plus velocity of detonation.
Physical return signal	Shock tube	Shock tube placed inside the charge hole leading back to an observation point.
Remote monitoring	Radio EM detection	Detection of the electromagnetic pulse generated by the blast process.
Remote monitoring	Impulse response / vibration analysis	Vibration conducted through the strata will propagate for many hundreds of metres and can be monitored at a safe remote location.

Each of the methods above could potentially provide a reliable indication of the status of a detonation event.

All of the eight candidate methodologies were finally rejected. Each approach was prone to generate either false positive or false negative outcomes when in relation to the physical condition of the detonator in particular. A detonator failure could either be missed all together; or a false result produced due to events other than a detonator failure.

3.5.1 Conclusions

In discussion with mining engineers both methods (but markers in general) did not promise reliable outcomes. Fundamentally both types could be buried completely either blocking the RF signal, or covering over metallic or chemical markers. If the intention is to ensure that no unfired detonators are present, neither method would fulfil the misfire detection system scope. It is accepted that they would both improve the probability of misfire detection in the right direction, but neither would solve the issue.

Further investigation into the use of tags and markers was abandoned.

3.6 Optical fibres

In preference to other sensor options optical fibres were selected for trial. The fibres can be monitored actively by transmitting a series of pulses into the fibre and by monitoring the flight time of an optical pulse reflected off the end of the fibre, the fibre length can be calculated. Alternatively the fibre can be used passively to capture light generated by the detonation event and transmit it reliably to a PIN photo diode detector at a remote monitoring site. The PIN photodiode receives the light pulse and converts it into an electrical signal.

Fibre optics have an initial attraction in that they are a passive medium. They are used in similar hazardous-event-sensing as ‘arch flash detectors’ in high voltage system monitoring where a loop of un-shielded optical fibre captures the flash of light created as an electrical discharge arc occurs. The light detected using the fibre trips the electrical generation system ABB, (2015).

In our case, we used the fibre as a passive light capture system, detecting any light generated by the detonation within the boreholes which were approximately 3 m deep. The optical fibres tried were both standard telecom plastic multi-mode fibres and glass core multi-mode fibres. Fibres were inserted fully into the back of the borehole to give us, in effect, a 3 m long sensor to capture the event. Two approaches were trialled in the initial stages of this research. Multiple fibres were coupled to a single receiver and then to individually assigned PIN photodiode receivers. The initial test setup comprised of a low cost multi-mode fibre which comes supplied with a protective opaque outer sheath. At the outset it was uncertain whether any preparation of the fibre would be necessary. The expectation was that any successful firing of the detonator would generate a flash of light that would be coupled into the fibre and carried to the receiver.

3.6.1 Optical fibre test set up

The test set up comprised of non-electric detonators being initiated via shock tubes, collocated with the optical fibres. In this controlled environment where individual detonators are fired, the blast outcome was self-evident for single shots. The fibre optic receiver was built by the Optical fibre lab at the University of Southampton and the analogue data acquisition system provided by CSM.

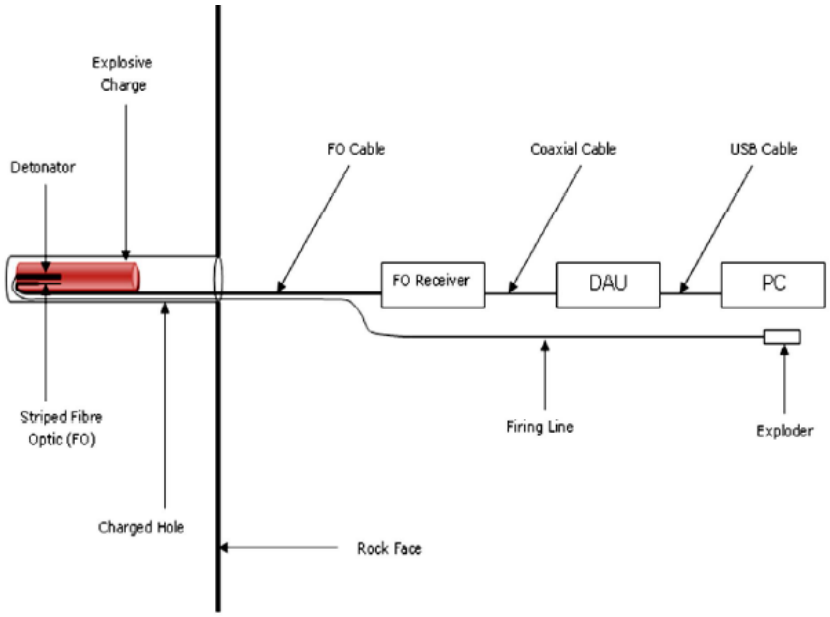

Figure 16 Schematic of test set-up for monitoring optical signals with single channel fibre optic Ewusi, (2013)

During set-up, detection was tested firing sparks/camera flashes close to the detecting end of the fibre, prior to loading the fibre/explosive assembly in the test holes.

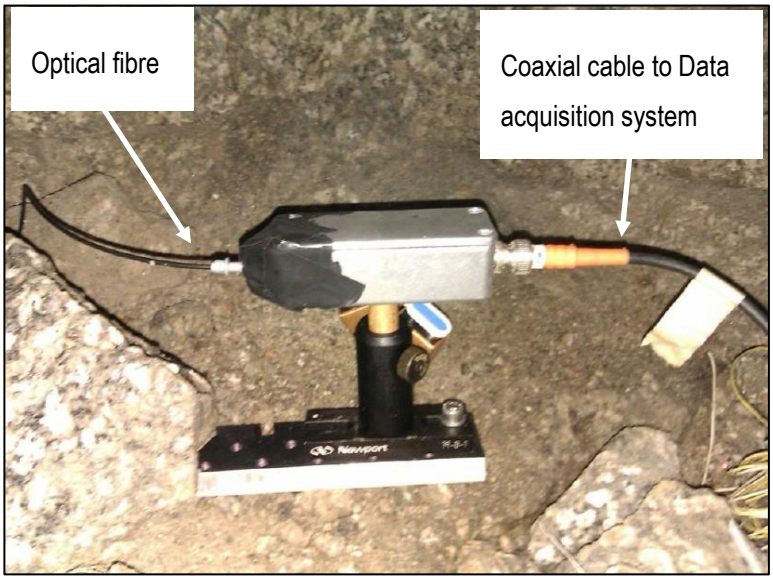

Figure 17 Single channel optical fibre receiver.

Further trials were conducted using a detonator and 200 g of Perunit™ nitro-glycerine based charges. This time the preparation of the fibre increased its heat resistance to maximise light capture opportunity. This was done initially by stripping away the opaque cladding and wrapping the now exposed translucent fibre core around the explosive charge. This also proved unsuccessful in detecting the light emitted by the blast.

The test arrangement of optical fibre and explosive charge is shown below.

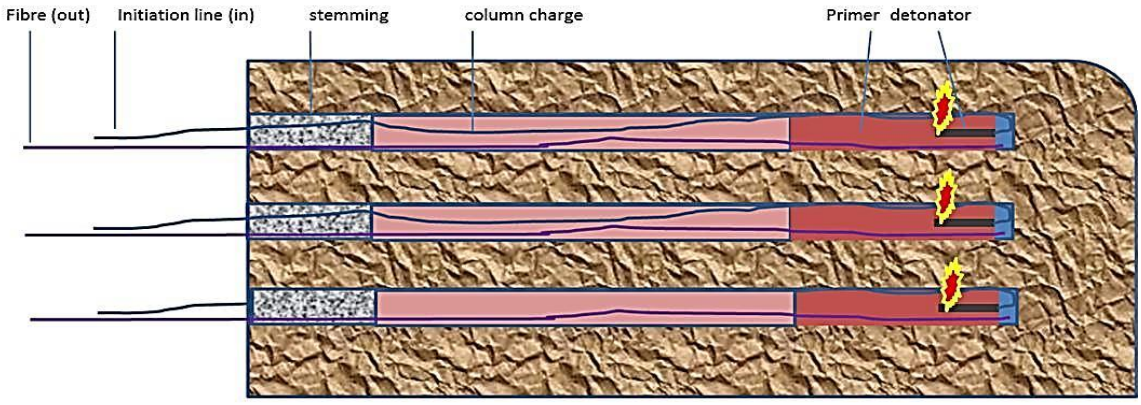

Figure 18 Arrangement of a fibre optic detection system

This arrangement was tried out in several physical configurations. The fibres were bound to the primer/detonator assembly and carefully loaded into the blast hole.

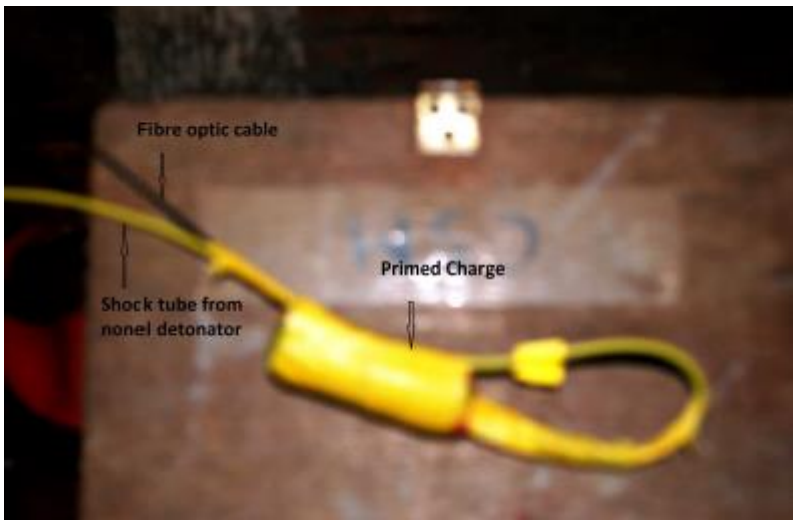

Figure 19 Primed explosive charge with electronic detonator and fibre optic cable

Further explosives are then loaded into the hole until the full charge was ready. Finally, stemming (containment) was used to partially seal the hole. The purpose of stemming is to prevent the unburned portion of explosive from simply being expelled from the bore-hole like a bullet from a gun.

The fibres themselves were routed back to a safe measurement location >100 m away from the blast area. Detection was by a fast photodiode arrangement with the output voltage recorded on a USB oscilloscope. For standard high explosives such as ANFO and Site Sensitised Emulsions (SSE) the rate of reaction VoD is around 3000 - 3500 m/s. For a column length of 3 m this directly translates to an explosive event of around 0.8 -1.0 ms. The effective VoD of an explosive depends on multiple factors: the explosive compounds, the power of the initiator, the hole diameter and the state of confinement of the explosive. Weakly initiated explosives may not instantly achieve a steady state velocity and can take a length equivalent to three hole diameters, or explosive cartridge diameters, to build up to the nominal VoD figure specified by the manufacturer.

3.6.2 Results of fibre trials

Although there is clearly a substantial amount of light generated from the explosive charge when it is fired, to our surprise no signals were measured at the detector at all. Multiple attempts to detect the event using both single mode and multimode optical fibres coupled to photodiodes failed.

Inspection of the fibres revealed that they had simply been cleaved cleanly by the actions of the detonators. No melting or charring on the fibre was apparent. The resulting exposed fibre end facets were functioning

apertures capable of coupling light from LED sources into the fibres, but no light from the firing detonator had registered at the detector.

Inspection of the fibres showed that both types had reacted poorly to the heat/pressure of the blast. Before sufficient light could be captured by the newly exposed fibre to trigger a signal from the photodiode detector. Heat from the blast had charred the fibre cladding preventing it from capturing light generated by the explosion. Together with a researcher from Exeter university, Ewusi, (2013) we conducted a number of additional trials to enhance the fibre end and found that once they were stripped of their opaque, protective sleeves and the clear optical fibre tails were inserted into thin glass philes, a signal was received. The fibre did not produce a signal when a detonator alone was tried, however a combination of a detonator and a small charge of Perunit™ did produce an impulse on the photodetector.

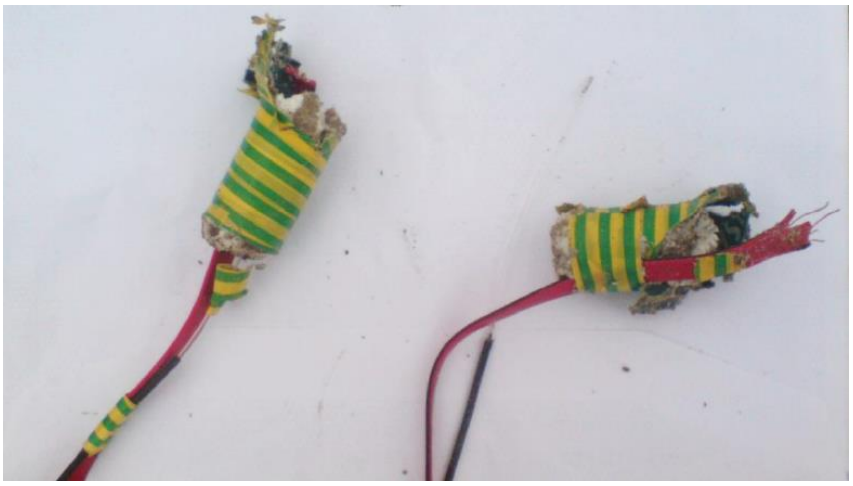

Figure 20 post blast condition of the optical fibre monitoring assembly

The intention was purely to detect a signal generated from the primer/detonator assembly; and this construction did successfully function in individual blast holes. However, when multiple holes were fired we immediately noticed damage to the 60 m long fibre by flyrock. It was clear that protecting the fibres leading away from the blast area would be essential to creating a reliable monitoring system.

3.6.3 Monitoring multiple shots with optical fibres

It is conceivable that a test rig could be constructed for optical fibre bundles with multiple-diode detectors, however the challenge lay with ensuring that potentially scores of closely spaced return-lines physically survived long enough at the blast face for each fibre to carry its signal back to the observation point.

3.7 Shock Tube

Shock tube technology was described in Chapter 2. Trials were carried out to establish whether shock tubes could be used to carry a return signal back to a safe, remote observation point. The design function of shock tubes is to initiate detonators and they themselves are generally fired with a percussion gun. Bundles of shock tubes are routinely initiated by a single detonator in blast sequence design, so by taping a shock tube to the detonator/primer assembly inside the charge hole it was certain that a return signal line would be initiated by a successful detonation. The speed of propagation of the shock wave inside blasthole is around 2000 m/s Farnfield, (2012) and that of the shock tube is 7000 m/s, therefore theoretically there isn't a reason why the detection signal shouldn't escape the charge hole before the rock fragments physically damage the shock tube itself.

This is in fact what was found. Manual inspection of the shock tube after our trials showed that the return line had fired in the hole and the signal arrived at the observation point where it was observed as an small explosion from the end of the tube.

3.7.1 Monitoring multiple shots with shock tube

The same challenge was apparent for the shock tube assemblies. The shock tubes were all initiated by the blast, but shock tubes that were designated to be fired later in the sequence were found to have failed due to physical damage close to the blast face by flyrock. Where the signal lines reached the ground they could be buried (trenched) quite easily, but protecting the mass of signal lines at the blast face proved unreliable. Different cable management options were tried to route signal lines, fibres and tubes away from the path of flyrock caused by preceding shots, but in the end protecting the lines sufficiently to ensure their survival was impractical. Operationally, an additional step to rig up the sensors and signal lines was impractical and unwelcome due to material and labour costs.

As outlined earlier, where multiple holes are being fired with varying programmed delays between each one, there could be a delay of milliseconds, or even seconds between one hole firing and its nearest physical neighbour since adjacent holes may not be programmed to fire consecutively in the sequence.

In numbers of multi-shot tests, we observed that return lines were cut off before adjacent holes had fired, thereby preventing the confirmation signal getting back to the observation point.

As we planned blast patterns for even simple arrangements we would occasionally only achieve three out of four successful returned lines fired, with the remaining holes having lost the continuity of their return signal path.

3.8 Sensors and return line conclusions

The conclusion of the physical return line trials was that it would prove impractical to physically protect return lines from flyrock and shockwave damage. It was therefore decided to abandon these approaches to detection.

Chapter 4 Blast Induced Vibration Utilisation

The aim of this thesis is to detect the incidence of misfires in the context of tunnelling. As the physical spacing between individual bore holes in a tunnel blast design is commonly of the order of 50 cm the ability to localise the point of origin of an impulse to an area with a similar order of magnitude would be advantageous.

The value in observing blast induced vibrations is the received mechanical wave holds information on the unique composition of media between any impulse source location and a receiver fixed at a remote and safe point. These waves potentially hold the information that could assist in identifying the point of origin.

As discussed in Chapter 2, current applications of far field blast monitoring have a deliberate focus on minimising the environmental impact of excessive blast induced vibration and not to detect and locate misfires. This investigation seeks to utilise the fundamental properties of wave propagation in solid media to localise the point of origin of a blast induced impulse.

Elasticity is a solid's most important property for restoring its shape and volume after the external forces acting on it have ceased. Therefore the medium, whose typical feature is elasticity, is referred to as "elastic medium." Nazarchuk, (2017). Consideration is given here to general wave propagation in idealised models of rock including compressional, shear and Rayleigh waves.

Local excitations in media are not instantaneously detected at locations that are distant from the region of excitation. It takes a finite period for a disturbance to propagate away from its point of origin. This phenomenon of propagation of disturbances, or excitations, is well known from physical experiences.

4.1 Propagation of mechanical disturbances

Mechanical waves occur due to the induced motion of a portion of a deformable medium. As elements of the mass are deformed due to an external force the disturbance is transmitted from one point to the next and this disturbance, or wave, progresses through the medium. Mechanical vibrations are characterised by the relative motion of particles about an equilibrium position. The process of elemental deformation must overcome the resistance arising from the nature of the medium and by the inertia of the material arising from its elemental mass.

As the disturbance travels it carries with it both potential and kinetic energy. The mechanism of energy transmission is sustained because motion is passed from one particle to the next and not by any global, or bulk movement of the entire medium.

It is the elemental inertia of the medium produces the time delay observed between an excitation occurring at some point and that excitation being experienced at a remote point of observation, as there would be an instantaneous transmission of energy from particle to particle. All real materials are elastically deformable and since they all possess mass, they all support the transmission of mechanical waves. The wave equation completely describes the behaviour of mechanical waves in an elastic medium.

At the initiation of a disturbance, the inertia of a material initially resists motion, but once the medium is in motion, inertia and the resilience of the medium sustains motion. If after a certain time interval, the external applied force is removed, the motion of the medium will eventually subside due to frictional losses and a state of static deformation will be reached.

The importance of dynamic effects depends on the relative magnitudes of the external application of the disturbances and the characteristic times of transmission of disturbances across the medium.

Continuum Mechanics (Spencer, 1980) is a branch of mechanics that deals with the mechanical behaviour of materials modelled as a continuous mass rather than as discrete particles. A continuum is therefore considered to be a body that can be continually sub-divided into infinitesimal elements with properties being those of the bulk material.

In the context of this research into mining safety with respect to explosives' safety, the rock between the excitation and the detectors is treated as a continuum. The development of wave mechanics is essentially based on theoretical spaces of infinite dimensions, half-spaces and smooth boundaries. The geometric arrangement between the explosive charge and detector and their subsequent relationship with respect to the propagation of mechanical disturbances will comprise thousands of permutations of both half-spaces and "infinite" spaces randomly created by the nature of the rock and its faults. In contrast to idealised models, the physical reality of the mine, or tunnel environment is messy. Mixed media coexist and come into physical contact with each other: rock types e.g., igneous and sedimentary rock, faults, cracks in the media, rough tunnel geometries, tunnel depths with corresponding embedded geotechnical stresses. Each tunnel will possess its own unique set of characteristics. Because we cannot produce a representative model of each tunnel at an elemental level, experimental measurements were conducted in the framework of continuum mechanics.

4.1.1 Elasticity

When an elastic material is deformed due to an external force, it experiences internal resistance to the deformation that acts to restore it to its original state if the external force is removed. There are various elastic moduli employed to describe the properties of a material, such as Young's modulus, the shear modulus, and the bulk modulus (Achenbach, 1973), all of which are measures of the inherent elastic properties of a material as it responds to deformation under an applied load. The various moduli apply to different kinds of deformation. For example, Young's modulus applies to extension and compression of a body, whereas the shear modulus applies to its shear strength properties.

Two types of waves propagate in an infinite elastic medium: dilatational and distortional with each having a characteristic velocity (Achenbach, 1973). The presence of a free surface boundary that forms a semi-infinite elastic medium introduces the interaction between shear and body waves induces the formation of Rayleigh waves.

The elasticity of a material is described by a stress–strain curve, which shows the relation between stress (the average restorative internal force per unit area) and strain (the relative deformation) (Achenbach, 1973). The curve can be approximated as linear for sufficiently small deformations (in which higher-order terms are negligible). If the material is isotropic, the linearized stress–strain relationship is described by Hooke's law and it is frequently applied only up to the elastic limit for most materials.

Two types of relationship are considered (Achenbach, 1973). The first type deals with materials that are elastic only for small strains. The second deals with materials that are not limited to small strains. The second type of relation is more general in the sense that it must include the first type as a special case.

For small strains, the measure of stress that is used is the Cauchy stress while the measure of strain that is used is the infinitesimal strain tensor; the resulting (predicted) material behaviour is termed linear elasticity, which (for isotropic media) is called the generalized Hooke's law.

4.1.2 Wave propagation

The inertia displayed by the media initially resists the motion induced by an externally applied force, however after the elemental mass has be displaced from its equilibrium position the material's inertia that then sustains that motion. For any solid material when a force F(t) is applied at a point P, the material responds with a stress ε(t) that creates a strain τ(t).

This disturbance will radiate away from the excitation position and due to the law of conservation of energy, it will decay in proportion to $1/r^2$, where r is the radius from the point of origin of the disturbance.

Mechanical waves originate in the forced motion of a portion of a deformable medium. As elements are deformed about their equilibrium position, the disturbance is transmitted from one point to the next and the wave progresses or propagates through the medium carrying both Potential and Kinetic energy with it.

Both the material stiffness and inertia must be overcome for the disturbance to propagate.

4.1.3 Wave propagation without boundaries

Body waves in solids without boundaries are modified by the material properties of the mass, predominantly density. Two types of body waves discussed are longitudinal waves and transverse waves.

Longitudinal waves are waves in which the displacement of the medium is in the direction of the wave propagation. Figure 21. Like all elastic wave motion, the displacements oscillate back and forth around an equilibrium position. It travels in the form of compressions and rarefactions. These compression waves are known as P-waves and are the fastest propagating waves in solids.

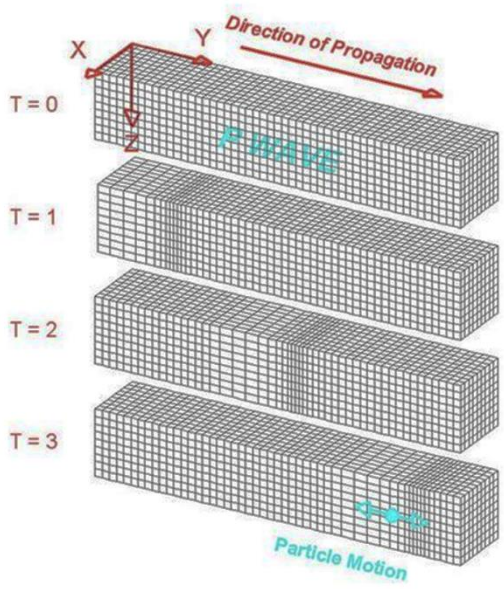

Figure 21 Illustration of a primary (compression) wave propagating through a solid.

Adapted from Wikipedia 2020. Royalty free.

Wave propagation within an infinite elastic medium that is unbounded in all directions, gives the most general analytical description.

The governing equations describing propagation in an infinite elastic medium, in terms of displacements are the Navier stress Equation of Motion (W. Michael Lai, 2009)

$$(\lambda+\mu)\nabla(\nabla\bullet\mathbf{u})+\mu\nabla^2\mathbf{u}=\rho\frac{\partial^2\mathbf{u}}{\partial t^2}, \tag{4.1}$$

Where λ and μ are the Lamé constants (Achenbach, 1973), defined as:

$$\lambda=\frac{\nu\cdot E}{(1+\nu)\cdot(1-2\cdot\nu)}, \tag{4.2}$$

$$\mu=\frac{E}{2\cdot(1+\nu)}, \tag{4.3}$$

Where E is the Young's modulus of the medium, v is the Poisson's ratio of the medium, ρ is the density of the medium, (•) is the scalar product, ∇ is the nabla operator, defined in Cartesian coordinates:

$$\nabla=\left(\frac{\partial}{\partial x},\frac{\partial}{\partial y},\frac{\partial}{\partial z}\right), \tag{4.4}$$

$\boldsymbol{u}$ is the deformation displacements vector in Cartesian coordinates defined as u (x, y, z) = ux uy, uz) and ∇2 is the Laplacian, defined as the gradient of the nabla operator.

If the vector operation of divergence is performed on each side of the governing displacement equation (4.1), we get:

$$\nabla^2\Phi=\frac{1}{V_P^2}\cdot\frac{\partial^2\Phi}{\partial t^2}, \tag{4.5}$$

Where

$$V_P=\sqrt{\frac{\lambda+2\mu}{\rho}}, \tag{4.6}$$

Where V_P is the propagation velocity and

$$\Phi=\nabla\bullet\mathbf{u}, \tag{4.7}$$

As the wave diverges, it corresponds to an increase in volume of the media undergoing deformation by the propagating wave. The direction of motion is coincident with the direction of propagation with the non-dispersive Propagation Velocity of V_p.

4.1.4 Shear Wave Velocity

Mathematically the shear wave velocity is derived from performing the curl of the governing equation.

$$\nabla^2 \mathbf{H} = \frac{1}{V_S} \cdot \frac{\partial^2 \mathbf{H}}{\partial t^2}, \tag{4.8}$$

where

$$V_S = \sqrt{\frac{\mu}{\rho}}, \tag{4.9}$$

and

$$\mathbf{H} = \nabla \times \mathbf{u}, \tag{4.10}$$

Where $(\times)$ is the product vector.

This rotational wave propagates with a non-dispersive velocity Vs, in a direction perpendicular to the direction of propagation, as the curl operator describes the circulation of a vector field along a closed path. Vs is the characteristic velocity of shear waves.

The relationship between the shear wave velocity and the compressional wave velocity is defined by the Poisson's ratio. σ_{SP} defined as:

$$\sigma_{SP} = \frac{V_S}{V_P} = \sqrt{\frac{\mu}{\lambda + 2\mu}} = \sqrt{\frac{1 - 2 \cdot \nu}{2 \cdot (1 - \nu)}}, \tag{4.11}$$

In the case of transverse waves, the oscillations displace solid elements away from their relaxed position in directions perpendicular to the propagation of the wave as illustrated in Figure 22. This secondary, transverse wave moves slower through the medium than the primary wave.

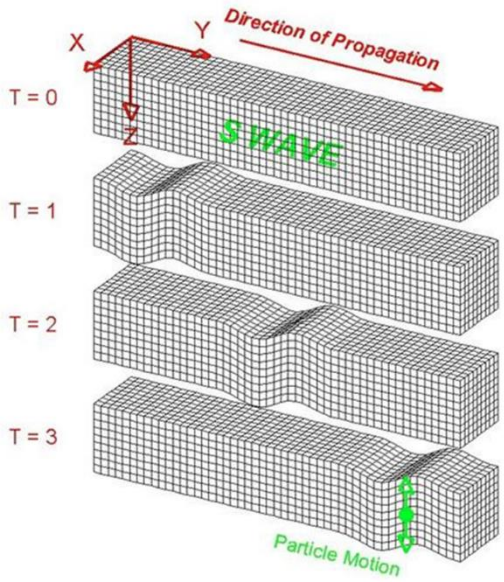

Figure 22 Transverse waves - motion perpendicular to the direction of travel.
Adapted from Wikipedia 2020. Royalty free

Since these displacements correspond to a local shear deformation of the material, a transverse wave of this nature is described as a shear wave, Secondary Waves or S-Wave.

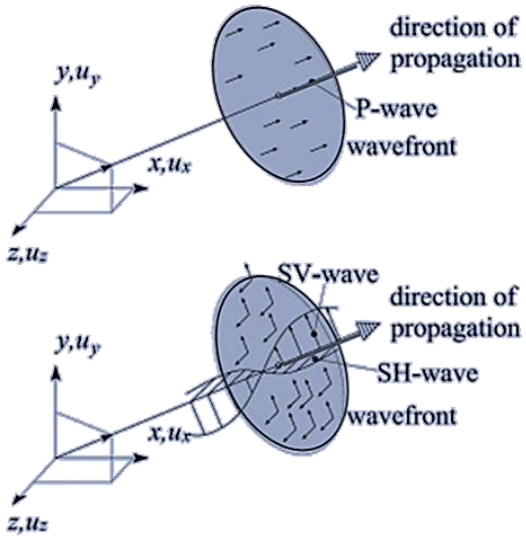

Figure 23 Comparison of displacements for P-wave and S-wave. Adapted from (Wolf, 1986)

Transverse waves are contrasted with longitudinal waves, where the oscillations occur in the direction of the wave.

4.1.5 Half-space subjected to surface interactions

One of the most common examples in wave mechanics is the consideration given to the half-space subjected to uniform surface forces. This situation displays many of the features of wave propagation through an initially undisturbed, homogeneous, isotropic, elastic medium (Graff, 2012).

In this 1-dimensional context, it can be shown that all stress components vanish identically at the boundary of the half-space, denoted by setting x=0.

In the half-space, the deformation caused by the propagating wave εx, is completely described by the single strain component.

$$\varepsilon x = \frac{\partial y}{\partial x} \tag{4.12}$$

The half-plane can be described as in a state of one-dimensional, longitudinal strain. It can be shown that a wavefront defining the boundary between disturbed and undisturbed medium propagates through the medium with a velocity C_L, where C_L is the longitudinal velocity (Achenbach, 1973). The description of this plane wave is essential as in linear time invariant systems all other wave forms can be represented by the superposition of multiple individual waves. In an infinite half-space the plane longitudinal wave is also the Primary (or P) wave.

The introduction of the infinite half-space leads into the physical situation encountered in *drill and blast processes* where boreholes are loaded with explosive materials. The inner surface of the borehole can be considered as the physical boundary of the infinite half-space.

In this description of wave propagation in a semi-infinite half-space the free surface is assumed to lie in the x-z-plane, also called the “horizontal” plane, in contrast with the x-y plane, also called the “vertical” plane, with y positive in the downward direction.

The particle motion due to the dilatational effects lies in the vertical plane, while the particle motion due to shear effects may have components in the vertical and horizontal plane. Each shear wave can be decomposed in its two components, a *SV-wave* that polarizes in a plane perpendicular to the plane of the interface, and a *SH-wave* that polarizes in a plane parallel to the interface.

The general situation is displayed in Fig 23. Finally, since every point along the vertical plane is undergoing the same displacement (plane strain), the motion is invariant with respect to the z direction if the wave is in the vertical plane.

The governing equations for the investigation (Graff, 2012) are:

$$u_x = \frac{\partial \Phi}{\partial x} + \frac{\partial H_z}{\partial y},\ u_y = \frac{\partial \Phi}{\partial y} - \frac{\partial H_z}{\partial x},\ u_z = -\frac{\partial H_x}{\partial y} + \frac{\partial H_y}{\partial x} = 0 \tag{4.13}$$

where Φ and H are potential functions related to the dilatation and to the rotation of the medium. The motion of the medium can therefore be viewed as superposition of compressional and rotational motions. (G.F. Miller, 1954) (Graff, 2012) Substituting the potential form of displacement into the equation of motion of the system gives:

$$\rho\frac{\partial}{\partial y}\left(\frac{\partial^2\Phi}{\partial t^2}\right)-\rho\frac{\partial}{\partial x}\left(\frac{\partial^2 H_z}{\partial t^2}\right)=(\lambda+\mu)\frac{\partial}{\partial y}\left(\nabla^2\Phi\right)-\mu\frac{\partial}{\partial x}\left(\nabla^2 H_z\right), \tag{4.14}$$

$$\rho\frac{\partial}{\partial x}\left(\frac{\partial^2\Phi}{\partial t^2}\right)+\rho\frac{\partial}{\partial y}\left(\frac{\partial^2 H_z}{\partial t^2}\right)=(\lambda+\mu)\frac{\partial}{\partial x}\left(\nabla^2\Phi\right)+\mu\frac{\partial}{\partial y}\left(\nabla^2 H_z\right), \tag{4.15}$$

for the y-direction and for the x-direction. Two wave equations are obtained, one for each potential:

$$\nabla^2\Phi=\frac{1}{V_P}\cdot\frac{\partial^2\Phi}{\partial t^2},\ \nabla^2 H=\frac{1}{V_S}\cdot\frac{\partial^2 H}{\partial t^2}, \tag{4.16}$$

They have velocities corresponding to the compressional and shear wave velocities. The two equations can be solved by applying the boundary conditions at the free surface:

$$\tau_{zx}=\tau_{zz}=\tau_{zy}=0,$$

Where τ_{ij} is a stress indicating the plane and the direction respectively the stress is acting. It can be shown (Graff, 2012) (Wolf, 1986) that the two boundary conditions result in the following equation:

$$\left(2-\frac{V_R^2}{V_S^2}\right)^2=4\sqrt{\left(1-\frac{V_R^2}{V_P^2}\right)}\sqrt{\left(1-\frac{V_R^2}{V_S^2}\right)}, \tag{4.17}$$

Where V_R is a characteristic propagation velocity of Rayleigh waves and is a function of both the compressional and shear waves and varies with the media Poisson's ratio. In general, the velocity of the compressional wave is the fastest and the shear and Rayleigh wave speeds are similar.

The existence of Rayleigh waves was predicted in 1885 by Lord Rayleigh and John W. Strutt, after whom they were named. In isotropic solids these waves cause the surface particles to move in ellipses in planes normal to the surface and parallel to the direction of propagation – the major axis of the ellipse is vertical.

At the surface and at shallow depths this motion is retrograde, that is the in-plane motion of a particle is counter-clockwise when the wave travels from left to right. At greater depths the particle motion becomes prograde. In addition, the motion amplitude decays and the eccentricity changes as the depth into the material increases. The depth of significant displacement in the solid is approximately equal to the acoustic wavelength.

It was shown (Graff, 2012) (G.F. Miller, 1954) that the resulting motion of the two components of the Rayleigh wave results in an elliptical motion of the element of the media.

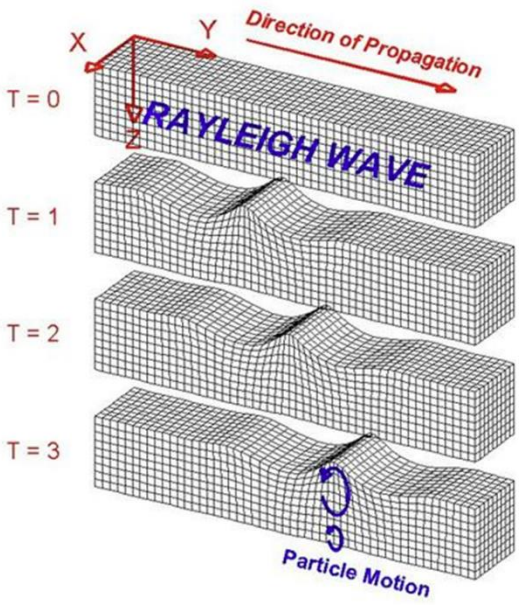

Figure 24 Illustration of Rayleigh Wave propagation. Adapted from Wikipedia 2020. Royalty Free.

In the drill and blast scenario, the internal surface of the bole hole establishes the boundary of what is in effect, a semi-infinite half-space. This interface is then subjected to dynamic surface pressure which at any given point location varies in time as the induced gas pressure builds then decays. This pressure builds from the blind end of the hole and progresses to the free tunnel face. It is self-evident that the nature of a disturbance generated by a blast is radically different from the idealised P-wave in many respects. Considering a single blast hole the external force is not applied at the same time along the length of the hole. The chemical reaction resulting in the generation of expanding gases that induce the pressure in the hole is progressive in nature.

Summary

Relevant sections of the theory of elastic wave propagation in infinite and semi-infinite media was reviewed in this section, concentrating on the mechanical propagating wave and on the media properties. The characteristics of Rayleigh waves in particular were highlighted.

4.2 Considering the media as a filter

In the mining context once again, it might be useful to consider the media between source and received as a filter where the exact nature of the filter is spatially dependent, but linear time invariant (LTI). Any system that selectively modifies certain frequency components relative to others has the characteristics of a filter.

Impulse response of a filter is its output when presented with a brief input signal, called an impulse. It is the reaction of any dynamic system in response to some external change. In both cases, the impulse response describes the reaction of the system as a function of time (or possibly as a function of some other independent variable that parameterizes the dynamic behaviour of the system). In the context of drill and blast

operations, the physical media and the unique characteristics of the geology create the dynamic system and its impulse response between excitation source and receiver.

Since the impulse function contains all frequencies, the impulse response defines the response of a linear time-invariant system for all frequencies.

Figure 25 Basic schematic of a filter system.

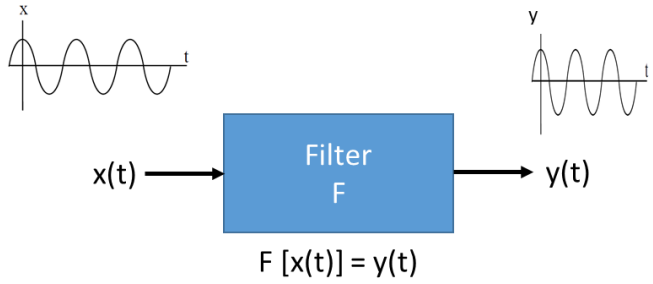

Figure 25 Basic filter schematic

If we assume the filter is linear time invariant (LTI) the impulse response tells us what the output will be if we input a very short sharp pulse into the filter Figure 26.

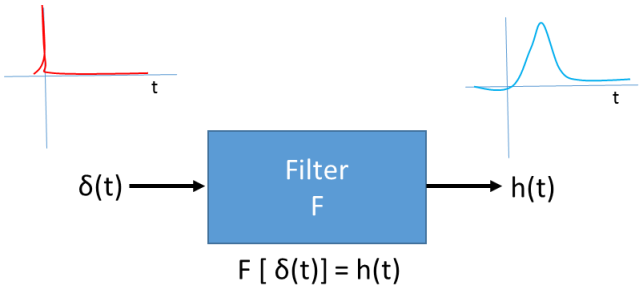

Figure 26 Filter response to an impulse response

We can approximate any input signal as a sum of weighted pulses (in the limit of an infinitesimally narrow pulse, i.e. a Dirac delta or impulse, we can make this exact by replacing the sum with an integral). - that is:

$$y(t) \approx \sum_{i=0}^{N} x(ti)h(t-\tau) \qquad (4.18)$$

$$y(t) = \int x(\tau)h(t-\tau) \qquad (4.19)$$

1. If we input a signal which is the sum of two separate input signals with known outputs, we can compute the output to the summed signal by just summing the outputs to the individual signals

2. Since the system is LTI, if we scale the input by some constant the output scales by the same constant

3. The output for a given input is the same irrespective of where the input is located in time, then we can compute the output of the filter to any input which can be expressed as a linear combination (weighted sum) of inputs which we know the output for, and so if we know the filters impulse response we can compute the output for any input by expressing it as a sum of a series of impulses Green function's use the same basic concepts but generalise to arbitrary linear (differential) systems rather than just LTI systems.

Rather than considering a system which just takes an input which is a function of time, in general the input may now be both a function of time t and of spatial coordinates. Also, rather than expressing the system as an input-output relation as with the filter typically for more general linear differential systems, the relationship is expressed as some linear operator L applied to an unknown state/output $\mathrm{y}(\mathrm{s},\mathrm{t})$ subject to some known input forcing term $\mathrm{x}(\mathrm{s},\mathrm{t})$ i.e.

$$L[y(s,t)] = x(s,t) \tag{4.20}$$

Here the linear operator L is effectively the inverse of what we defined for the filter F. In general, L is some linear combination of time and/or space derivative operators.

4.3 Green's functions and impulse correlation

It has been shown by various authors, including Wapenaar, (2004), that the Green's function of a random medium, or an irregular finite body can be obtained by cross correlating the recordings of a diffuse wave field at two receiver positions. The resulting Green's function is the wave field that would be observed at one of these receiver positions if there were an impulsive source at the other. This theoretical result has been successfully demonstrated with seismic surface waves. The accuracy of the reconstructed Green's function depends on the degree of inhomogeneity, or disorder of the medium parameters and the duration of the signal. Ideally the cross correlations should be done where the net energy flux is equal to zero, which takes place after sufficiently long multiple scattering of the wave field between the heterogeneities in anisotropic medium.

In the context of earthquake monitoring that the autocorrelation of the transmission response of a horizontally layered earth yields the superposition of the reflection response and its time-reversed version the source signature in the reconstructed reflection response is the autocorrelation of the source signal in the subsurface. Claerbout, (1996) proposed that for the 3D situation by cross-correlating noise traces recorded at two locations on the surface, the wave field that would be recorded at one of the locations if there was a source at the other could be constructed. These modelling studies showed that longer time series, and a white spatial distribution of random noise events would be necessary for the conjecture to work in practice. This corresponds to investigations currently underway at the Institute of Micro-seimology, Tasmania Lynch, (2013).

A relationship was derived Wapenaar, (2004) between the elasto-dynamic Green's function and the cross-correlation of observed wave fields that holds at the free surface of random, as well as deterministic media. Their derivation is based on correlation reciprocity theorem which relates two independent elasto-dynamic states (wave fields and sources) in one medium. Wapenaar, (2004) derived the elasto-dynamic Green's function of any inhomogeneous medium (random or deterministic) from the cross-correlation of two recordings of a wave field at different receiver locations using a reciprocity theorem of the correlation type

An additional complication for more general linear systems is that as well as specifying the linear operator L we also need to specify how the system behaves at the boundaries. The Green's function G is then the

state/output which corresponds to the solution of a differential system (specified by a differential operator L plus boundary conditions) for a Dirac delta / impulse input - it is effectively the impulse response of the solution operator (i.e. the operator which solves the differential equations, giving the output $y(s,t)$ for a specified input $x(s,t)$).

As we are assuming the system is again linear, as for the filter if we know the solution for an impulse input we can construct the solution for any arbitrary input by considering it as a weighted sum (integral) of impulses. Therefore we can solve any linear differential system with an arbitrary input term if we know the Green's function corresponding to the differential operator and boundary conditions.

4.4 Spatial positioning of blast induced impulses

There are a variety of industry needs that drive the work on spatial positioning of impulse signals in rock or in fluids. To date, several techniques have been employed to spatially position the points of origin of impulses in rock. They are classified essentially as methodologies that utilise the frequency and amplitude content of the source signal at one, or more detection locations some with signal correlation techniques, or utilising the time difference of arrival of the impulse signal at multiple known sensor positions.

Safety of personnel and the legal duty of care encourage every reasonable precaution to be taken to predict and prevent tunnel or mine collapse. The routine seismic monitoring of mines to detect ground movement in response to mining operations can give advanced warning of the probable location of rock failure in a 3D space.

In the context of misfires detection, the charge location will be bounded to a two dimensional plane that is the drilled tunnel face.

In the tunnelling scenario, it is to be expected that errors in wave speed estimation will be introduced by the variable composition of surrounding strata formations between the point of origin of any signal and sensors situated at varying distances and locations.

The idea of using a signal processing techniques to match and compare blast induced impulses does offer possibilities in our scenario.

4.5 Vibration signal triangulation and tomography

Blast events are typically a few hundred milliseconds long and optimising the position of the sensors is important to acquiring the vibration data. During the construction of a tunnel there are constraints in selecting the location of sensors and it is not always possible to arrange the optimum geometrical sensor configuration with respect to the blast face. Significantly, during a blast, the signal path from vibration source to receiver will be disrupted

during the blasts sequence, and the velocity of propagation will certainly vary locally through fractured and fragmented rock.

Wright C., (2000) studied localised variations in seismic velocity in underground mines and observed velocity ranges of 4.2 to 5.2 km/.s resolved over very small distances of 15 m. It follows that for a direct path between source and sensor that the seismic velocity features as a parameter to calculate, or reconstruct a wave front, then a natural precision error will result. The Wright study was in underground tunnels which means that the rock had been disturbed from its natural state due to a lack of rock confinement as in a tunnel scenario.

The Institute of Microseimicity (IMS) based in Tasmania, Australia Lynch, (2013) conducted research into the applications of passive microseismic detection in the context of caving mines. This method called block caving is carried out where large, weak ore deposits are found. The method is based on building a tunnel under the ore body then punch a hole in the tunnel roof into the ore that is so weak that it cannot support its self. This initiates a collapse of the rock under its own weight. Block caving (also called panel or sub-level caving) is illustrated in Figure 27, relies on cave mining in structurally weak rock. As material is removed from below the ore body the confinement is removed and the weak rock at the top of the void simply fails under the influence of gravity. The process continues and a cave grows.

The rate of growth is dependent on how much material is removed around the base of the cave and the direction of cave growth is influenced by where the material is extracted via draw points that are made by tunnelling under the target cave.

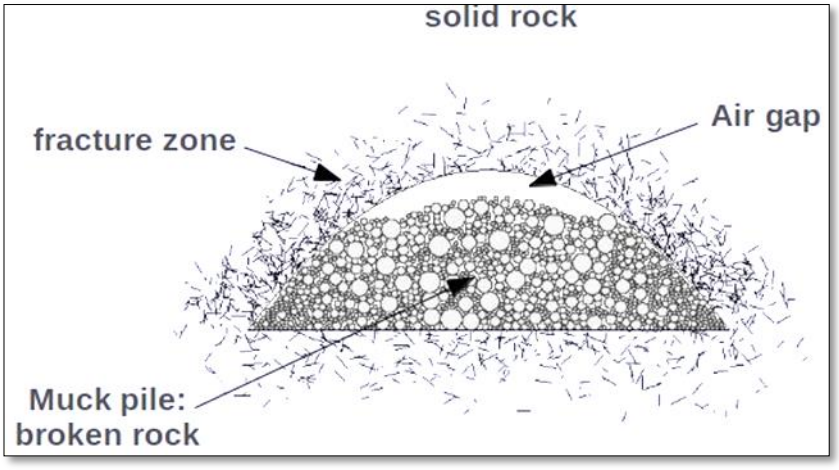

Figure 27 Schematic section though a cave, showing the interior filled with broken material, the fracture zone surrounding the cave and the weak host rock.

The challenge for this method of mining is to understand how the cave is developing as the broken rock is removed from the floor of the cave. There are production risks if the cave is developing in largely low grade ore zones or if the cave progressing rapidly towards the surface where it has been known to cause a dangerous ground failure such as the North Parkes accident in Australia in 1999.

IMS passively monitor seismic emissions from the rock fracturing using multiple sensors in known locations around the cave to gauge where the inner surface of the cave actually is and in which direction(s) the cave is developing.

The principal technical challenge in using 2D Tomography or in 3D (where the technique is described as seismic velocity inversion) is the localised variations in seismic velocity due to fracturing and stress relieving in the so called zone of seismicity surrounding the cave. IMS refer to the aseismic gap – the unknown distance between the actual cave back and the seismic cloud – which prevents a reliable estimation of the cave geometry.

One technique employed by IMS to reduce the error in seismic velocity estimations it to *induce a seismic event at a known location* close to the presumed vicinity of the zone of seismicity Lynch, (2013). The seismic event can be created using either a pneumatic hammer or a piezoelectric impulse. Both techniques create a seismic impulse from a known location with respect to the microseismic sensors and therefore the errors in the assumptions of the seismic velocities can be minimised. With this parameter being more understood, the positioning estimates for the seismic activity can become more precise.

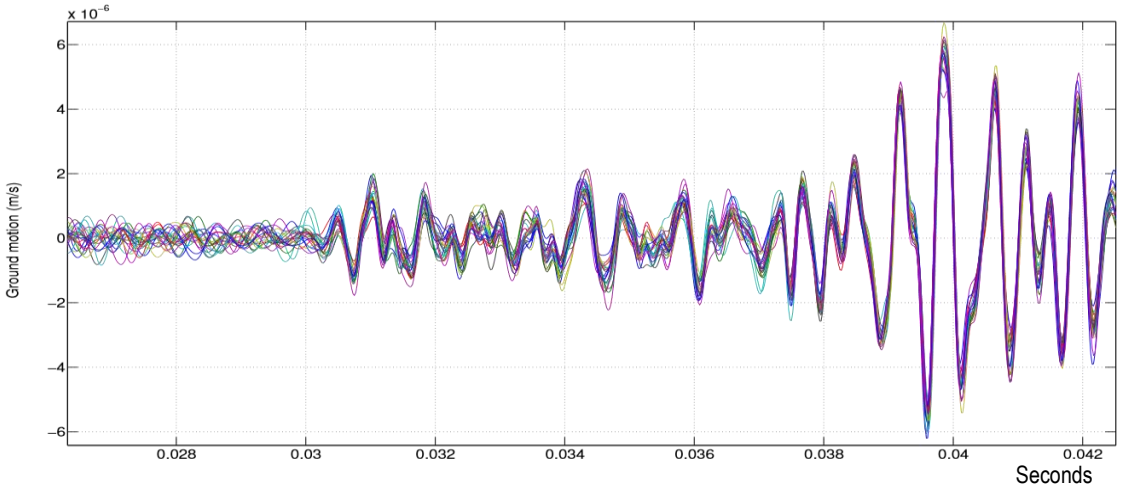

Figure 28 Time trace for multiple induced seismic impulses from a pneumatic hammer Lynch, (2013).

The figure above from Lynch, (2013) illustrates the repeatability of this technique over a range of 80 m between impulse location and the geophone used to capture the signal. Significantly, IMS aim to utilise the power radiated over the 1,200 – 2,600 Hz band. The dominant frequency observed in their environment was 1,500 Hz. The positioning accuracy achieved for seismic events using this technique is currently around 70 m Lynch, (2013).

4.6 Time reversal mirror background

The relevance of time reversal mirror (TRM) techniques to this research is driven by the need to identify the point of origin of the blast induced vibrations. Although we would not be aiming to conduct a TMR process and reproduce a facsimile of the original impulse at its original source, the relevance to this work is that TMR theory and practice implies that signals originating from an excitation source in a solid medium will be uniquely influenced by the boundary of that medium and when sampled at fixed point the 'output' function will possess both a spatial and temporal dependency. TRM exploits the fact that the signal is not a simple wave form, but a group of waves comprising of many propagating, reflecting and refracting waves that when sampled at a specific point(s) in space generate a discrete time signal that is unique to the relative spatial arrangement of source and receiver within an elastic solid medium. The identification of each blast signal source, in the context of a misfire, will lead us to derive the identification and therefore the location of any impulse source and to determine if there has been a misfire.

Work by Parvulescu and Clay described a 'matched-signal technique' Parvulescu, (1965). They applied the technique to underwater communication and object detection to recover the location of a remote signal. The

significance of the time reversed invariance of the acoustic wave equations means that every diverging wave radiating from a source will experience reflection, refraction, scattering and absorption by the propagation media. There will hypothetically exist a set of waves that will precisely retrace all of the complex paths that the original wave experienced and this set of waves can be made to synchronously converge at the point of origin, as if time were going backwards. Theoretically TRM transducers must completely surround the volume of material being monitored. This bounded volume is described in their work as the acoustic cavity. To sample all of the information available about the shape and nature of this space, or between the impulse source location and sensors, all of the wave fronts that are propagating in all directions need to be sampled. In practice time reversal cavities are difficult to realise and the time reversal operation is performed by a utilising a limited number of transducers over a reduced angular area. This process was referred to by Draeger, (1997) as a Time Reversal Mirror (TRM). It is composed of a reversible transducer array surrounding the incident acoustic field to be sampled, once the sampling is complete the signals are time reversed and reemitted by the TRM transducers. At the point where the waves combine there will be a facsimile of the impulse that generated the original wave train.

Derode, Roux et al., (1995) established that the focusing quality is improved if the waves can traverse a multiple scattering medium before arriving at the transducer array. Media with higher order multiple scattering widens the effective focusing aperture due to the large length of paths involved. i.e once the TRM operation has been performed, the whole cavity behaves as a coherent focusing source.

The study of TRM in solids differs substantially from that in a purely acoustic case in fluids, due to the excitation of bulk compressional waves and shear waves and the continual conversion that would take place between them due to scattering, absorption and re-radiation into multiple modes Sutin, (2004). For time reversal to function the waves generated in an elastic medium (and the subsequent, multiple reflected waves) need to arrive at the detectors, or TRM. Wave trains that experience excessive mixing become ‘foggy’ and lose the information relating to the structure of the acoustic cavity. Significantly in the context of tunnelling in rock, Sutin, (2004) demonstrated that time reversal still works in granular solid media where unwanted wave conversions and high losses could easily be expected to ruin the time reversal process. Sutin, (2004) conclude that a single channel can also be used to effectively focus time reversed acoustic energy in time and

space. This was studied in 3-dimensional solids where multiple compressional-shear wave conversions could have potentially destroyed the process. Frequency filtering was seen to improve the TRM focusing quality.

Derode A. (1995), Fink (2012) established the principle of linear superposition of waves propagating in multiple scattering media. They demonstrated that TRMs can be applied to reconstruct the location of an excitation in bounded and in unbounded, chaotic cavities for media such as solid silicon wafers and even in fluids as shown in Figure 29 below.

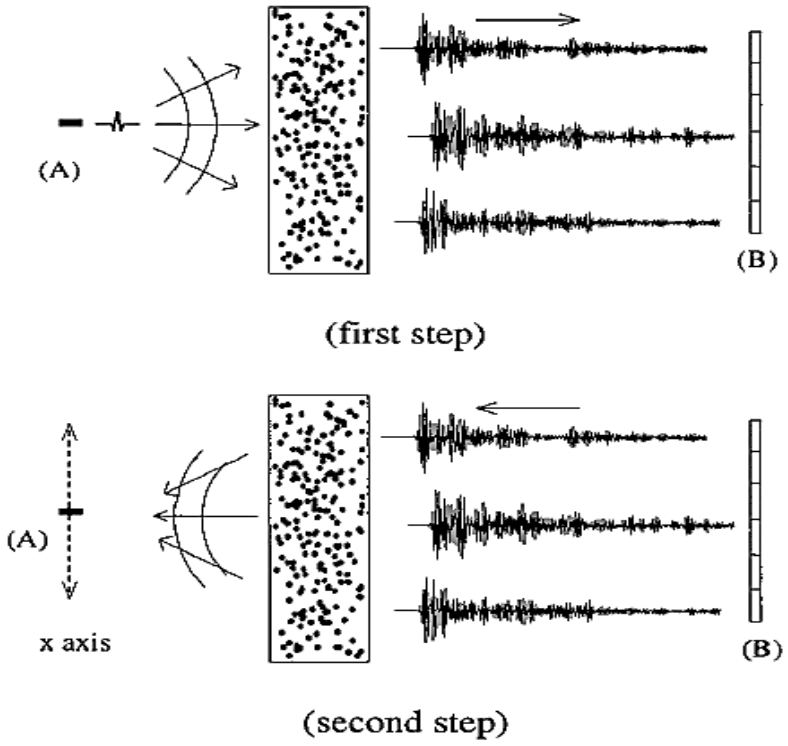

Figure 29 Experimental set-up in Time Reversal in chaotic cavities. Reproduced from Fink 1999.

In the first step the source (A) transmits a short pulse that propagates through the rods. The scattered waves are recorded on a 128-element array (B). In the second step, the 128 elements retransmit the time-reversed signals through the rods. The piezoelectric element (A) is now used as a detector. It can be translated along the x axis while the same time-reversed signals are transmitted by B, in order to measure the directivity pattern. In the second step is to reconstruct the original excitation at the original location. The recorded signals were time reversed and replayed through the 128 transducers, which then produced 128 unique wave fronts that passed back through the chaotic cavity. Observations around the point of origin of the initial excitation / impulse showed that a localised facsimile of the original event was produced, representative in time and space.

The importance of this phenomenon is that the received acoustic wave holds information on the unique acoustic path between any point of origin of an acoustic impulse and a fixed receiver and hence information identifying the point of origin.

Draeger, (1997) Cassereau, (1994) demonstrated time reversal invariance of acoustic waves in chaotic cavities. He experimented with ultrasonic waves transmitted by a transducer into silicon wafers which then reverberated inside the cavity, creates a long pulse at a receiver, hundreds of times longer than the initial excitation. The long and complex acoustic field is measured at a second transducer (or series of transducers); time reversed and re-emitted from the receiver(s). The acoustic field is shown to propagate back to the source position; recreating a facsimile of the short initial pulse.

Sutin, (2004) investigated single channel time reversal in elastic solids and recorded the first results presented for TRM experiments in granular materials. A series of TRM experiments were carried out with a single-channel piezoelectric transceiver in 3D reverberant solid media. The two materials chosen were doped glass and sandstone. They found that the technique worked extremely well in the light of large numbers of mode conversions generated by compressional to shear wave conversions at the boundaries of dissimilar media and the TRM provided excellent spatial and temporal focusing of elastic waves. They observed that both the temporal and spatial focusing are frequency dependent and that they are also dependent on the dissipation characteristics of the medium. The doped glass substrate followed the earlier work by Fink et al (1998) and enabled a focus at around half of the shear wavelength. Sandstone on the other hand, showed a focusing width of over one wavelength. Elastic waves are highly attenuated in sandstone in comparison to the doped glass substrate. The effect of this is that sandstone allows fewer reflections of the elastic waves and therefore supports fewer (virtual) TRM elements created by wave reflections.

Following an impulse generate at the source, a relatively long wave-train consisting of the initial arrival and its reverberation, or coda, was detected at the receiver, then time-reversed. This TR signal could either be radiated from the receiver to produce a focused displacement at the original source, or replayed at the original source to produce a focused displacement at the receiver, demonstrating the reciprocity of the system.

In sandstone, the attenuation is substantial resulting in received signal with smaller amplitude and of shorter duration. This allowed an estimated 20 traverses of the cavity before the signal was overcome by noise. This

produced a corresponding reduction in the number of (virtual sources) restricted the focusing properties of the TR system in sandstone. They measured the focal width at -3 dB was around 8 mm; wider than in glass and almost equal to the shear wavelength. They deduce that this will be the case for lower Q materials in general.

4.6.1 Relevance of early experimental work on time reversal

TRM in granular solids has been shown to works very well. Sutin, (2004) observe that one can virtually ignore the complications of mode conversion and treat the TRM process 'blindly'. They propose that focusing resolution will lie between the compressional and shear wavelengths in granular material with a low Q. Quieffin, (2005) applied Draeger's experimental work which demonstrated the time reversal invariance of acoustic waves in chaotic cavities to the localisation of small mechanical impacts on an objects surface. Ing, (1998) aimed to turn the surface of any solid object into an interactive interface. They demonstrated that the number of potential discrete positions on a surface is directly related to the mean wavelength of the detected acoustic wave.

4.7 Conclusion

The value in observing blast induced vibrations is the received mechanical wave holds information on the unique composition of media between any impulse source location and a receiver fixed at a remote and safe point. These waves potentially hold the information that could assist in identifying the point of origin.

In this section we outlined the mathematical representation of mechanical waves and the development of the wave equation, and the definition and propagation characteristics of iLongitudinal, Shear and Rayleigh waves in an elastic medium.

In the context of tunnelling with explosives, the advantages of considering the rock as a continuous medium lead into treating the intervening rock between signal source and detector as a filter was discussed. The potential applicability of Green's functions was introduced. Finally the section looked at investigations into mechanical wave localisation.

Chapter 5 Determining the Spatial Dependence of Impulse Correlation

The research carried out in this investigation aims to determine whether analysing the vibration time trace can derive sufficient information to identify the location of a specific charge in a firing sequence. It is clear that examining the vibration time trace will permit ‘peak counting’, but as previously highlighted, for a number of reasons such as when pairs of charges are fired simultaneously; or the charge firing times are very close together or detonator timing errors overlapping impulse are possible. This makes the process of identifying misfires from peak counting alone more uncertain.

Previous work on long range, far-field ‘signature-hole’ analysis has been applied and developed in tunnelling to predict peak levels of blast induced vibration Anderson, (2008). In the early 1980s a method for controlling blast vibrations was sought that did not mean manipulating the mass of the explosive charge and distance. The intent was to control blast vibration by firing a representative charge in a signature hole close to the production area of the tunnel under construction. The resultant vibration was then monitored at critical locations such at the foundations of buildings. Using a computer to superpose the resultant vibration waveforms with varying delays and by choosing delay times that create destructive interference at frequencies that were favoured by the local geology, the "ringing" vibration that excites structural elements in houses and annoys neighbours could be reduced.

The time-reversal principals and the application of cross-correlation/cross covariance techniques can be applied to localise the point of origin of impulses in the context of tunnel drill and blasting.

5.1 Scenario

If it could be determined from the experimental results that an impulse response could be identified from information in its discrete time signal, then a misfire detection and localisation methodology was conceivable as a three stage process.

1. Create a pre-blast signature impulse at each of the borehole locations on the blast face.

2. Monitor and record the impulses from the tunnel production blast
3. Correlate each production blast impulse with each corresponding signature impulse

In this way it was hoped that by establishing whether a signature signal was lacking a corresponding production signal, then we could identify the misfire location.

5.2 Experimental concept

Work carried out by Fink, (2006), demonstrated that a bounded acoustic cavity (sic. acoustic environment) will produce a unique relationship between an impulse signal location and a remote measurement location. They measured this relationship in many types of media and applied the results to time-reversal experiments, whereby the detected signal is recorded at one or more transducers and then played back in reversed chronological time sequence. The resulting wave fronts combine to reproduce a physical displacement at the point of origin of the original measured impulse as the time-reversed waves combine. We wish to exploit the unique signal filtering that takes place in the acoustic media that lies between the impulse emitter source and the transducer.

It is worth noting that the experiments conducted for this thesis differ greatly from earlier work on time reversal mirrors in several key respects, namely:

- Earlier experiments on time reversal mirrors were conducted on centimetre scale acoustic media.
- We carried out cross-correlation of dramatically dissimilar impulse signal amplitudes as there is a massive disparity between the initial signature-impulse and the second impulse from the production blast.
- The acoustic environment will itself be damaged, or partially destroyed during a tunnel production blast.
- Isolating a specific unknown candidate impulse in the presence of overlapping, or simultaneous impulses from other locations may be necessary
- Rock will by its nature produce an inhomogeneous acoustic medium and not the monolithic crystal used by Fink et al.

A series of scalable experiments were designed to identify the spatial limits of accuracy achievable in the intended context of a sequence of impulses culminating in a series of explosive shots. The experiments outlined here each used a single fixed-location detector to record the impulse vibrations. They were conducted on/in:

1. Composite wood substrate – small impact comparisons
2. Cast concrete slab – hammer impact comparisons
3. Quarry - detonator induced vibration comparisons
4. Underground mine - detonator and full explosive shot comparisons

5.3 Bench top experiment - Discriminating between impulse signals

The initial acoustic test bench chosen was a standard work bench. It was assumed that if the influence of the bounded acoustic media was consistent on the impulse signal, as observed in the signal correlation experiments and in time reversal experiments, then each impulse generated close to the original signature impulse location would deliver the highest cross-correlation coefficient results. Conversely computing the cross-correlation coefficient between impulses that were physically further apart should result in a relatively lower value of correlation coefficient.

A second investigation was made to observe whether the acoustic test bench changed its behaviour effect of the media on the impulse signal was stable over time. A series of measurement was made at each test point over a period of two days.

A third set of observations were made after making small changes to the test bench by loading it with weights.

5.4 Test method

Four target impulse positions were marked out on the 1600 x 800 mm workbench as shown on Figure 30 and a single geophone fixed to the benchtop as indicated. Signals were measured by a Model SM-4 geophone manufactured by IO Sensor Nederland b.v. Each impulse was sampled by the geophone connected to a

Picoscope™ USB oscilloscope. The sample rate applied to all desktop measurements was 9,766 kS/s and 4,888 samples recorded per impulse. The resolution of each sample is 8 bits. The geophone element generates an output voltage of 24 V/m/s. The geophone was rigidly secured to the edge of the bench top using a P-clip and thermosetting epoxy, which prevented any rocking of the geophone in its mount. This gave us the ability to measure physical displacements in the vertical axis.

Impulses were induced by sequentially dropping a small, 10 g, steel ball bearing onto the bench at the four target positions designated A – D in figure to create the library of 'signature signals', see Figure 30 and Figure 31. The ball bearing was dropped from a height of 10 cm and care was taken to capture it after the first bounce.

Figure 30 Desktop test set-up (1600 x 800 mm)

Figure 31 Schematic of showing the relative positions of the four target locations and geophone position

5.5 Impulse signal comparison

The sensor would receive not only the direct-path signal, but also attenuated and delayed replicas of the source signal coming from reflections from the random boundaries of medium i.e. the edges of the bench and the holes in the bench itself. The aim of the experiment was to ascertain whether impulse signals could be classified and consistently assigned to a unique location in a bounded acoustic environment.

Cross-correlation of two discrete time series is a well-established technique to establish the similarity or otherwise of the two discrete time signals. To establish the characteristics and similarity of impulses generated at various positions around a solid medium, multiple sets of impulses were recorded which were then compared to each other with one set being designated as target, or 'signature' signals.

In other applications such as in sonar target detection it is commonly used for searching a long signal for a shorter, known feature by finding a component of an emitted target signal in a noisy received signal. The process of cross-correlation (or cross-covariance) consists of the displaced dot product between two signals. In our case, since all measurements were recorded using digital acquisition systems, all signals under study have been recorded in discrete time, so that the correlation between two signals x and y with the same N samples length is expressed by the following expression Eq 28:

$$Corr\{x, y\}[n] = \sum_{m=1}^{N} x^*[m] \cdot y[m+n] \qquad (5)$$

Where x^* is the complex conjugate of $x(m)$ and the bullet operator $\cdot$ denotes the cross correlation.

By using the cross correlation function, we identify the degree of similarity by using the magnitude of the first positive peak. For our purposes, we are disregarding the negative-going peak as we are seeking a positive correlation between our two candidate time series signals in a linear, time invariant system. The maximum of the first positive peak calculated in the correlation function was used to indicate the level of correlation of the two signals.

In addition, as signals of greatly dissimilar energies would be compared, they were normalised prior to conducting the correlation function.

By calculating and comparing the cross-correlation coefficients, it was found that there was a distinct spatial degradation in the observed values between the signature signals made at the target position and signals originating at any other position on the test bench. The spatial decay was characterised around the four locations on the bench and the results tabulated and mapped.

It was decided to employ the cross-correlation coefficient to compare the signature impulse with the candidate impulses. The cross-correlation coefficient for each comparative calculation was then mapped onto the test bench.

5.6 Cross-correlation coefficient Stability

Repeated impulse measurements were made at each test point to ascertain the variability of the cross-correlation coefficient. A typical waveform is shown below in Figure 32.

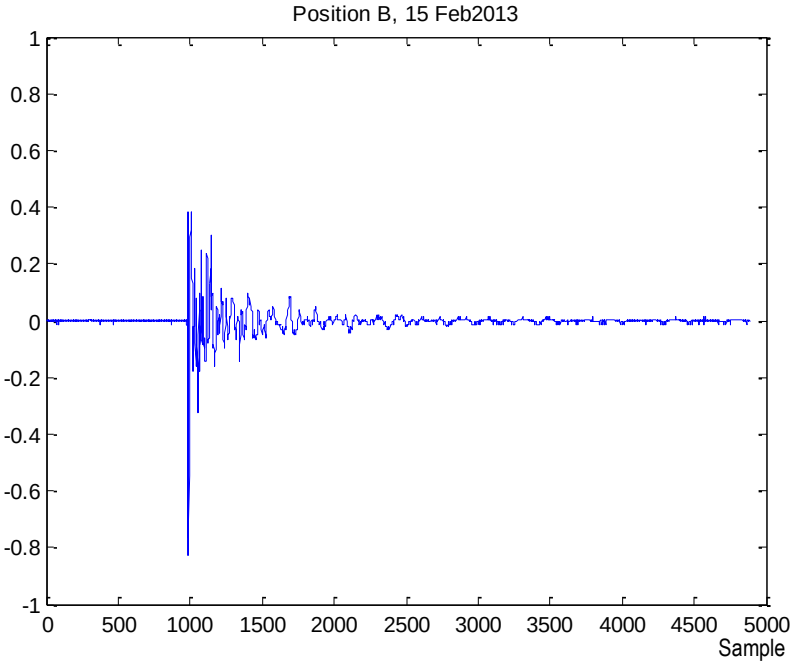

Figure 32, Impulse Position B

The cross-correlation function was calculated in Matlab for five impulse samples at each of the four locations.

This cross-correlation result displayed as the normalised value with respect to the standard deviation.

The output of this processing returns an output between zero and 1 and was plotted.

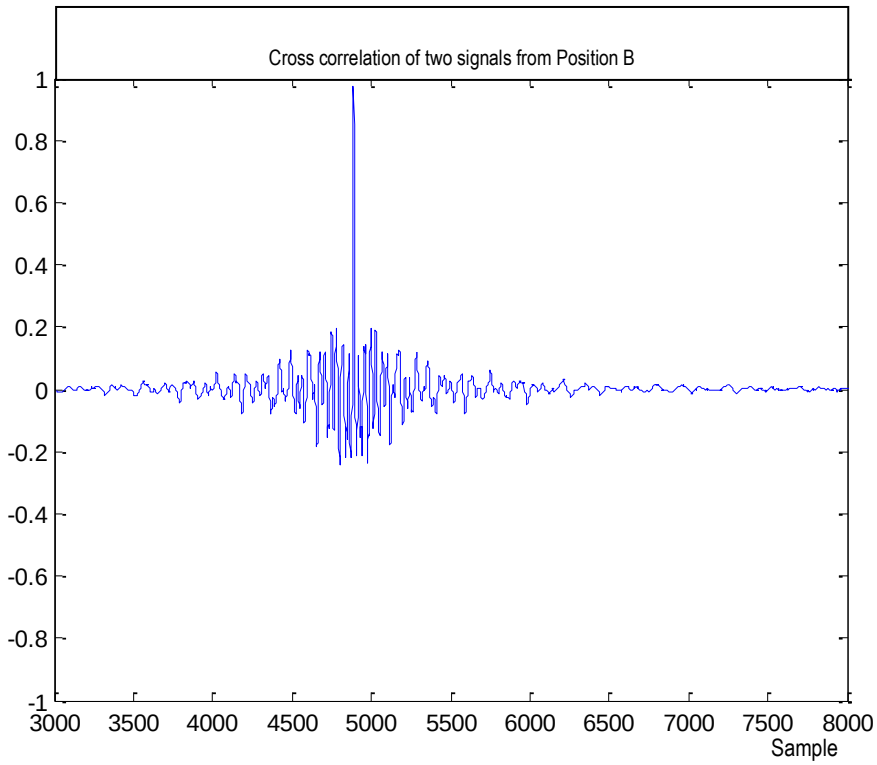

Figure 33 Cross-correlation coefficient, Position B

Once again the distinctive peak indicating that there is good correlation between the two consecutive signals was present. The presence and contrast of this peak was used to assess the results of the changes in impulse location and in the time delay observations.

5.7 Signature impulse measurements

At the outset of the investigation into the spatial decay of the cross-correlation coefficient, a set of quickly-spaced, base-line signature impulse measurements was made for each of our four target positions. These signals were sampled and compared using cross-correlation. An example of the cross-correlation output observed from impulses made at the same location is shown below in Figure 34.

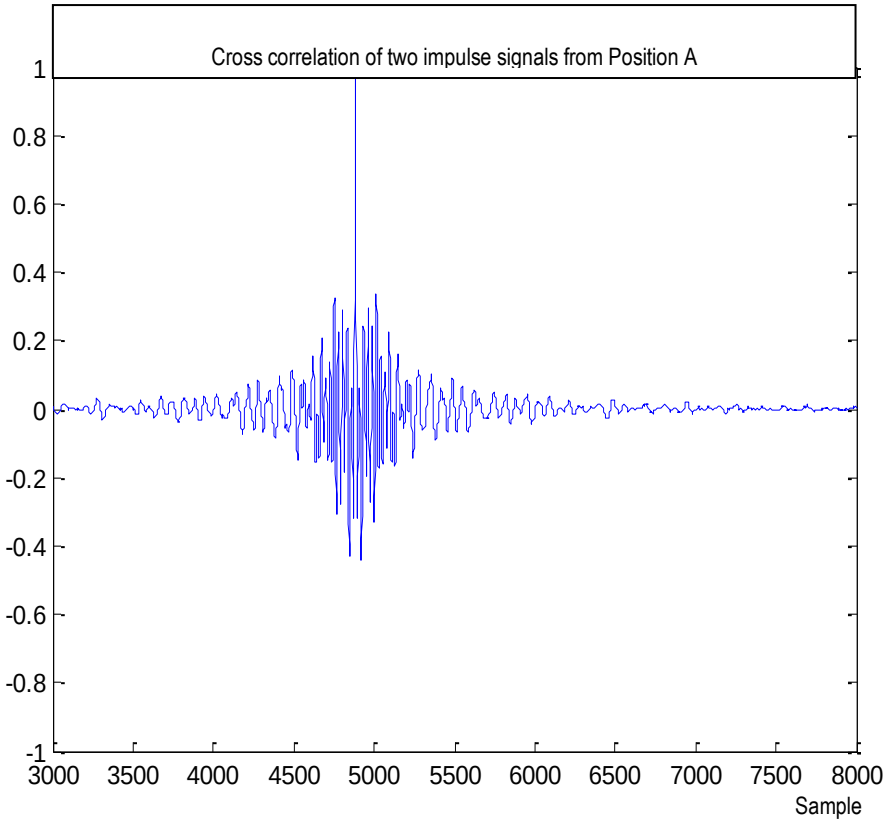

Figure 34 Cross-correlation of two Impulse Signals at Position A

Typical variations in the values of cross-correlation coefficients are shown in Table 6, Cross-correlation coefficients for 5 Impulses at Position A.

In this example there is very little variation in the cross-correlation coefficient indicating that the technique of using cross-correlation was a useful tool to compare the impulse signals. A series of 5 impulses was recorded at each of the designated target locations, the same repeatability with high correlation coefficients was achieved.

Table 6, Cross-correlation coefficients for 5 Impulses at Position A

Position A	Impulse 1	Impulse 2	Impulse 3	Impulse 4	Impulse 5
Impulse 1	1	0.9692	0.9688	0.9664	0.9547
Impulse 2		1	0.9619	0.9551	0.9614
Impulse 3			1	0.9639	0.9724
Impulse 4				1	0.9486
Impulse 5					1

Figure 35 shows the cross-correlation coefficient for signals from position A and from Position B. Our fundamental aim is to differentiate signals originating from different locations and conducting a cross-correlation of signals from different locations gave a result showing little similarity between signals.

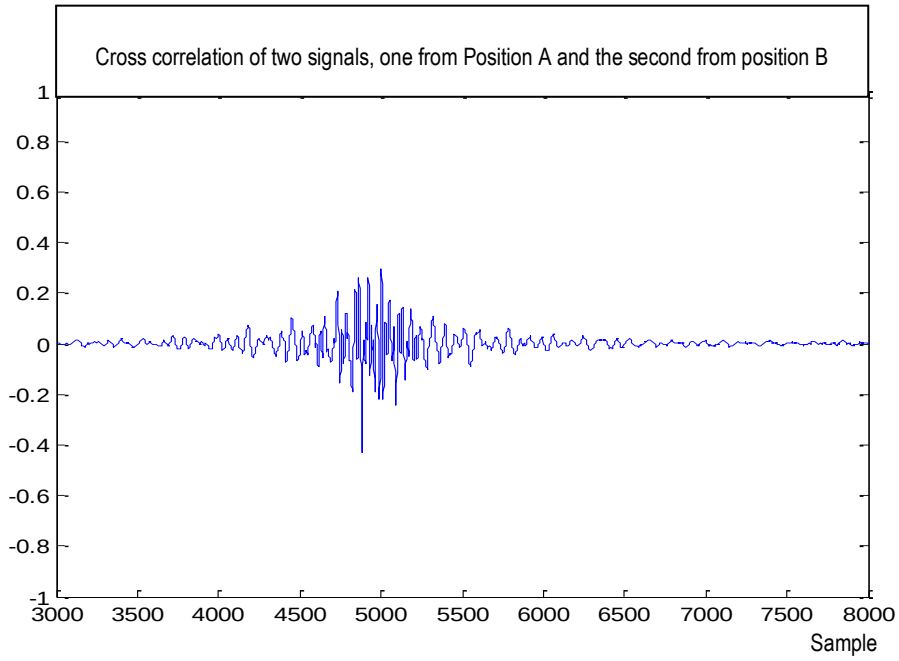

Figure 35 Normalised cross-correlation of Signals from Position A and Position B

In the example shown Figure 35, the correlation coefficient peak value is 0.2932. This is clearly lower than the values obtained from correlating signal made between repeated impulses made at the same location, which gave values closer to unity.

This procedure established that the correlation coefficient could be used as an indicator to localise the origin of an impulse signal by comparing signals from an unknown source and comparing it with the library of signature signals. Establishing which signature signal from positions A, B, C, or D best matched any unknown signal using the correlation coefficient as our measure enabled to classify its point of origin.

5.8 Spatial Cross-correlation coefficient decay results

Investigations were carried out on the spatial decay of the correlation coefficient as consecutive impulses re made when increasing range from the original impulse position. Measurements were systematically recorded at each signature impulse point then at a series of points of increasing radius from the original impulse location. Figure 31 shows the relative positions of the four test points.

Figure 36 shows how the calculated cross-correlation coefficient between a signature impulse signal and a target signal varies as around the central position of Position A.

The first set of measurements was made at a radius of 5 cm from the signature impulse, and the second set made at 10 cm.

As the test positions were close to the edge of the bench itself variation of the cross-correlation coefficient was expected depending on the specific orientation and the range from the signature impulse origin. Measurements were made in four quadrants Q1 – Q4 clockwise around the origin for each position.

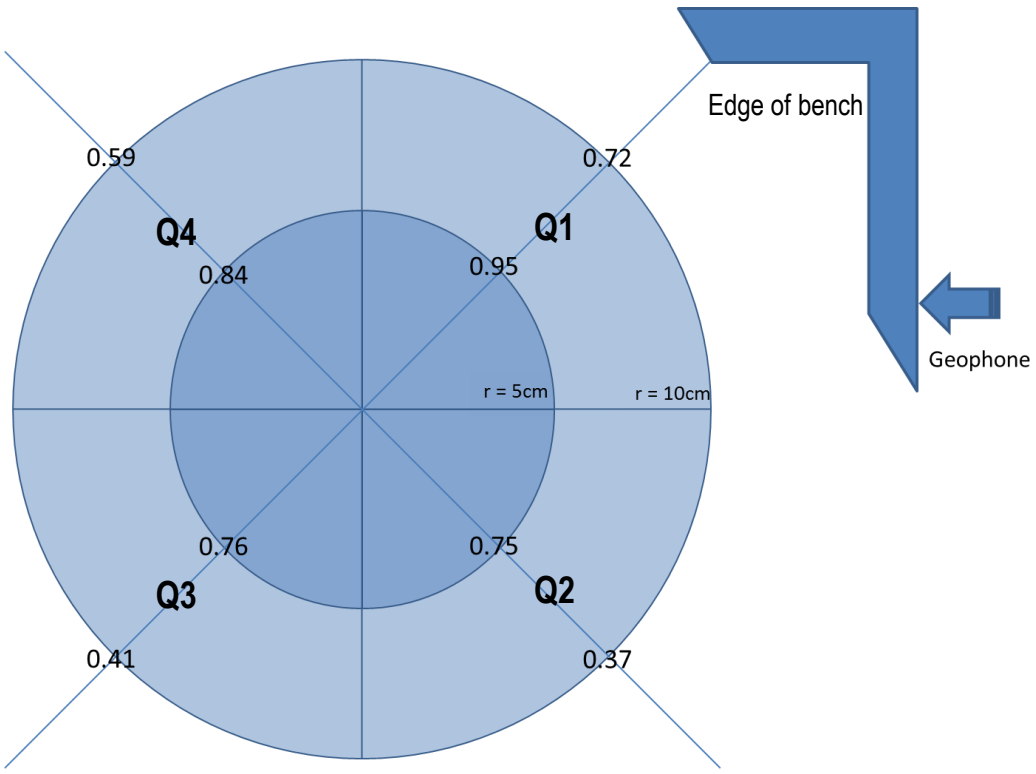

Figure 36 Position A, Correlation coefficient calculations

Position A is in the top right hand position of the test bench as shown on Figure 31 and it is the closest to the sensor. It is worth noting that repeated calculations of correlation coefficient made at any of the centres of each test Position A-D, yielded a coefficient value of 0.95, or above.

Figure 30 maps the values of correlation coefficient obtained by correlating signals made at the centre position and signals from impulses made at a radius 5 cm and at 10 cm from the centre of the target.

The results show that impulse signals generated away from the initial centre will resulted in an expected degradation in cross-correlation coefficient from levels > 0.95, to levels < 0.9; with the single exception of test Position A, Quadrant 1.

Additionally, it was seen that increasing the radius in any direction resulted in a reduction in cross-correlation coefficient. Again, one exception to this. Position C, Q3 which gave an increase in the cross-correlation

coefficient at the higher radius from the centre of Position C , but only in 1 quadrant. The other three quadrants returned the expected reductions in the cross-correlation coefficient.

The cross-correlation coefficient maps for the remaining positions are shown in Figure 37Figure 38Figure 39, below.

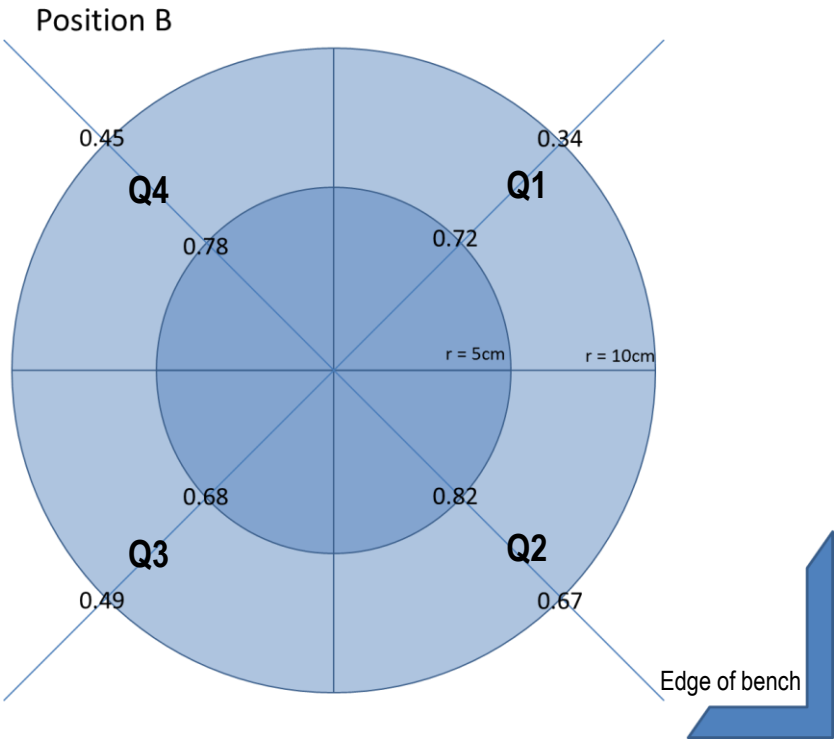

Figure 37, Position B, Correlation Coefficient calculations

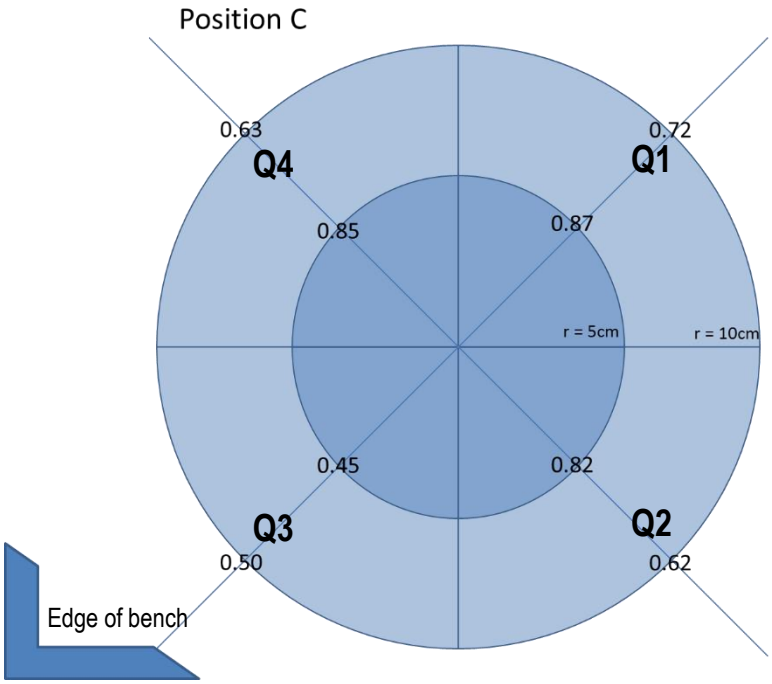

Figure 38, Position C, Correlation coefficient calculations

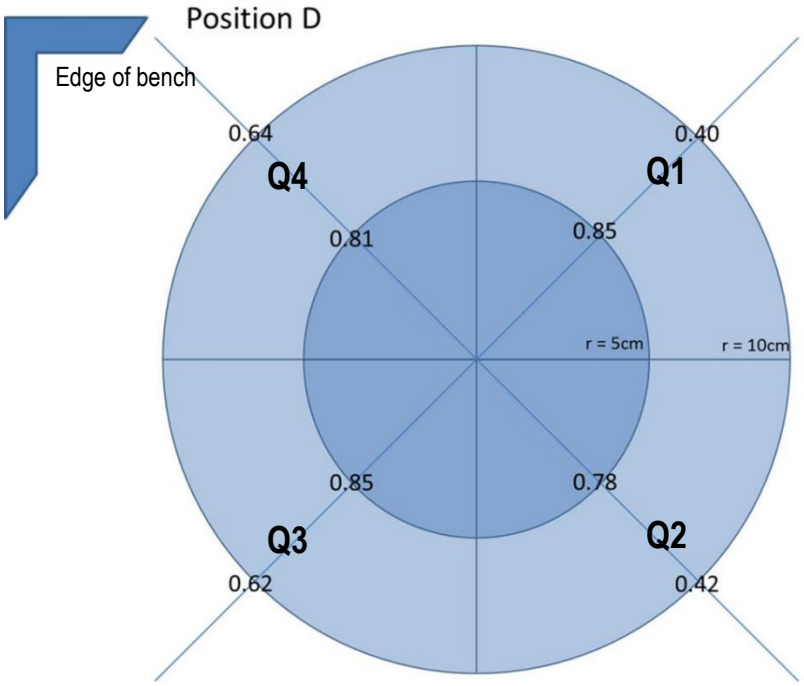

Figure 39, Position D, Correlation coefficient calculations

In conclusion for each of our target signature source positions, it was seen that a consistent change in the calculated cross correlation coefficient within 5 cm of the signature location to average values of 0.75 – 0.83 across the four target positions. At a range of 10 cm correlation coefficient values had fallen to average values of 0.49 – 0.62 across the four target positions. Clearly the expected outcome of decreasing correlation coefficient with respect to increasing distance between impulse positions was present in data.

5.9 Degradation of impulse discrimination with distance

A second set of experiments was conducted to establish the influence of distance on the ability to discriminate between impulse locations using signal cross-correlation.

A 1 cm grid pattern was marked out on the test bench and impulses were again made by a dropping a 10 g weight onto the bench surface. Taking care to prevent bouncing. A nominal signature impulse location was chosen at the centre of the grid for the purpose of the experiment. The cross correlation coefficients between our signature impulse and every other impulse were then calculated in Matlab and the output mapped against location.

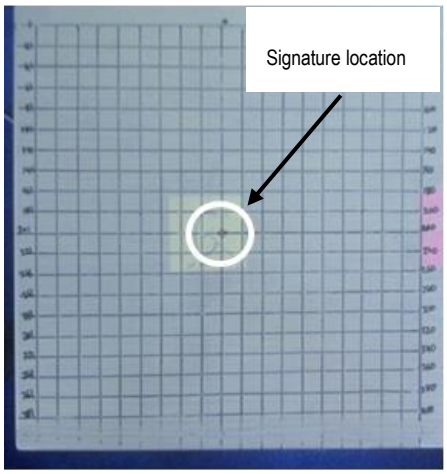

Figure 40 20 x 20 cm grid on composite fibre board experiments

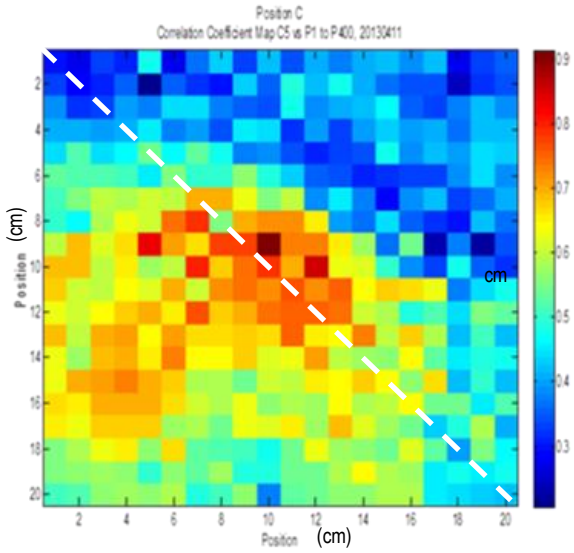

Figure 41 Spatial map of Cross-correlation coefficients calculated from composite fibre board experiments

Figure 40 shows an image of a 20 x 20 cm grid that was marked out on a 0.6 x 1.6 m rectangular fibre board base. Impulses were made at each of the 400 positions on the grid, and the resulting impulses measured using a single axis accelerometer fixed with bees wax at a position around 70 cm distant off-grid. Signals generated at each of the grid points were correlated against a signature signal that was recorded from an impulse made at the central point (indicated by the white circle) in Figure 40. Cross-correlation coefficients were calculated and then plotted in a 20 x 20 matrix in Matlab, with the higher coefficient values (best match) represented by a dark red colour, and the lower values in dark blue.

Figure 36 shows that the correlation coefficient decays as impulse points moved progressively away from the target signature position at the grid centre. Although it doesn't decay homogeneously, it can be seen that the normalised, on-target cross-correlation coefficient value is close to 1, with the next nearest position returning a value of around 0.75.

Given the earlier results with target locations at the four extremes of the workbench, these results imply that higher values of cross-correlation coefficients should be expected as we progressively move towards the location of the signature impulse.

Using this technique signature impulse positions could be consistently identified to within ~ 5 cm.

So the edges of the media were adjacent to Row 20, and Column 1 as shown Figure 41. It can be seen that there is a clearer differentiation between the centre position and point on the upper right half as demarcated by the diagonal line running from R1,C1 and R20, C20. Given that calculating the cross-correlation between impulse signals from any two points establishes a measure of the similarity of those signals, there is clearly less similarity between points further away from the edges of the test bench. The speed of sound in timber is approximately 3000 m/s. The impulses propagating on a direct path from the impulse location to the geophone will arrive after approximately 0.55 ms. Impulses originating to the right of the signature point will be composed of waves reflected from the edge of the bench with a lag of approximately > 0.14 ms. Groups of waves originating to the left of the diagonal will travel through the signature impulse position within fractions of a millisecond and propagate to the geophone all the while and continue to radiate towards the bench

boundaries. The reverberation in composite timber will be less than natural timber due to the nature of the glues and soft wood used in their manufacture, but it is clear from the cross-correlation results that longer impulses measured at the accelerometer are a result of multiple reflections within the bench. It is also clear that moving the impulse source, even marginally, results in a significant change in the nature of the group wave arriving at the geophone and that performing a cross-correlation demonstrates that difference.

5.10 Signal comparison with a modified test bench

In order to ascertain how modifications to the test bench would affect composition of the media. Impulse measurements were taken before and after placing a 5 kg weight at centre of the bench. It was expected that this would change the way the effective volume and spatial boundaries of the material and how it reverberates. A series of five impulses were made pre and post loading. Figure 42 shows that there is still a distinct peak in the cross-correlation coefficient, but it is significantly degraded.

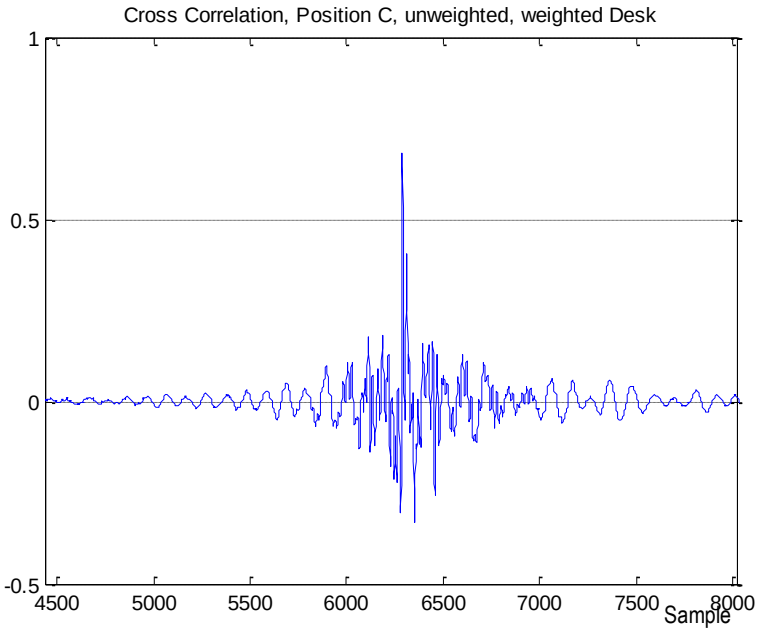

Figure 42 Cross Correlation Coefficient of impulse signals before and after modifications with a load

The cross-correlation coefficient results measured at between the original unweighted bench and the weighted bench measured at Position C ranged from 0.6711 to 0.6801 . This is in comparison to values of 0.95 and higher that were realised between impulse made before modifications were made to the test bench. This pattern of a reduced, but still distinct correlation was repeated at each position on the test bench.

5.11 Conclusions

Comparing sets of impulses made at a fixed location with impulses made at an increasing radius for the original position there was a significant reduction in the cross-correlation coefficient at a radius of 5 cm from the initial impulse location. A further marked degradation was apparent at a range of approximately 10 cm from the initial signature excitation point.

There was no measureable change over time in the cross-correlation coefficient values between impulses made at the same location but on different days. This indicates that the influence on the impulse by the acoustic media remained stable at least over a period of days; returning repeatable, high peak values of cross-correlation coefficients.

In addition, moderate changes to the acoustic media could be made (in our case by loading the bench with weights) and a high correlation coefficient value was still observed. This level of correlation would depend on the method by which the weights are applied to the bench. If the additional weights presented a large surface area to the bench, this not only modified the bench's behaviour, but in effect added a volume of material to the acoustic environment and change the shape of the bounded media, which would consequently influence the impulse.

Applying these results to the blasting context, the implication of the observations on signal correlation is that each acoustic path between each shot hole and the location of the detector could potentially be characterised by a signature impulse measurement. Our intent in carrying out observations on modified acoustic paths is to begin to appreciate factors in the blasting context where the physical shape of the rock will change, but to exploit the unique influence on the impulse signal experiences from the remaining intact rock and thereby to consistently identify the point of origin of an impulse.

Additionally it implies that if the path between the excitation source location and receiver doesn't overlap positions of other candidate impulse locations, we may achieve higher discrimination using impulse cross correlation coefficient

From these results it was decided that it was valid to conduct further tests on larger scale cavities and in situ tests underground and attempt to isolate the location of impulses created by more energetic explosive charges.

It was decided to use the cross-correlation coefficient as the comparative measure for all of the subsequent tests to observe the spatial dependency of signal correlation.

Chapter 6 Impulse Correlation in a Particulate Composite Matrix

In the preceding chapter the spatial dependency of the acoustic path in a low density solid media was examined. It was found that for a macro-scale acoustic cavity, a map the decay of spatial coherence by computing the cross-correlation coefficient from sets of impulse signals could be made.

In the next experiment investigated the influence of an increase in range between impulse source and detector in an elastic medium, two sets of tests were carried out with similar dense media i.e. concrete, but with increasing magnitude of detection range and impulse energy. The two test media were (a) Steel reinforced concrete beam and (b) Steel reinforced concrete slab.

6.1 Concrete Beam

Concrete is classified as a particulate composite matrix and on the macro scale concrete can be considered a homogenous material. The concrete beam used for the first experiment is 150 x 150 x 900 mm. the beam was simply supported on narrow bearings at two points close to the ends.

Figure 43 Test set-up - spatial decay of coherence in a particulate composite matrix with the accelerometer location highlighted in yellow

As in the previous experiments on a composite timber bench, a set of five impulses was made. In this case a small hammer was used to produce impulses at 10 cm intervals along the length of the beam shown in Figure 44. The resulting signals were recorded with a single PCB model 353C22 accelerometer fixed with beeswax at one end of the beam on the top surface. The accelerometer signal was fed into an ICP Conditioning amplifier LM-148 the output was then sampled by a Picoscope 2-channel USB oscilloscope.

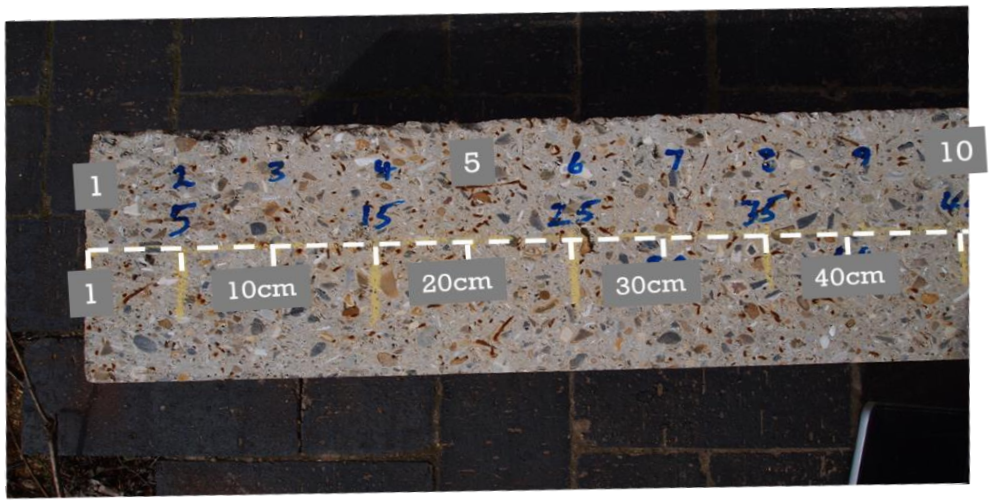

Figure 44 Impulse positions along the concrete beam

A second set of signals was made at the same positions and the impulses recorded. The samples in Set 2 were then correlated with the initial signature set of impulses using Matlab. A nominal target location was chosen at the centre line of the beam as a reference point.

6.2 Results

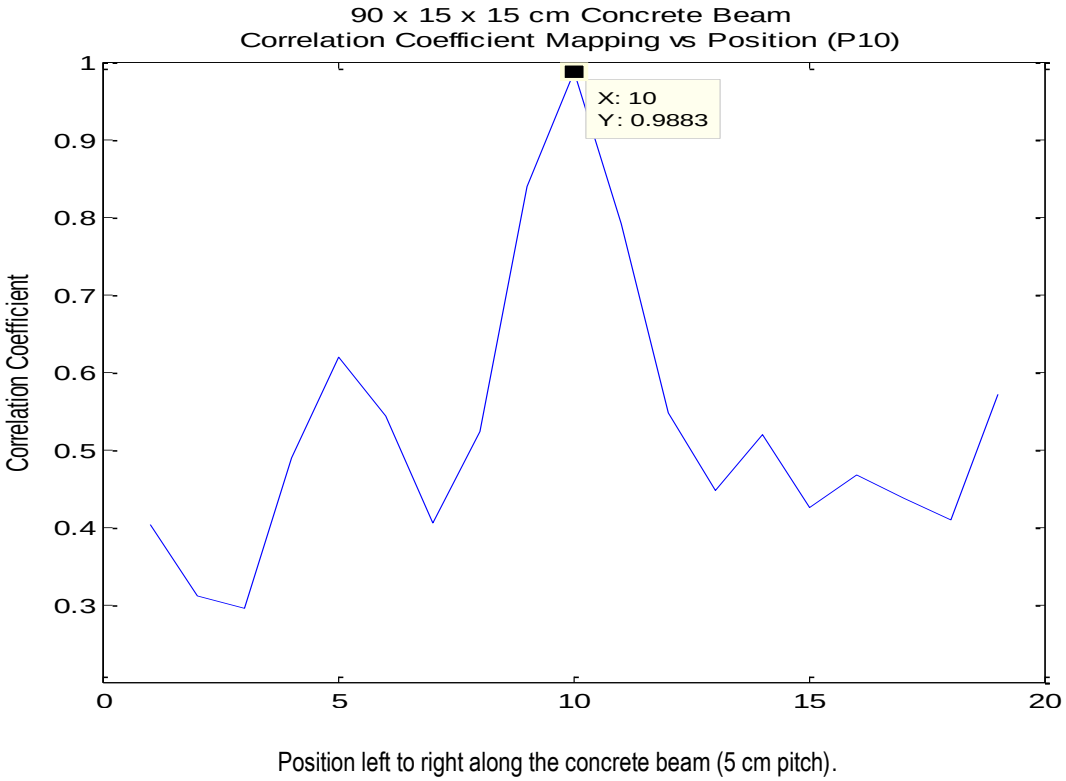

Figure 45 Decay in spatial coherence in concrete media with the signature impulse at Position 10

The strongest correlation was seen between two impulses generated at the same position. For this beam geometry it was observed that the correlation coefficient reduce as impulses were made further away from the signature impulse location, however it did not decay linearly with range. There was a substantial decrease in the correlation coefficient value (from 0.99 to 0.45) at short separation distances of around 10 -15 cm. The presence of two side peaks in the correlation coefficient is noteworthy.

Both longitudinal and sheer velocity *Vs* in concrete is of the order of 3000 m/s for normal strength concrete with an unconfined compressive strength of ~35 MPa given by the equation:

$$Vs = \sqrt{\frac{E}{\rho}\frac{1}{2(1+2\vartheta)}} \qquad \text{Equation (6)}$$

Where E is the Young's modulus, ρ is the material density and ϑ is the Poisson ratio.

The test beam was struck on the top surface to generate the impulse required for the correlation comparisons. The beam cross section was 15 x15 cm. Given the frequency spread observed between 50 -200 Hz the impulse will effectively generate a plane wave with λ of 15 - 50 m, with its source at the medium bounded surface. The wave will traverse the beam twice in a period of around 0.10 ms and losing energy to the elastic excitation of the concrete. The peaks and troughs are of the correlation coefficient between the signature impulse and subsequent impulses moving away from the signature position and not to be confused with standing waves of interference modes. Given that the accelerometer was located at the end of the beam, it is not surprising that the waves have strong similarities since they all contain waves reflecting from the top surface of the beam that propagate to the ends of the beam and reverberate under the energy has dissipated. However it is clear from Figure 45 that that there is a clear contrast in the peak of correlation coefficient. This was born out comparing other locations on the beam.

There is a flattening of the correlation values to the right of the central peak. These locations lie between the signature position and the sensor, so there may again be a more significant difference between the impulses generated between the positions whose initial paths do not propagate through the position of the signature location.

6.3 Experiments on a steel-reinforced concrete slab

A similar experiment to that described in Section 6.1 was conducted on a concrete slab.

The slab was a large area of concrete which was approximately 3 x 5 m attached to a multi-storey building along one edge and into a set of cast concrete steps. Figure 46 shows the test grid marked out on a 1.0 x 1.0 m square, with 10 cm spacing between measurement positions. The white circle shows the position of the nominated signature location at Position 55.

Impulses were made at each position across the grid by means of a drop hammer (shown in Figure 46). The hammer consisted a 1 kg steel mass guided by a bar through its centre. It was used to deliver single point impulses and two-point impulses into the slab. Signal measurements were made by a single PCB model 353C22, 1 to 10,000 Hz range accelerometer, fixed with beeswax. The sensor was mounted at a distance of 50 cm to the right of Position 100. The accelerometer signal was fed into an ICP conditioning amplifier LM-148 and the output was then sampled by a Picoscope 2203 2-channel USB oscilloscope at a sampling rate of 8kH.

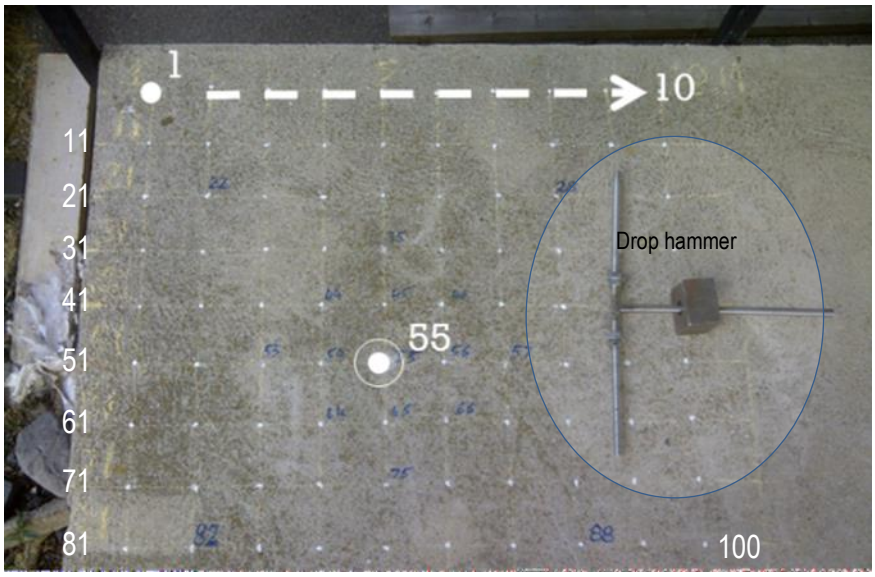

Figure 46 Test set up of investigation into spatial coherence in concrete slab

The cross-correlation coefficients were calculated between each candidate impulse and the impulse from the target signature position P55. The correlation coefficient values were plotted against impulse location.

Independently of where the nominal signature location was chosen to be across the grid, the maximum correlation between was consistently observed at that target position.

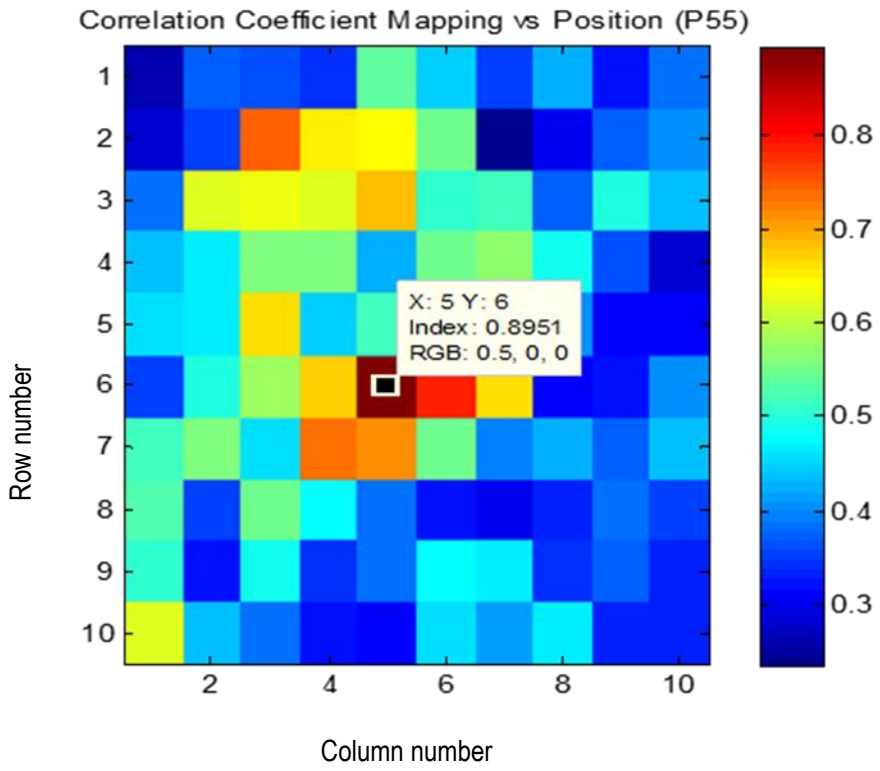

Figure 47 Decay of spatial coherence in an concrete media

Repeating the exercise at alternative target signature locations across the slab yielded similar results.

With reference to Figure 47 we can see that the correlation coefficient is lower at the lower right hand diagonal of our test matrix. The location of the accelerometer is on that side of the matrix and in line with that last row. i.e. location R10,C10 is the closest to the sensor. In that quadrant of the matrix within 20 cm of the target signature point, there is a 60% reduction in the correlation coefficient. The edge of the concrete slab is clearly visible to the left of column 1 in Figure 46 and impulses from positions in this column will generate a reflection from the edge within 0.06 ms that will become part of the wave travelling towards the sensor. In comparison impulses generated at R10,C10 which will radiate out in all directions and reach the sensor after 0.2 ms. Reflected waves from the edge would not arrive at the sensor until 0.9 ms, given a propagation distance of 2.7 m and an estimated wave velocity of 3000 m/s. Given that correlating the signals reflects the degree of similarity between the signals, we can then infer that the signals whose source locations that lie between the signature impulse location and the sensor can be more clearly differentiated than those further away from the receiver.

6.4 Finding a Target Location in the Presence of an Interferer

In the context of tunnelling the firing sequence may by design initiate multiple charges at the same time, or the blast impulses may overlap essentially occurring simultaneously.

It would be advantageous if this method could match a signature impulse to a candidate from the target point of origin in the presence of one, or more interfering noise signals. To this end, additional experiments were conducted on the concrete slab to compare sets of signature impulse signals with a subsequent set which comprised of one impulse generated at the target location plus an off-set interferer impulse. This was achieved by designing a simple drop hammer to have two points of contact with the slab. Figure 48 shows an example of such a correlation coefficient.

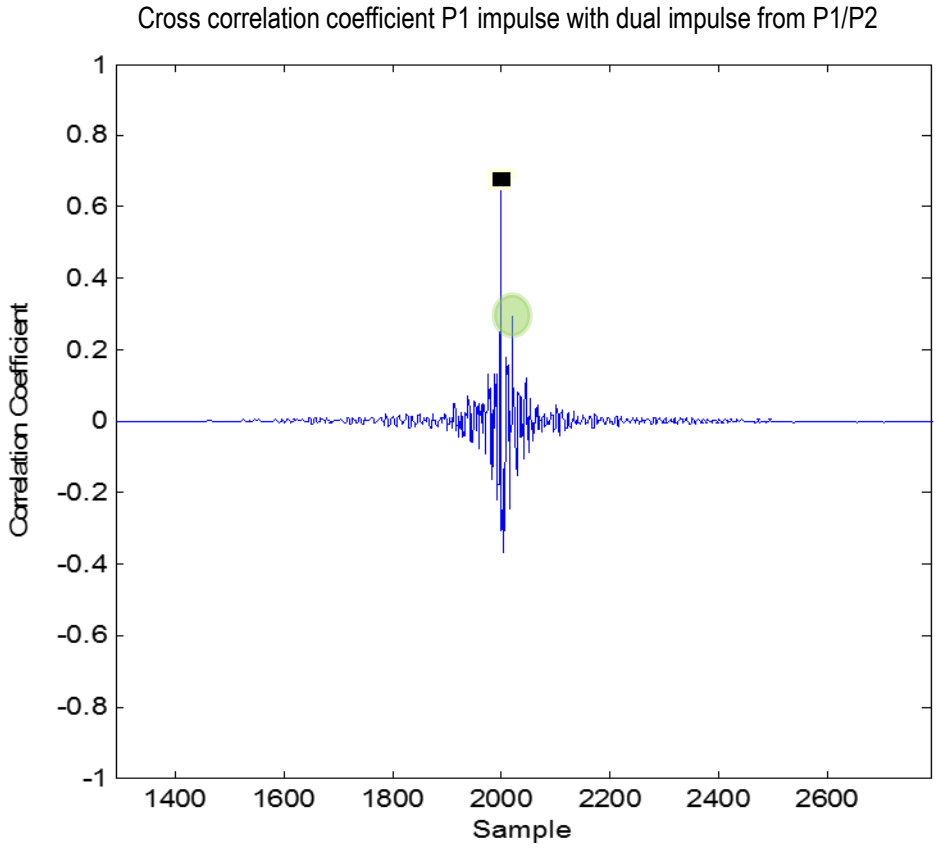

Figure 48 Correlation of the signature impulse with one from the signature location plus interferer

The distinct peak indicated in the figure above shows a strong correlation peak between the signature impulse and an impulse containing mixed signals from the signature impulse location and a 2nd off-target interference impulse was generated at a position 10 cm away from the target location.

Figure 48 also shows a smaller peak (highlighted in green) to the right of the main peak resulting from the interfering signal giving a lower level of correlation with the signature impulse generated at our target location but still with a degree of similarity between the two signals. The correlation trace shows this as a lag off-set and a significantly smaller correlation coefficient value of close to 0.3.

6.5 Conclusions

From the results of these three experiments there appeared to be scope to use the cross-correlation coefficient as a metric to understand the behaviour of the decay in spatial correlation of impulse signals.

We demonstrated that in a relatively large scale, particulate composite matrix such as concrete, the spatial correlation of impulse signals is highly localised and that signals can be differentiated at separation distances of around 10 - 20 cm. This order of magnitude is of significance in our context as the spacing between explosive charges in underground tunnelling is of the order of 30 - 50 cm.Being able to discriminate between impulse source locations origins that are 10 - 20 cm apart from one another gives promise to this technique in the context of drill and blast in tunnelling. Demonstrating some applicability of this method in concrete suggests that it could be viable in certain types of natural rock environments.

Chapter 7 Utilising the Blast Vibration Signature

Having demonstrated that the use of the cross-correlation coefficient could help differentiate impulse source locations in a concrete particulate composite matrix, the next practical step was to extend the scope of the investigation to conduct higher energy impulse comparisons in rock. Since no such facilities were available in the University of Southampton an approach to the Camborne School of Mines (CSM) a part of the University of Exeter was warmly received and plans were made for a series of scaled experiments.

7.1 Camborne School of Mines Test Mine

The CSM test mine is located near Truro in Cornwall, United Kingdom. Prior to becoming an asset of the University of Exeter, CSM was owned by the mining equipment company Holman Brothers of Camborne. It was used as a demonstration site for their world-class range drilling equipment manufactured by them at that time. The test mine is composed of a gallery of development drives and sub-levels over an area of approximately 150 x150 m. The mine reaches into a hillside from a quarry entrance to a maximum depth of around 20 - 30 m from the ground surface above. Access is via a 'walk-in' from the quarry so there is no vertical shaft.

The geological nature of the rock in this area is 'coarse grained Semi-Megacrystic Biotite Granite Selwood, (1998). This region is part of the Cornumbian Batholith which goes to depths of more than a kilometer. The underground galleries have significant numbers of veins and elvan dykes LeBoutillier, (2002). For the purposes of these experiments the area around the mine and the galleries provided a competent stable and dense rock structure in which to conduct multiple blasts. Granite in this quarry has uniaxial compressive strength of around 120 -150 MPa, in comparison to concrete used in earlier experiments with a uniform consistency and compressive strengths of approximately 40 - 60 MPa. Earlier research identified three principal joint sets in this granite. This did not impact our experiments as we selected competent zones with no visible joints, or discontinuities in our detection path between impulse source and receiver. The acoustic velocity in this type of rock is around 5950 m/s.

In addition to mining research, the mine played host to numerous student cohorts being trained in the use of explosives underground which provided opportunities to monitor production blasts.

A map of the entire test mine is shown below in Figure 49 .

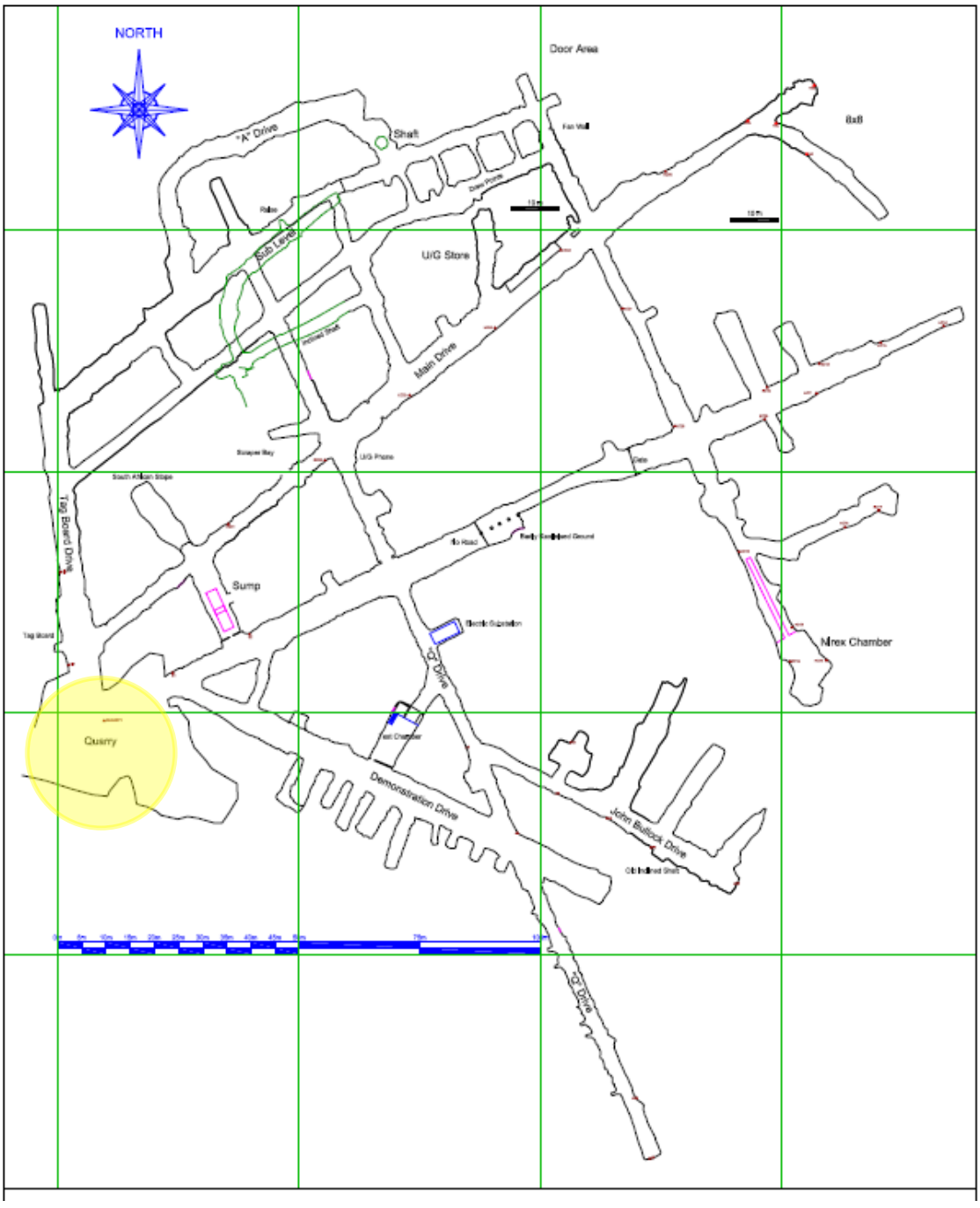

Figure 49 Map of the CSM test mine

CSM use a variety of detonator types. Due to the availability of nonel shock tube and detonators at that time it was decided to use these to generate impulses for the initial experiments in the CSM quarry. We chose mass manufactured, #8 strength detonators that ensured near identical quantities of explosives were fired in each shot. The detonators used in the first set of experiments were used to generate relatively low magnitude impulses, they are not normally powerful enough to fracture, or fragment rock.

Downhole detonators are composed of both a primary charge of Lead Azide and a base charge composed of PETN, or poly-coated PETN to provide the explosive strength necessary to detonate modern explosives. The timing precision is of the order of ±0.025 s Silva, (2017). This timing variation is insignificant in our experiments as we fired only individual charges, or deliberately aimed to overlap some impulses.

7.2 Peak Counting

Early investigations examined information that could be derived from remotely monitoring the vibration time trace signals using geophones, or accelerometers. In conjunction with a fellow PhD researcher at the CSM, together we prepared several multi-shot blasts with the purpose of observing the resultant vibration trace. Ewusi, (2013) went on to make an extensive assessment of the applicability of peak counting comparing the viability with PED and nonel initiation systems.

7.2.1 Peak Counting Test Set-up

Small production blasts were made at a location known as “The 8x8 Drive” as shown in Figure 50. The blast-induced vibration monitoring was conducted with geophone-based seismographs at 5 sites (also shown in Figure 50). The geophones were mounted on the tunnel wall onto rigidly anchored steel plates and connected by foil shielded cable to protect the transmitted data from any potential atmospheric interference from the many electrical pumps and transformers underground connecting back to a central data acquisition unit Adderley, (2009). Particle velocity data from the blasts was sampled at a rate of 10,000 samples per second on each of the three orthogonal channels. All blastholes were drilled using the mine’s jack leg drill to a

diameter of 35 mm. Some holes were reamed to create a larger free face/void (the cut) and so were enlarged to 75 mm diameter. Wooden spacers were placed in between explosive cartridges to distribute the explosive strength along entire depth of the blastholes We prepared the holes over a period of a week. The blast was not designed to be an actual tunnel development blast and consequently each hole contained only one 200 g cartridge of Perunit™.

This set up had been established in the test mine to facilitate regular monitoring of mine activity. Each geophone consisted of three mutually perpendicular SM-6 long-coil geophones having natural and frequency of 4.5 Hz and 140 Hz respectively. Each tri-axial geophone unit was mounted in a sealed plastic case sealed with silicon to prevent water ingress. The tri-axial geophone unit was configured such that a zero value corresponding to zero movement would indicate a voltage level of approximately 5.8 V. An IOTech Personal DAQ 3000 data shuttle implemented as the data acquisition unit (DAU) was used to capture the signals from the geophones in their operating mode and converted to a digital format for analysis with conventional commercially available software packages. The data acquisition unit was capable of sampling up to 1 MHz speed across 16 channels of analogue inputs. The data acquisition was triggered using an outsider trigger window which allows the DAU to commence sampling when the geophone voltage deviated outside a range of 5.733 - 5.83 V.

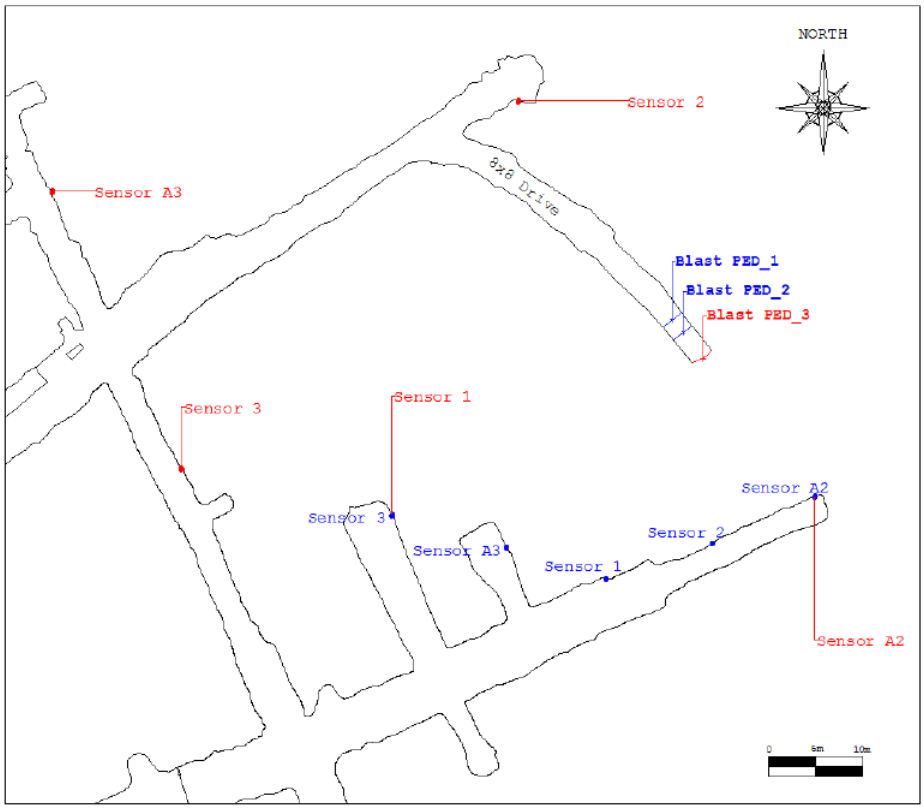

Figure 50 Map showing the location of the site used for programmable electronic detonator (PED) initiated blasts (PED_1, PED_2 & PED_3) and the geophone locations

To make the task of peak counting easier the results are displayed as absolute values. Used in conjunction with the plan of the firing sequence goes a long way to providing an understanding of what has taken place during the blast.

7.2.2 Observations from PED initiation systems

A typical example of the vibration trace using PED initiation system is shown in Figure 51. This was planned to be a 24 discrete shots blast Ewusi, (2013) with identical charges; each charge set to fire individually in sequence on a 50 ms delay. This signal was recorded by a geophone situated 36 m from the blast face.

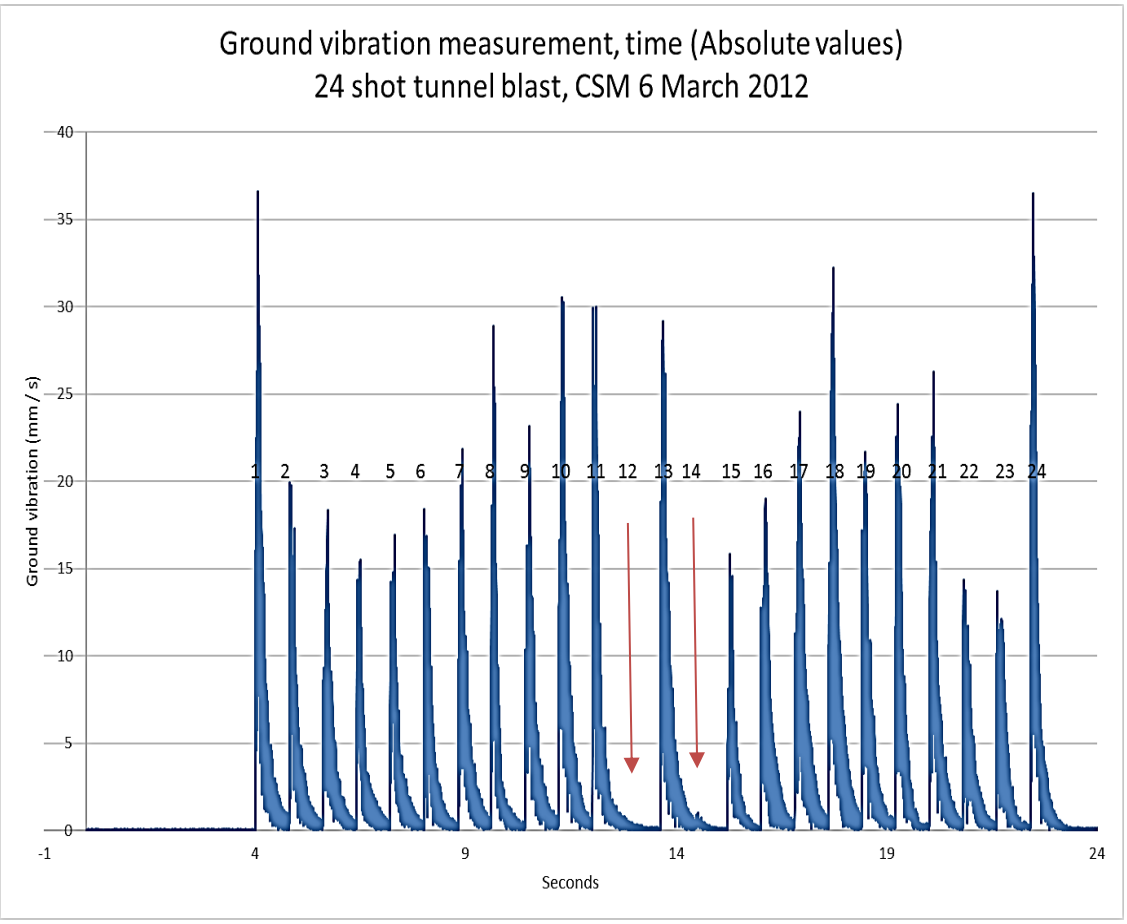

Figure 51 Full face blast time trace at the CSM test mine. Blast PED1, Sensor 3 (36 m from blast site)

The peaks generated by the individual shots can be clearly observed. A cursory glance at the time trace is sufficient to see that Shot number 12 is a concern. Either it has failed to fire entirely, or perhaps fired at the same time as shot number 11 (which looks like it could be a double peak), or it fired along with #13. Since both #11 and #13 show no apparent anomalous characteristics, it is possible that #12 has misfired. From the test plan on the day, there were no expected gaps in the firing sequence and we see that shot #12 is completely missing in the sequence and #14 appears to be a partial detonation. Altogether, there are causes for concern. As #11 is high, there is a possibility that the missing #12 fired at the same time. Another possibility for #11 being

disproportionately large is that the rock burden could have been excessive and excess energy was coupled into the rock rather than fracturing and expelling the rock.

Despite the amount of information that can be derived from the figure above, the identity of potential misfired shots can only be inferred from the data. The trace cannot definitively identify the source location of each peak, or if any one peak is comprised of one, two, or even three individual shots firing together, or whether an individual shot fired out of sequence. Other performance characteristics of this blast could be inferred from the trace. The vibration trace associated with each shot fired offers information on how each one performed and whether or not the blast has been effective. Higher peak amplitudes could have resulted from a larger explosive charge being fired, or multiple charges programmed for the same delay, or that of a disproportionate amount of energy was coupled into the rock mass. Rather than energy being spent on fragmenting and moving the newly released rock from the face the burden, or confinement may have been too great for the charge to fracture the rock.

It is clear in this case that the blast did not fire as planned. Shots #1 and #24 show excessively high peak particle velocities and may have produced poor rock removal, fragmentation, or throw (rock movement).

The facts of what happened in this blast was corroborated by an inspection of the blast area. Extreme caution was taken in the blast zone where there was a potential for the unfired remnants of shot #12 to be found. Since there was a complete absence of a peak on the trace there was a working assumption that the detonator was still intact and a hazard. No traces of #12 were found and it was certain that it fired at the same time as #11. Charge #14 was a partial misfire and some of the explosive material was present in the fragmented rock.

7.2.3 Observations from nonel initiated blasts

As stated earlier, due to the lack of timing delays in commercially available nonel detonators while conducting their own experiments into misfires, Ewusi was compelled to design the nonel experiments with several groups of charges on the same timing. From Figure 52 the variability in timing precision is apparent in the case of 3000 ms and 6000 ms delays. Figure 52 shows the result from two detonators fired together both with a nominal 7000 ms delay.

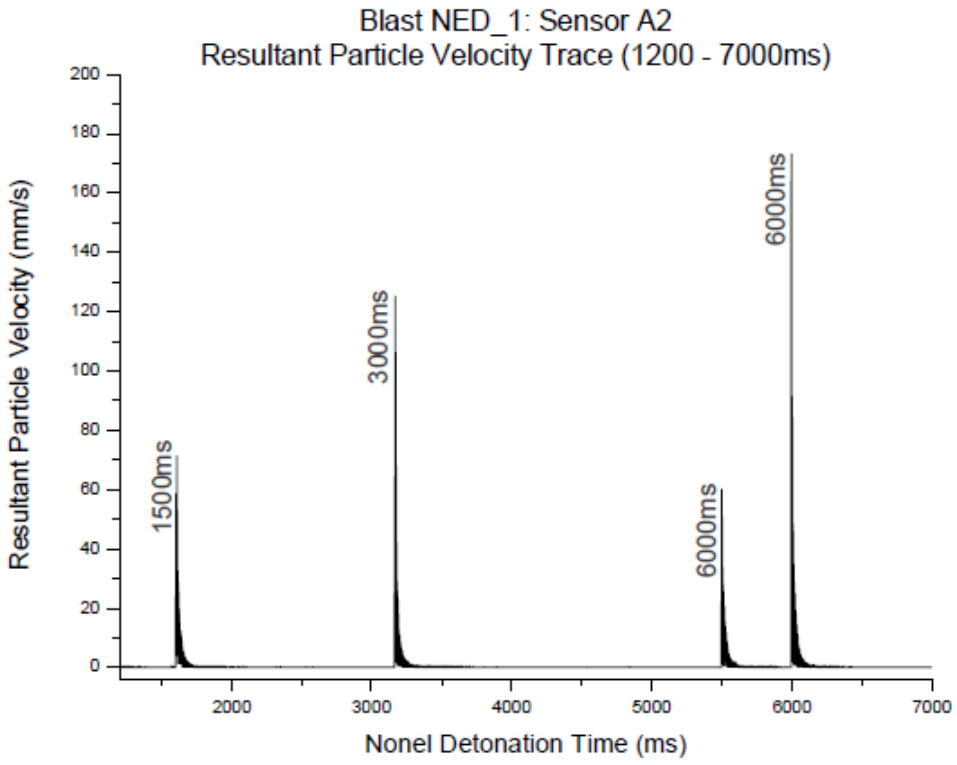

Figure 52 Blast NED_1 vibration trace from Sensor A2 (21m from blast)

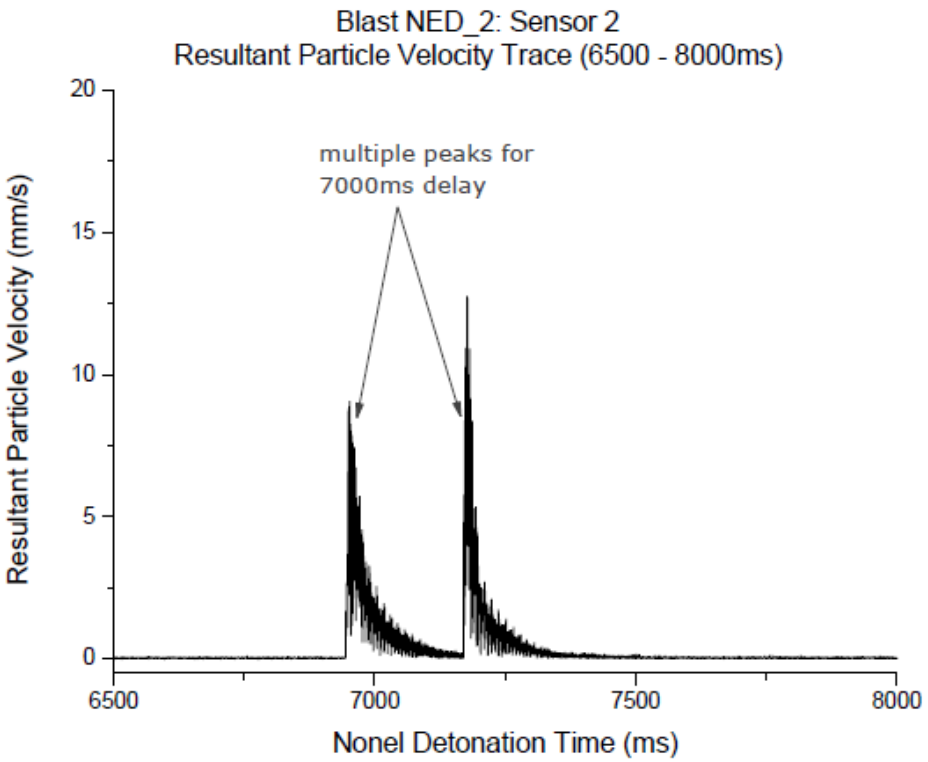

Figure 53 Variation in delay firing time for nonel detonators

7.2.4 Peak counting conclusions

It can be seen from this one PED example that so long as each blasthole is allocated an individual firing delay time and with the minimum achievable firing time deviation, a one-to-one correspondence between blasthole detonation time and the vibration trace, which will permit identification of potential misfires. The information contained in the trace highlights several characteristics of this firing event: the total number of shots fired; their timing delays and potentially, if a gap is apparent, the identity (and hence location) of the misfired shot.

The limitations of this technique are seen in practice with non-electric (pyrotechnic) based detonators especially with long delay times. Specifically with nonel initiation systems the timing variation can be in the order of 10s of milliseconds Silva, (2017) which could then inadvertently generate overlapping detonation timings. In addition, there are limited choices of timing delays available with commercially available nonel detonators which results in groups of holes being programmed to be fired together. In this case overlapping vibration traces are guaranteed with large numbers of shots being fired due to the practical limitations.

In the case of nonel detonators, due to the limited choice of timing delay options and the variability in timing precision, it could prove impossible to infer the location of a misfire from peak counting alone.

7.3 Higher Energy Impulse Experiments

The first series of experiments aimed to compare impulse signals from a series of co-located shots using cross correlation. The second series of experiments compared impulses from a fixed observation location with a second set of impulses generated at an increased range from the first. The third experiment aimed to identify a target impulse made at the same location as a signature impulse in the presence of an interferer impulse. The final experiment compared signature impulses made by #8 strength detonators in production blast holes and run a correlation with impulses generated by a fully charged production shot with a much higher magnitude. The outcome of these experiments would indicate whether the technique could be applied to larger detection ranges, and between impulse signals of significantly disproportionate magnitudes and significantly, whether the technique could be developed for misfire detection

7.3.1 Quarry blast experiments with detonators

The quarry environment at CSM enabled an increase in the physical range of detection and permitted the use of varying types and quantities of explosives. We hoped to develop a technique to compare pre-blast, signature impulses with those from a full face blast. We also intended to establish whether, or not impulse signal correlation would be adversely affected by any damage, or removal of rock that would compose the signal path between the signature impulse source location and the detector. The premise that these investigations are based upon, is that the physical relationship of the bounded surfaces of the rock i.e. the free face of the rock, the orientation of the plane of the blastholes to the sensor location, the multiple perpendicular free faces of the blastholes themselves, the voids created for the cut and condition of the natural rock surrounding the blast site, all impart a unique influence on the signature impulse as it propagates from the impulse source position to the detector. The original state of the rock mass will evidently be disturbed during rock expulsion (spalling) during the production blast as well as introducing fissures propagating into the surviving rock. It is therefore to be expected that these changes to the rock will impact the shaping experienced by the production blast induced impulses potentially degrading signature and production blast signal correlation.

It had been demonstrated during this research that mechanically generated impulses showed excellent correlation and repeatability which spatially decayed over distances of 10 - 20 cm in concrete. It remained to be seen whether impulses induced by explosive charges would exhibit similar spatial dependency, even without removing rock. Clearly the impulse generated by mechanical means can be repeated at precisely the same position. An impulse generated in a drilled hole is created by rapidly increasing gas pressures acting around the surface area at the blind end of the borehole. The forces imparted to internal surface of the borehole is more diffuse than a mechanical impact and the force generated from the detonator are dependent on the quality of the gas containment achieved by the stemming of the detonator, or shot amongst other physical factors. Despite the difficulties in ensuring an adequate gas seal inside the test holes drilled for these experiments, detonators generated significantly higher impulses than could be generated mechanically and were adopted for this trial.

The first test site for the impulse correlation experiments in rock were conducted at the open air quarry that forms the entrance to the test mine shown in Figure 54 below.

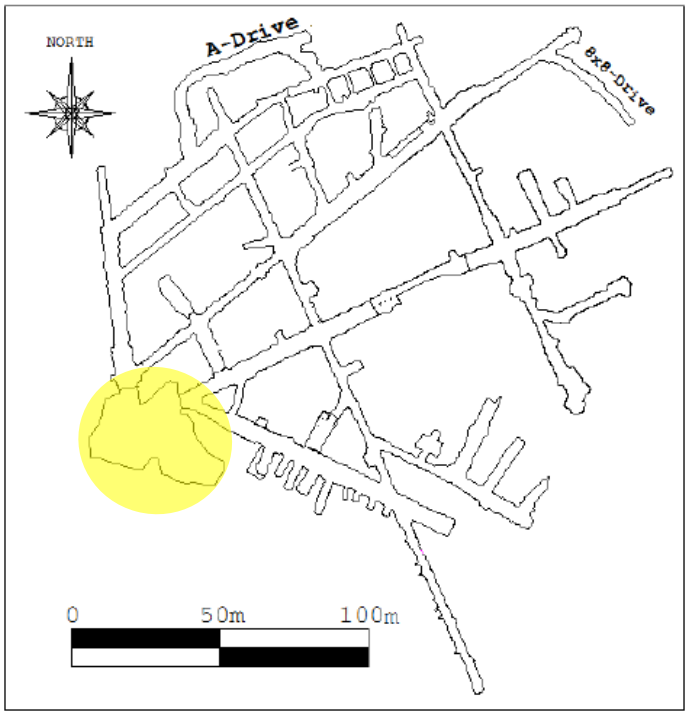

Figure 54 Quarry location (indicated in yellow) at CSM

Figure 55 shows the setup used to determine the spatial decay of the cross-correlation decay in natural rock. In this instance it was decided not to create a centimetre scale grid, but aimed to replicate the hole spacing more representative of blasting processes i.e. 20 - 50 cm.

In this set up we also placed one of the two geophones close to the plane of the impulses (highlighted) and a second behind the free face (not shown).

Figure 55 Open test area for the quarry blast experiments showing weathered rock face.

Figure 56 close up of the detonator hole arrangement with one of two positions of the geophones

The experiment involved drilling seven 150 mm deep, ø10 mm holes to accommodate the ø7 mm nonel detonators in the rock face. The holes were spaced at 100 mm A-B-C, 100 mm A-E-F and 200 mm C-D and F-G. the geophone was approximately 1.2 m distant from the farthest detonator hole position.

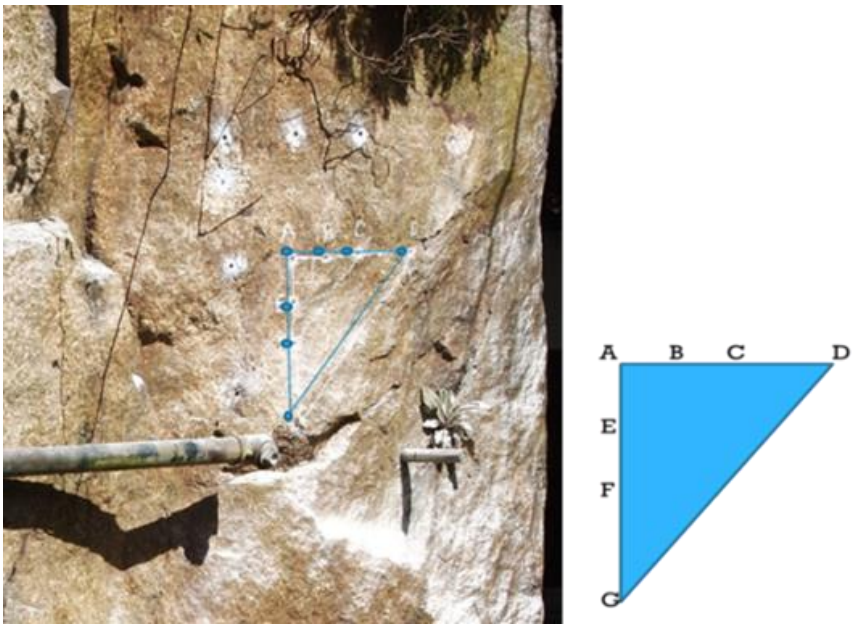

Figure 57 Image of drilled holes and schematic of hole references A – G

Two individual detonators were fired sequentially in each hole (where possible). Once a detonator was in placed, the hole was stemmed (sealed) with putty to prevent the detonator being ejected from the hole and ensure the maximum energy was coupled into the rock. The pressure front created by the detonator would generate an impulse that would radiate away from the free face and radiate into the surrounding rock mass.

Two single axis geophones were installed close to the test location. The geophones were equipped with ground spikes and they were coupled to the rock by embedding them in pre-drilled holes in the rock using a 2-part hard setting epoxy to prevent them rocking.

Figure 58 Geophone #2

The resulting impulse measurements were captured using a Prosig P8004 which is an ultra-portable 24-bit data acquisition system (Figure 59) with 4 analogue inputs with industry standard BNC connectors. Its maximum sampling rate is 100k samples/sec/channel at 24-bits, or 400 k samples/ sec/channel at 16-bits. A sample rate of 8 kHz was selected for all measurements at CSM.

Figure 59 Prosig P8004 data capture system

7.3.2 Experiments on spatial decay of cross correlation

Earlier experiments on the use of cross-correlation techniques to differentiate impulses showed that as we compared two mechanically generated impulse signals at two separate points, the cross-correlation coefficient decreased with increasing distance between signature impulse source and a candidate impulse, however, two impulses originating at different, but equidistant points from a target position would not result in identical wave-forms, or show a high degree of correlation. We note here that we are not only observing the relationship between the correlation coefficient value and the separation distance between the first and second impulses, but that the correlation value is spatially-dependent and therefore also range dependent.

7.3.3 Impulse correlation – single position.

Using the quarry setup described above, a series of detonators were fired at each position. It had not been previously determined whether the use of explosives to generate impulses in rock would result in signals that would demonstrate the correlation observed earlier from mechanically generated impulses.

Where possible, multiple detonators were fired in the same position and the resulting impulse signals were then compared by calculating the cross-correlation coefficient for spatial repeatability.

Some initial failures were observed when the first signature impulse caused physical damage in and around the hole. As a result of this damage the gases from the subsequent detonators escaped into the surrounding rock without generating a measureable impulse due to a lack of pressure build up within the hole. Consequently no impulse was recorded and these holes were abandoned. Despite this problem several successful pairs of impulses were recorded from a single position and the correlation coefficients calculated.

Table 7 Correlation coefficient between high energy impulses

	A	B	C	D	E	F	G
A	0.5	0.36	0.18	0.16	0.3	0.1	0.14
	0.6		0.3	0.24	0.35	0.28	0.2
B		0.18	0.3	0.17	0.18	0.11	0.13
		0.46	0.3	0.36	0.46	0.3	0.18
C			0.5	0.32	0.18	0.14	0.11
			0.48	0.5	0.3	0.3	0.14
D				0.31	0.2	0.17	0.12
				0.44	0.31	0.24	0.17
E					0.36	0.13	0.12
					0.43	0.16	0.16
F						0.43	0.11
						0.3	0.19
G							0.31

High values of correlation coefficient were consistently observed when two impulse were generated at the same position. When cross-correlation was carried out of signals from successive detonators in the same hole, the first pairs of correlation results showed the highest level of correlation. This trend was seen at each of the four locations. Where more than two detonators were fired in the same hole the signal correlation decreased as the holes was increasingly damaged and the confinement of gases decreased. This was observed at each of the four positions A-D.

Mapping the cross correlation coefficients for Positions A-D show that the value of the coefficient drops off as we compare signals from increasing ranges from the original signature position. Figure 60,Figure 61,Figure 62,Figure 63.

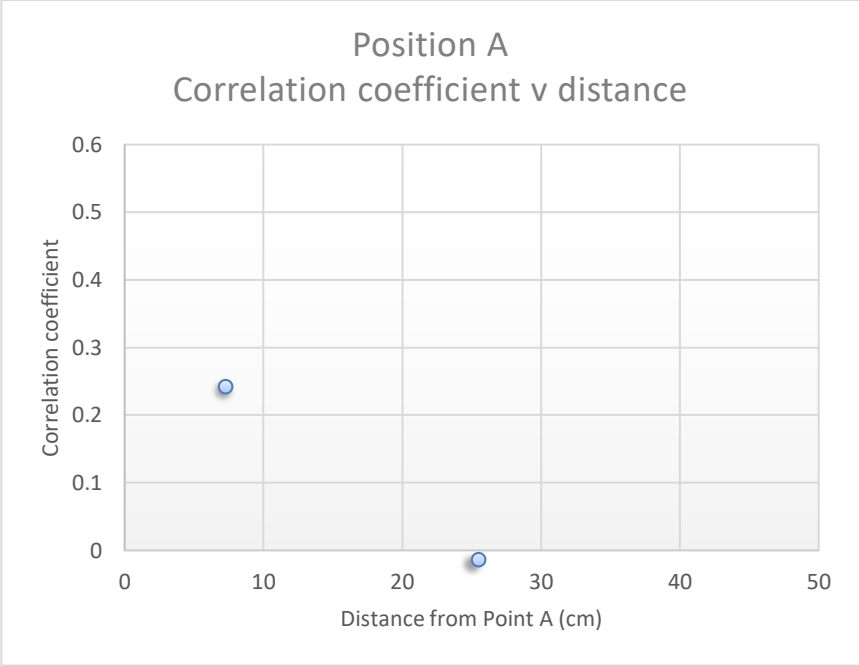

Figure 60 Cross correlation coefficient v distance from Position A

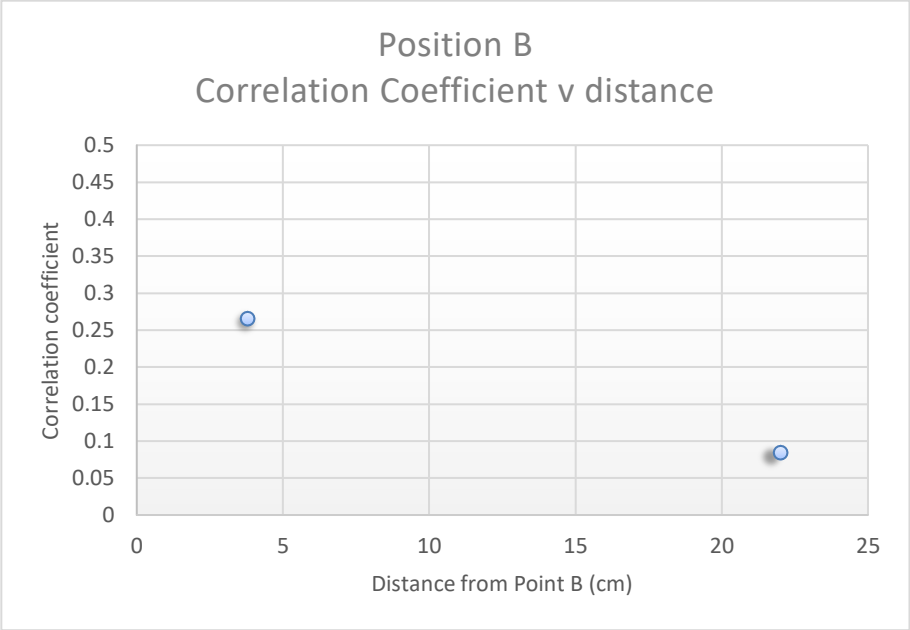

Figure 61 Cross correlation coefficient v distance from Position B

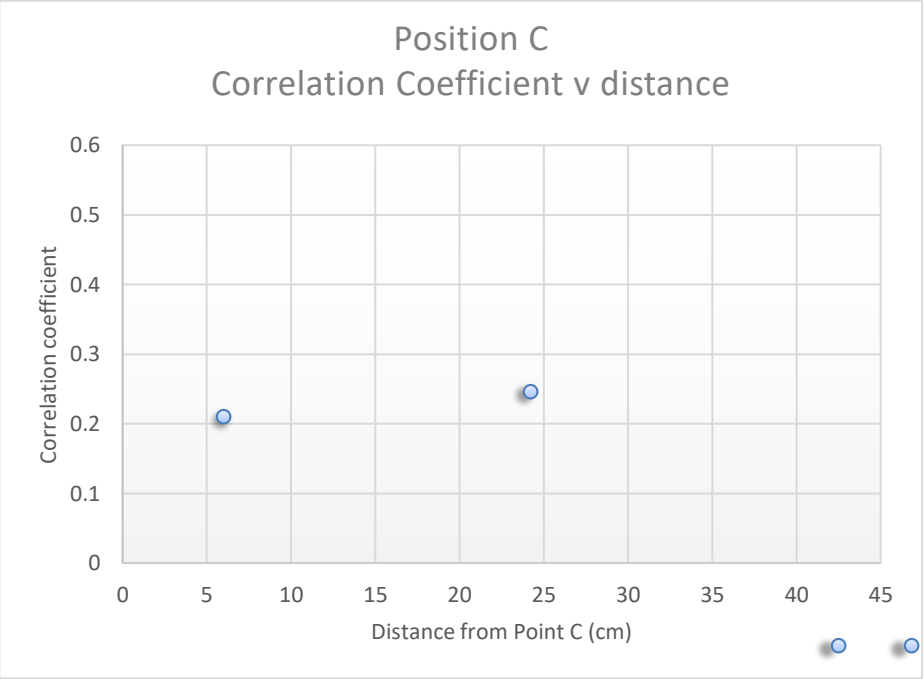

Figure 62 Cross correlation coefficient v distance from Position C

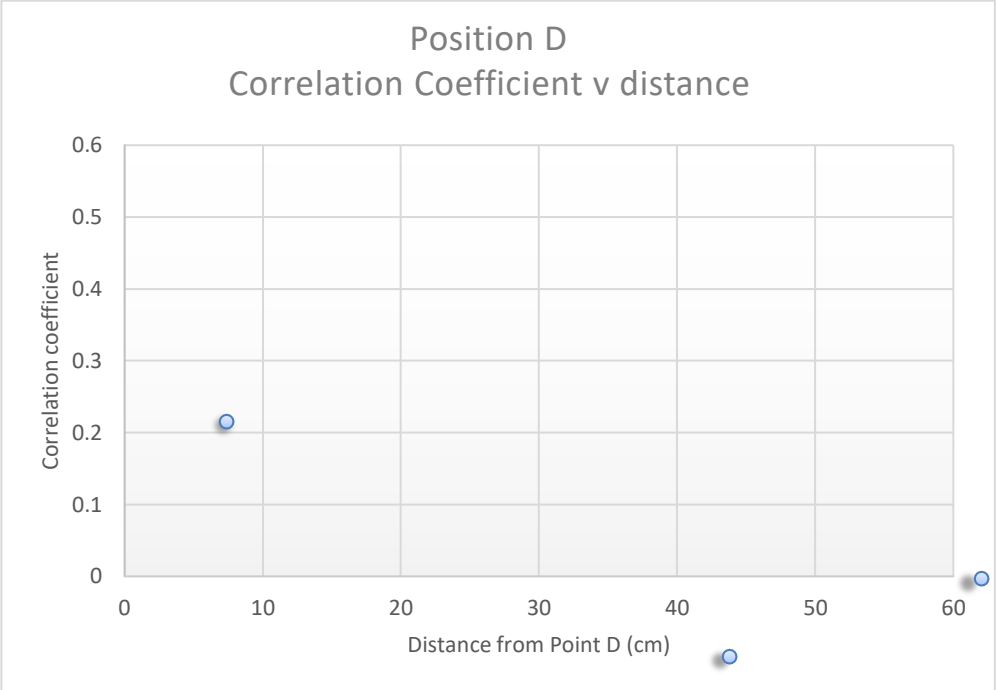

Figure 63 Cross correlation coefficient v distance from Position D

The maximum correlation coefficients calculated ranged from 0.48 to 0.50. The results are plotted in the graph shown in Figure 64.

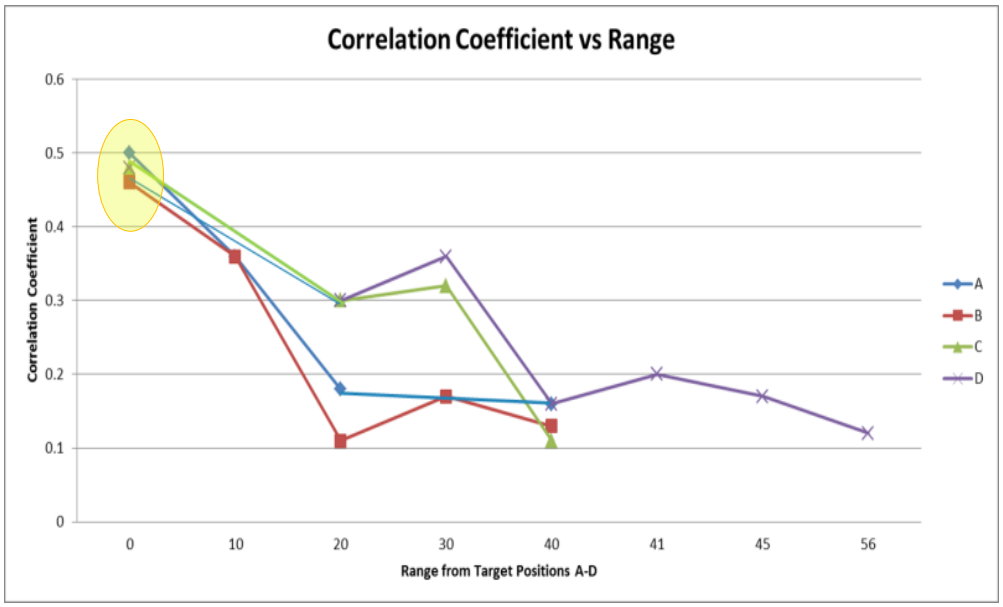

Figure 64 Correlation coefficient versus range from all four locations A, B, C, D (shown in Figure 57)

7.3.4 Spatial dependency of impulse correlation

Figure 64 shows the summary of spatial decay in correlation coefficient from all four different starting positions A – D (schematic of test hole positions shown in Figure 57).The test set up permitted steps of 10 cm, 20 cm and 40 cm along two perpendicular axes. As we compare signals from progressively distant positions, similar to the behavior observed in concrete. At ranges greater than 40 cm there was no further degradation in the calculated correlation coefficient value.

Given the results above, where the correlation coefficient appears to be a function of distance, in the context of blasting, where hole spacing is of the order of 20-50 cm there appears to be scope to develop this technique further.

It is also of interest that the detection range is of the order of a few meters. The most effective geophone was located at a range of approximately 3.5 - 4 m distant from the firing face. In the context of tunneling drill and blast, this is very close indeed. Placing any instrumentation at this distance exposed to a blast face, would necessitate protecting signal cables from flyrock, or could be carried out by using entirely wireless transmission eliminating the need for cables from the sensor to the data processing location.

7.3.5 Impulse Correlation with an interfering signal

Having observed repeatability with individual shots, pairs of detonators were fired in two steps: firstly as individual shots to generate the signature impulse, followed by pairs of detonators, one of which was at the signature impulse firing position. The loading arrangement is shown in Figure 65 below.

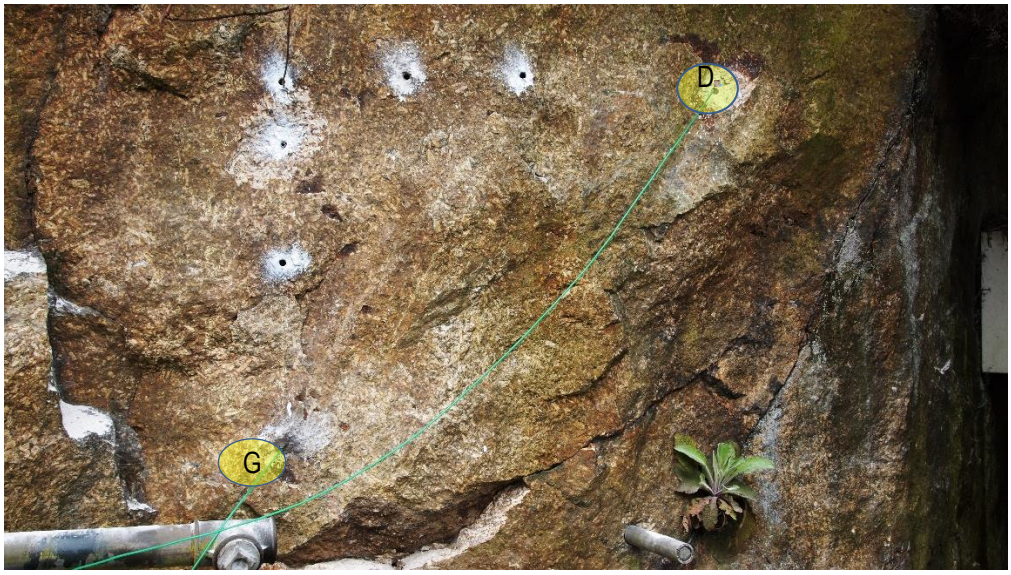

Figure 65 Set up at stage 2, Signal correlation with interference

Figure 65 shows the test set up to determine whether the presence of an overlapping second signal would prevent correlation with a signature impulse made at the target location. Two detonators were installed at test position D with second interfering impulse generated at position G and fired simultaneously.

Impulse signals were monitored by the same geophone / Prosig DAQ as before. An individual signature impulse generated at Position G was cross correlated with an impulses created by firing two detonators simultaneously at locations D and G.

Figure 66 shows that there is a distinct correlation between the signature impulse and the signal recorded with a second impulse from that location in the presence of overlapping off-target impulse.

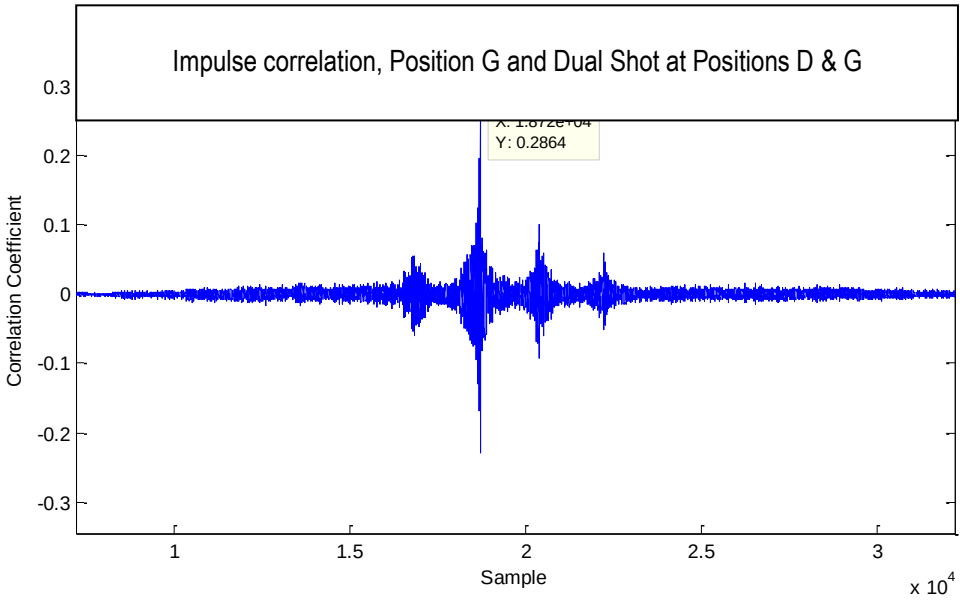

Figure 66 Correlation of Single shot (Position D) and Dual shot at Positions D & G)

The importance of the outcome in a tunneling context is that with overlapping impulse time signals arising during a development blast, there is the possibility to employ this two-stage process to identify misfire locations by creating a library of pre-blast signatures from each hole prior to the production blast then comparing them to the signals from the main charges.

7.4 Small blast experiment

Until now, a method of comparing low-energy signature impulses with high energy impulses from production blasts, for the purposes of misfire detection, had not been tried. Therefore a series of experiments were conducted, similar to the ones carried out on concrete to establish whether it would be possible to obtain repeatability with correlation comparisons. The ultimate aim at this stage in the investigation was to discriminate between impulses generated by small quantities of explosives, but with limited volumes of rock removed. The introduction of rock removal is the significant new factor at this stage. Whether, or not the removal of even small volumes of rock during a modest production blast would result in the impulse signals losing significant identifiable features of the information that would potentially characterise the signal path that the signature impulse had possessed.

An opportunity arose at CSM test mine to trial the pre-blast signature hole method during a small production blast. The blast was designed to widen and extend a small cross cut at the blind end of the A-drive. There were four pairs of charges fired in series, followed by a fifth individual shot Figure 68. The physical layout is shown in Figure 68 and actual timing sequence of the blast in Figure 69.

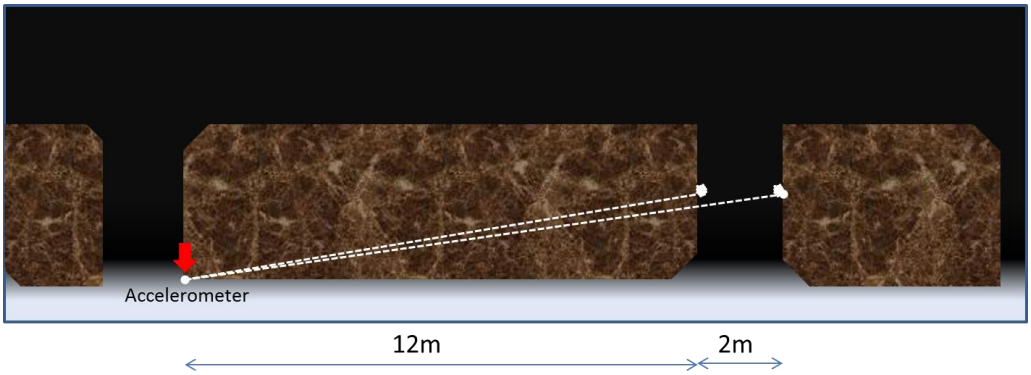

Figure 67 Small production blast arrangement and sensor range

The final individual charge was very small and designed to remove a small unwanted protrusion of rock to result in a smoother surface. Very little energy was coupled into the surrounding rock as it was a small charge and small rock burden.

Once we had drilled the nine blast holes, we were given permission to fire a couple of signature signal detonators for later comparison with the signals from the main charges. Only two Nonel detonators were fired couple of holes and stemmed using timber and clay. The blast was monitored using PCB model 353C22 accelerometer fixed with beeswax. The accelerometer signal was fed into an ICP Conditioning amplifier LM-148 the output was then sampled by a Picoscope 2-channel USB oscilloscope and the signal sampled at 8 kHz.

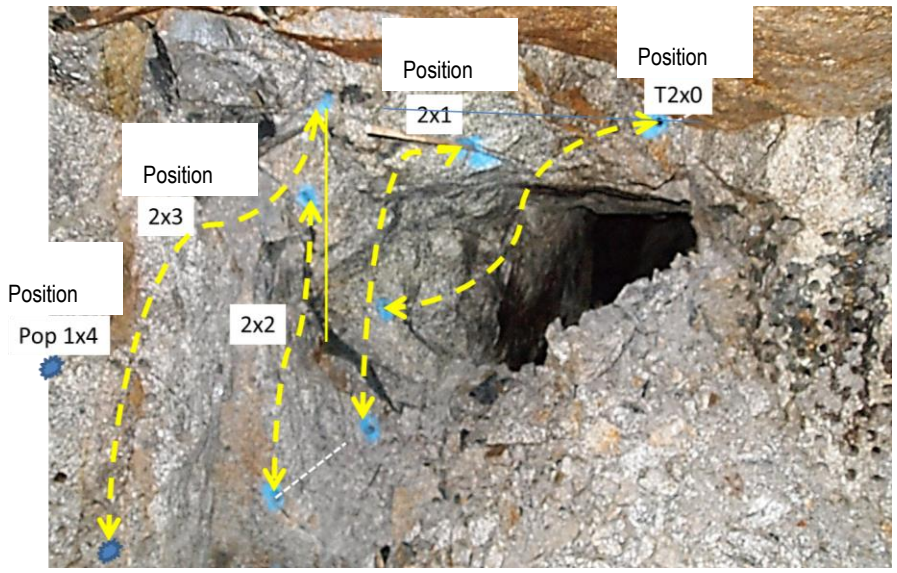

Figure 68 Blast configuration and sequence

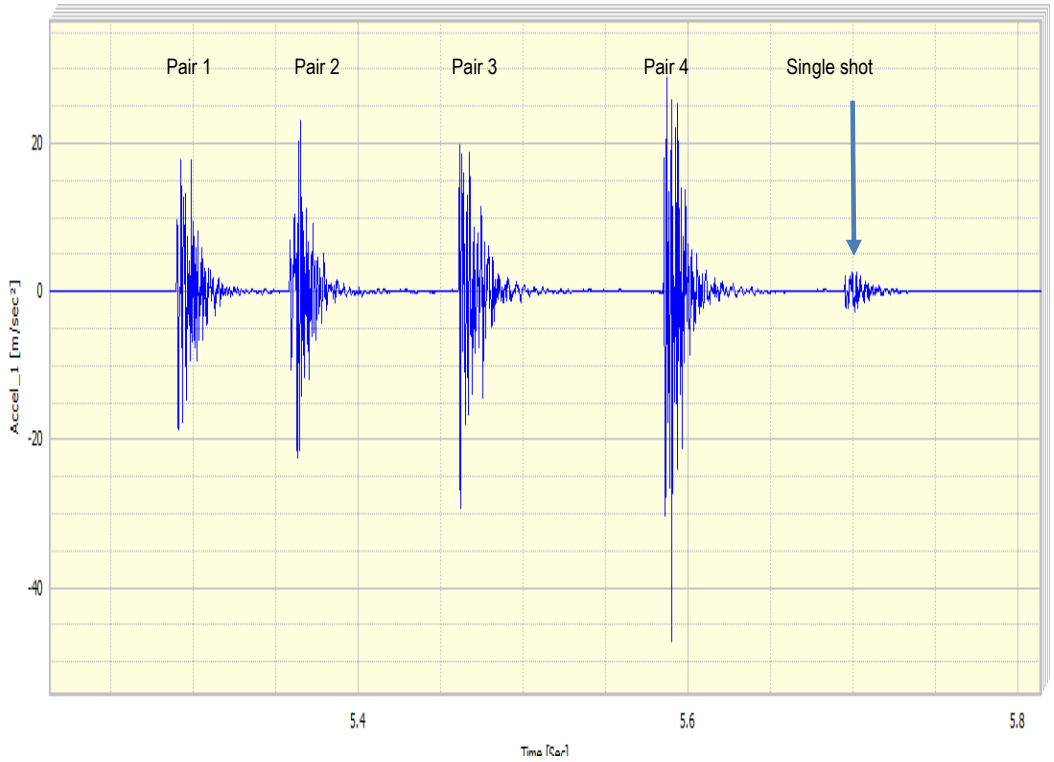

Figure 69 Cross cut expansion blast vibration trace

In this case the expansion of the cross cut required a variety of hole depths and explosive charge weights to be used. In regular tunnel advancement it's typical that the hole depths at would be similar in depth and charge size.

Simply monitoring the impulse magnitude alone is not a good indicator of misfire event. In this blast, firing pairs of holes together was the intention, therefore if one had failed to fire, it would not be obvious from the vibration trace alone whether or not one, or both had been successful before a physical inspection of the site. If a misfire had occurred, the vibration trace would not have indicated which of the two had fired successfully.

After the blast was complete and the site fully ventilated, re-entry was permitted the following morning. The positions of the holes were marked where evidence of the original hole remained.

Figure 70 Cross cut expansion post blast with the remnant of the blast holes marked by blue paint

Figure 71 shows details of one of the original blast holes and rock breakage. The remnant of the blast holes were sprayed with blue surveyors paint to highlight them against the broken rock. The blind end of the hole was still intact for some of the holes. For the pre-blast signature hole concept to be effective it is this surviving mass of rock that would be the acoustic path between the blind end of the hole, where the detonator generated the signature impulse, and the detector.

Figure 71 Cross cut expansion post blast detail

The cross-correlation of the signature impulse signal that had been generated by a detonator, and the full trace from the main blast. In the far field there were effectively five charges fired, 4 four simultaneous, but partially separated pairs plus one individual shot. We had one signature detonator in Position 3, at the roof of the newly expanded cross cut, and a second at final individual shot.

No correlation was recognisable between the signature impulse generated by the last shot (the final hole with a small explosive charge of 200 g Perunit nitro-glycerine based explosive). The correlation calculation yielded nothing at all. The result of the correlation between the pre-blast signature impulse from Position 3 (see Figure 68) and the production blasts is shown in Figure 72.

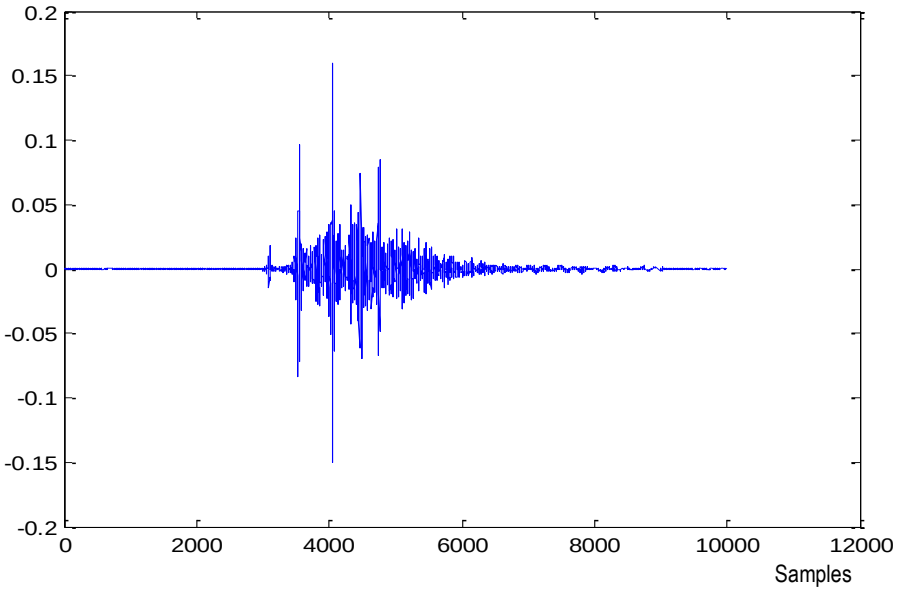

Figure 72 Cross-correlation of #3 pre-blast signature impulse and main blast signals

It is important to note that despite the removal of significant volumes of rock, correlation could still be observed between the pre-blast #3 signature impulse and the main blast signal. Indicating that the residual vibration path from blast hole to sensor and the original rock in its undamaged state shared sufficient similarity to provide a distinctive signal correlation. From Figure 72 we can see that there is a stronger correlation at Position 3 than at any of the other positions. This result was achieved despite the presence of an interfering signal from the other hole in the pair being fired on the same timing (T2), but physically separated by approximately 2 m. Earlier experimental work carried out for this investigation on peak counting falls short in being able to distinguish between such simultaneous, or overlapping signals. By contrast the use of cross-correlation here appeared to uniquely identify one of the two charges fired.

We observe that there are other, smaller correlation peaks at the timings offset from the main peak, evidently indicating some, all be it lower, signal correlation than the target position. It raises the question of why there should be any correlation, since each of the holes were spatially quite separate. The physical separation was >1 m. Earlier we saw that signature impulses could be used to segregate impulses down to around 40 cm.

Given the nature of an acoustic wave front radiating out in all directions from the shot location, the strongest signal received at the detector will be from the first arrival of the compression wave from any individual shot. The wave train will be elongated and augmented by the many reflections from rock compositions, mineral inclusions, mud, water, rock facets, voids and faults etc. Therefore every portion of direct path between the furthest away charge, to the detector, that is shared by intervening shots, will overlay a portion of the same propagation path as the most distant shot. It's not unreasonable to expect some degree of correlation to be seen between all shot locations between source and receiver. This is corroborated by the early experiments on the concrete slab where target positions that lay between the signature impulse position and the sensor displayed less similarity and produced a lower correlation coefficient. Whereas impulses that were on the opposite side of the signature position with respect to the sensor, had marginally higher correlation coefficients.

It is of interest to note that the impulse signatures in this experiment were created by detonators only. It appears that at least one of them created a viable signature impulse for the hole. Overall, the magnitude of the correlation coefficient was very small in comparison to previous experiments on concrete media.

Chapter 8 Conclusions

The investigations presented in this thesis aimed to develop a practical approach to identify the specific locations of misfires in tunnel blasting. The early stages of this investigation examined the feasibility of using various signal line options and sensors types to detect misfires. A series of practical blast monitoring experiments conducted at the University of Exeter's test mine located near Camborne investigated the viability of using electrical wires, optical fibres and shock tubes to carry signals from the charged tunnel blast face to a safe, remote observation point. These investigations concluded that such approaches were impractical and unreliable due to the high probability flyrock cut-offs impacting the signal integrity.

Previous blast monitoring investigations into blasting operations were aimed at optimising the blasting process, or emphasised environmental impact protection from tunnelling operations by limiting the peak particle velocity and modifying the impulse frequency content.

In contrast, this research focused on spatially locating the source of individual shots by utilising their unique blast induced impulse signals which were measured from a remote, safe observation point. Acoustic signal detection and analysis have been employed to uniquely identify the impulse signal and derive its point of origin. Signal localisation experiments were initially carried out on small mechanically induced impulses and progressed up to small-scale tunnel blasts.

Initial results have shown that there is the potential to employ cross-correlation to impulse signals in larger meter-scale media and to blast induced impulse response signals in particular. Furthermore, the signals can be successfully sampled by a single sensor and still yield a useful result. We have shown that in concrete and in rock, multiple impulses, made at same position, correlate strongly, but impulses originating from different positions showed significantly lower levels of correlation. We found that impulse signals generated by mechanical impacts exhibited strong correlation as did impulses made by small explosive charges. Significantly, early experimental results showed a strong correlation between low energy impulses and high energy impulses originating at the same location in a variety of mixed media substrates and in natural rock.

8.1 Outline of contributions to knowledge

The current methods for the detection and identification of misfires in tunnelling are essentially based on post-blast visual inspection. The contributions to knowledge provided by this research are:.

- Monitoring the vibration trace from a blast induced impulse sequence does not provide sufficient information about the specific location of any specific hole firing out of sequence. e.g. one hole in a pair that failed to fire, or the identification of sympathetic detonations.
- We also established that signature hole techniques are useful for estimating the resultant vibration magnitudes and frequency content at some remote point from a blast location.
- Established that the concepts of Time Reversal Mirror theory applies from millimetre scale to meter scale acoustic paths.
- Established that mechanically induced impulses were useful to demonstrate impulse correlation
- Established that blast-induced impulses were useful to demonstrate impulse correlation.
- Established that high energy impulses could be correlated against low energy signature impulses made at the same location.

8.2 Recommendations for further work

Arising from the promising experimental work that showed that high energy impulses could be correlated against low energy signature impulses, further work to optimise the blast face – detector arrangement. Location range should be addressed. A compromise between detection range and equipment protection will need to be ascertained.

Further testing with multiple sensors could provide corroboration of misfire location due to increased signal integrity and could increase the confidence of signal correlation repeatability.

Utilising the impulse noise generated by the drilling process as signature impulses could be investigated to eliminate the addition of an additional process step of creating a signature impulse as the drilling process will automatically generate continuous impulses as the rock is drilled. There is a real possibility to utilise these signals to characterise the acoustic media from blasthole to detector. Avoiding additional processes would deliver an economic benefit by eliminating the signature impulse generation step.

An investigation into optimising surface blasting operations, such as road, or railway cutting blasts, could be easier to implement than tunnel blasting and the benefits to safety would be easier to realise due to the simplicity of sensor deployment. It is thought that the signature/main blast signal correlation could be used here. Given the scale of surface blasting operations for civil works for transport infrastructure development multiple sensors could easily be deployed.

References

ABB. (2015, 2017). "Arc Flash Protection: tripping the light fantastic " Retrieved 1.06.2015, 2015, from http://www.abb.com/cawp/seitp202/f8e7a4a7e7496bddc125792900742d15.aspx.

Achenbach, J.D. Wave Propogation in Elastic Solids (1973), North-Holland Publishing ompany

Adderley, G. (2009). Blast vibration analysis. PhD, University of Exeter.

Anderson D.A. (2008). Signature Hole Blast Vibration Control.

Anderson, D. A. (2008). "Signature hole blast vibration control - twenty years hence and beyond " Explosives Engineers 2: 12.

Andrews A.B. (1981). Design criterion for sequential blasting. 14th Annual conference on Explosives and Blasting Techniques, Pheonix, AZ, USA.

Armstrong L.W (2000). "Blast Induced vibration monitoring and wave form analysis."

Bajpayee, T. S., T. R. Rehak, G. L. Mowrey and D. K. Ingram (2004). "Blasting injuries in surface mining with emphasis on flyrock and blast area security." Journal of Safety Research 35(1): 47-57.

Bajpayee, T. S., T. R. Rehak, G. L. Mowrey, D. K. Ingram and Isee (2002). A summary of fatal accidents due to flyrock and lack of blast area security in surface mining, 1989 to 1999.

Cassereau, D. F., M (1994). "Time-reversal focusing through a plane interface separating 2 fluids." Journal of Acoustical Society of America 96(5): 3145-3154.

Claerbout, J. R., J (1996). Stanford exploration project technical report.

Crenwelge O.E. (1988). Use of single charge vibration data to interpret Explosive excitation 14th Annual Conference on explosives and Blasting techniques, Anaheim, CA, USA.

Decross, M. S., K. (2018). "Green's functions in physics." Retrieved 19/03/2018, 2018, from https://brilliant.org/wiki/greens-functions-in-physics/.

Derode, Roux and Fink (1995). Acoustic time-reversal through high-order multiple scattering. 1995 Ieee Ultrasonics Symposium Proceedings, Vols 1 and 2. M. Levy, S. C. Schneider and B. R. McAvoy. New York, I E E E: 1091-1094.

Derode A., R. P. (1995). "Robust acoustic time reversal with higher order multiple scattering." Phys Rev Lett 75(23): 4206_4209.

Dowding, C. (1985). Blast Vibration Monitoring and Control. . Englewood Cliffs, NJ., Prentice Hall, Inc.,.

Draeger, C. F., M. (1997). "One-channel time reversal of elastic waves in a chaotic 2D-silicon cavity." Physical Review Letters 79(3): 407-410.

Draeger, C. F., M;Cassereau, D;Fink, M. (1997). "Theory of the time-reversal process in solids." Journal of the Acoustical Society of America 102(3): 1289-1295.

Energy, D. o. M. M. a. (2013). Surface blaster's certification study guide. D. o. M. M. a. Energy. Virginia, USA, Commonwealth of Virginia.

EPC (2010). Quarry Blasting Course. D. M. Pegden. Nottingham.

Ewusi, S. (2013). Misfires Identification in Tunnel Blasts. PhD Research, University of Exeter.

Farnfield, R. (2012). Shot firing training course.

Fink, M. (2006). "Time-reversal acoustics." Inverse Problems, Multi-Scale Analysis and Effective Medium Theory 408: 151-179.

Fink, M. (2012). "Time reversed acoustics in chaotic cavities."

Graff, K. (2012) Wave Motion in Elastic Solids, Dover Publications

Hinzen K.G. (1987). A new approach to model and predict blast vibration. 13th Annual Conference on Explosives and Blasting techniques, Miami, FL, USA.

Hopler R. (2006). Blasters Handbook.

Ing, R. K. F., M (1998). "Time-reversed lamb waves." IEEE TRANSACTIONS ON ULTRASONICS FERROELECTRICS AND FREQUENCY CONTROL.

Kortnik J, B. J. (2010). "Use of Electronic Initiation Systems in the mining industry." RMZ - materials and Geoenvironment 57(3): 403-414.

Lai, W.M., Rubin, D., Krempl, E., Introduction to Continuum Mechanics, Elsevier Science

Langefors U., K. B., . (1978). the modern technique of rock blasting. LONDON, UK, john Wiley and sons.

LeBoutillier, N. G. (2002). The Tectonics of Variscan Magmatism and Mineralization in South West England. PhD, university of exeter.

Lee, J. P., A; Holmberg, R (1994). Rock Blasting and Explosives Engineering.

Liu, Q. (2011). "A Misfire Identification method using wavelet transform." International Journal of Digital Content Technology and its Applications 5(8).

Liu, Q. K., P. D. (1993). "A theoretical approach to the stress waves around a borehole and their effect on rock crushing." Rock Fragmentation by Blasting: 9-16.

Lynch, R. (2013). Review of Seismic Methods in Caving Mines. Hobart, Institute of Mine Seismology: 26.

Lynch, R. (2013). Review of Seismic Methods in Caving Mines.

McLaughlin, K. L., J. L. Bonner and T. Barker (2004). "Seismic source mechanisms for quarry blasts: modelling observed Rayleigh and Love wave radiation patterns from a Texas quarry." Geophysical Journal International 156(1): 79-93.

Millar, G.F, Pursey, H. (1954) Field and Radiative Imedance of Mechanical Radiators, Procedings of the royal Society of London, Series A Mathematical and Physical Science, 223, 521-541

Mishra, A. N., Y;Singh, D. (2017). "Controlled Blasting in a Limestone Mine using Electronic Detonators: A Case Study." Journal of the Geological Society of India 89(1): 87-90.

Murashita, T. S., N;Sakamoto, M;Isee, (1998). "Blasting in tunneling." Twenty-Fourth Annual Conference on Explosives and Blasting Technique: 347-358.

Nateghi, R. (2012). "Evaluation of blast induced ground vibration for minimizing negative effects on surrounding structures." Soil Dynamics and Earthquake Engineering 43: 133-138.

Nazarchuk, Z. (2017). Acoustic emission, foundations of engineering mechanics, Springer.

Olson (1972). ground vibrations from tunnel blasts in granite. RI-7653. Washington, U.S Bureau of Mines

Pain, H. (1999). The physics of vibrations and waves, John Wiley & Sons.

Parvulescu, A. C., C. S. (1965). "Reproducibility of signal transmissions in ocean." Radio and Electronic Engineer 29(4): 223-+.

Persson A., H. R., . (1994). Rock blasting and explosives engineering. Boca Raton, FL, USA, CRC Press LLC.

Quieffin, N. I., RK; Catheline S (2005). "In solid localization of finger impacts using acoustic time-reversal process." APPLIED PHYSICS LETTERS 87(20).

Revey, G. F. (1996). "Practical methods to control explosives losses and reduce ammonia and nitrate levels in mine water." Mining Engineering July 1996: 4.

Sandvik (1999). Rock excavation handbook. Brisbane, Sandvik.

Selwood, E. B. D., E. M; Bristow, C. M (1998). The geology of Cornwall and the Isles of Scilly, University of Exeter Press.

Silva, J. L., L: Gernand, JM (2017). "Reliability analysis for mine blast performance based on delay type and firing time." International Journal of Mining Science and Technology.

Siskind D.E. (1986). Frequency analysis and the use of response spectra for blast vibration assessment in mining. 12th Annual Symposium on Explosives and Blasting Research, Orlando, FL, USA.

Siskind, D. E., Stagg, M.S, Kopp, J.W. and Dowding, C.H. (1980). Structure response and damage produced by ground vibration from surface mine blasting.

Spathis, A.T. (2010). A brief review of the measurement, modelling and management of vibrations produced by blasting. Boca Raton, Crc Press-Taylor & Francis Group.

Spencer, A.J.M. (1980) Continuum Mechanics, Longman Group UK Ltd

Sutin, A. T., JA; Johnson, PA (2004). "Single-channel time reversal in elastic solids." Journal of the Acoustical Society of America 116(5): 2779-2784.

Thoenen, J. R. W., S.L. (1942). Seismic effects of quarry blasting, Unites States Bureau of Mines. 442.

Thornton, D. S., D; Brunton I (2005). Measuring Blast Movement to Reduce Ore Loss And Dilution. Brisbane, University of Queensland: 11.

Verakis, H. C. L., T. E;Isee, (2001). Blasting accidents in surface mines, a two decade summary. Cleveland, Int Soc Explosives Engineers.

Verakis, H. C. L., T. E;Isee, (2003). "An analysis of blasting accidents in mining operations." Proceedings of the Twenty-Ninth Annual Conference on Explosives and Blasting Technique, Vol 2: 119-129.

Verakis, H. C. L., T. E;Isee;Lobb, T (2002). Blasting accidents in underground mines: A two decade summary. Cleveland, Int Soc Explosives Engineers.

Wapenaar, K. (2004). "Retrieving the Elastodynamic Green's Function of an Arbitrary Inhomogeneous Medium by Cross Correlation." Physical Review L Etters: 4.

Wright C., W. E. J., Carneiro D., (2000). "Seismic velocity distribution in the vicinity of a mine tunnel at Thabazimbi, South Africa." Journal of Applied Geophysics 44(2000): 369-382.

Yuill, G. F., R; Isee, (2001). Variations in vibration signals from single hole quarry blasts. Cleveland, Int Soc Explosives Engineers.

Zare, S. B., A (2006). "Comparison of tunnel blast design models." Tunnelling and Underground Space Technology 21(5): 533-541.